Austrian Journal of Technical and Natural Sciences

№ 9–10 2018
September–October

PREMIER
Publishing

Vienna 2018

Austrian Journal of Technical and Natural Sciences

Scientific journal

№ 9–10 2018 (September–October)

ISSN 2310-5607

Editorial office Premier Publishing s.r.o.
Praha 8 – Karlín, Lyčkovo nám. 508/7, PSČ 18600

E-mail: pub@ppublishing.org

Homepage: ppublishing.org

Austrian Journal of Technical and Natural Sciences is an international, German/English/Russian language, peer-reviewed journal. It is published bimonthly with circulation of 1000 copies.

The decisive criterion for accepting a manuscript for publication is scientific quality. All research articles published in this journal have undergone a rigorous peer review. Based on initial screening by the editors, each paper is anonymized and reviewed by at least two anonymous referees. Recommending the articles for publishing, the reviewers confirm that in their opinion the submitted article contains important or new scientific results.

Premier Publishing s.r.o. is not responsible for the stylistic content of the article. The responsibility for the stylistic content lies on an author of an article.

Instructions for authors

Full instructions for manuscript preparation and submission can be found through the Premier Publishing s.r.o. home page at:
http://www. ppublishing.org.

Material disclaimer

The opinions expressed in the conference proceedings do not necessarily reflect those of the Premier Publishing s.r.o., the editor, the editorial board, or the organization to which the authors are affiliated.

Premier Publishing s.r.o. is not responsible for the stylistic content of the article. The responsibility for the stylistic content lies on an author of an article.

Included to the open access repositories:

Typeset in Berling by Ziegler Buchdruckerei, Linz, Austria.
Printed by Premier Publishing s.r.o., Vienna, Austria on acid-free paper.

Section 1. Biology

Rustamov Atham Ahmatovich,
Ph D., Degree
Kimsanboev Xojimurod Xamraqulovich,
professor
Jumaev Rasul Ahmatovich,
Rajabov Shohrux,
Toshkent state agrarian university
Uzbekistan in the department plant protection
E-mail: atham-rustamov@mail.ru

IN BIOCENOSIS THE DEGREE OF APPEARING ENTOMOPHAGOUS TYPES OF VERMINS WHICH SUCK TOMATOEY SOWINGS

Abstract: In the article ressarches are carried aut Tashkent region's tomato agrobiocenosis sucker pests and about their degree of appearing entomophagous types. In researches it is defined that kinds of predatory and parasitic entomophag which appropriate for mainly 7 family, belong to 20 sorts. According to it Aphidiidae, Neuroptera, Aphelinidae, Syrphidae, Coccinellidae, Anthocoridae, Phytoseiidae are concerned as a basic family sorts.

Keywords: Agrobiocenosis, tomato, pest, entomophagous, parasite, quantity, efficiency.

Introduction: Learnung entomofauna of earth surface is intimately connected with agriculture. Pests that are appeared in the tomato agrobiocenosis and their loss are damaging seriously for the harvest and quality of plants. Cultivating all food productions should be high quality and safe. In fact, many problems are increasing year by year, while planting sowings, as well as it isinfluencing the cost of productions. It means the part of poor people of the world population can't eat enough what they want because of faod shortage. So ti is required to learn this issue deeply [1; 3].

Observations of theoretical research: In nature, there are approximately 1000 pests of sucker vermins which are appeared tomato sowings (whitewinged, plant lice and specialized. However some sorts nourish only with vermins that belong to one type. In this way, it is considered chrysopidae, Miridae, Coccinellidae are more efficient among predator entomophags. According to world scientists (Naranjo; 2009) researches indicate controlling external, natural quantity of the only whitewinged nourishes. Some scientists suppose that researches are not adeguate by analyzing systematically and verifying in ruling the quantity of tomato sowings in dredatory entomophags [1; 2; 4].

In the condition of our country, there are a lot of entomophag types that nourish sucker pests that appear in tomato plant. Unfortunately, they haven't been analysed systematically till now.

Observations of practical research: So, entomophag types of sucker vermins that appear in tomato agrobiocenosis were learned in Tashkent regions of aur country.

Researches were held at the condition of open field as well as in the tomato field that damaged with plant lice and white winged. According to it, (0.5) cucumber, melon's agrobiocenosis was learned as a practical area and tomato was sowed in 5,0 area. Researches continued from The beginning of sowings season till the end. Each identified and gathered samples were analysed systematically in laboratory. All entomophags' appearing degree and quantity of population, plan lice and white-winged that have in tomato agrobiocenosis was learned perfectly.

Besides these, it was investigated appearing of entomophag types according to territories [2; 4; 5; 6].

In Tashkent region of our countiy as it was identified plant lice and white-winged types, there are different faunas of parasite entomophags. According to collected information, plant lice and (quality) wyite-winged's quality types of boss-parasite and boss-predatory that appears in tomato agrobiocenosis and their foodstuff chains were learned during investigation (1 time table).

Results of the research: Due to collected informations, it was defined that, kind of predatory and parasitic entomophag which appropriate for mainly 7 family, belong to 20 sorts. Due to these Aphididae, Neuroptera, Aphelinidae, Syrphidae, Coccinellidae, Anthocoridae, Phytoseiidae their families *Aphidius colemani, Aphidius matricariae, Aphidius rhopalosiphi, Chrysopa carnea Steph, Chrysopa septempunctata Wesm., Chrysopa formosa Br., Chrysopa dubitans McL, Encarsia partinopea Masi, Encarsia formosa Gah, Sphaerophoria rueppelli Wied., Sphaerophoria philanthus Mg, Syrphus ribesii L, Coccinella undecimpunctata, Adonia variegata, Scymnus frontalis, Stethorus punctillum, Scymnus rubromaculatus, Campylomma diversicornis Reuter, Metaseiulus occidentalis, Phytoseius rubii* representatives were registered. Above mentioned foodstuff speciality of family represent tetives is mainly considered plant lice imagoes and larvas of white-winged, lymphas and grown-up imagoes.

It is very important the relationship between boss-predatory and boss-parasite of insects in biocenosis. Because one type may increase highly or decease at all if parasite or bass relationship is destroyed [2; 5; 6].

Identified types of entomophags were collected by vegetable agrobiocenosis in Bekabad, Buka, Okkargan, Kibray, Zangiota and Yangiyul districts of Tashkent region.

Table 1. – Encounting degree and typical structure of entomopgagous sorts as well as sucker vermins in tomato agrobiocenosis. (Tashkent region 2018-year)

No.	The names of entomophagous types	The period of damaging of boss	Parasite: proportion of boss	Encounting degree of parasite thpes
1	*2*	*3*	*4*	*5*
1	**Aphidiidae family**			
Aphidius colemani *Aphidius matricariae* *Aphidius rhopalosiphi*		imago	1:15	+++
2	**Neuroptera family**			
Chrysopa carnea Steph, *Chrysopa septempunctata Wesm.*		imago, larva, egg, lymph	1:20	+++

1	*2*	*3*	*4*	*5*
3	**Aphelinidae family**			
Encarsia partinopea Masi. *Encarsia formosa* Gah.		3–4 ages of lymph	1:20	++
4	**Syrphidae family**			
Sphaerophoria rueppelli Wied. *Sphaerophoria philanthus* Mg. *Syrphus ribesii* L.		imago, larva, egg, lymph	1:24	++
5	**Coccinellidae family**			
Coccinella undecimpunctata *Adonia variegata* *Scymnus frontalis* *Stethorus punctillum* *Scymnus rubromaculatus*		imago, larva, egg, lymph	1:15	+++
6	**Miridae family**			
Campylomma diversicornis Reuter,		imago, larva, egg, lymph	1:23	++
7	**Phytoseiidae family**			
Metaseiulus occidentalis *Phytoseius rubii*		imago, larva, egg, lymph	1:21	+

It is obvious that collected entomophag kinds are various by Tashkent region. In this case, the majority of wild birds have a population of Kangyoo beetle and Semitic family. This parasite entomophagus found that the setting of the vegetable agrobiocenosis was controlled by a certain amount of sucrose pests.

References:

1. Alimukhamedov S. N. Ecologization of plant protection in Uzbekistan // Plant protection. 1991.– 12.– P. 13–15.
2. Kimsanbaev X.X. and others. Development of parasite entomophags of plant pests in biocenosis. (Tutorial). NMIU of Uzbekistan. – Tashkent. 2016.– P. 14–21.
3. Myartseva S. N. and Yasnossh V. A. Parasites of the hothouse and cotton whitefly (Homtortera, Aleyrodidea) in Central Asia // Entomol. browse 1993.– No. 4.– P. 785–793.
4. Sulaymonov B.A. and so on. Biological protection of plants. NMIU of Uzbekistan (Tutorial). – Toshkent. 2015.– P. 56–59. Hamraev A. Sh., Nasriddinov K. Biological protection of plants.– Tashkent. Folk Meros. 2003.– P. 171–178.
5. Naranjo S. E., Cañas L. Ellsworth P. C. Mortalidad de Bemisia tabaci en un sistema de cultivos múltiples. Hort. Internacional 43(Febrero): 2004 a.– P. 14–21.
6. Naranjo S. E., Cañas L., Ellsworth P. C. Mortality and population dynamics of Bemisia tabaci within a multi-crop system. 2009.– 18 p.

Section 2. Biotechnology

Shehu Matilda,
Department of Biology,
Faculty of Technical Sciences
University of Vlora, Albania
Plant Biotechnology PhD., candidate
E-mail: matildazeqo@gmail.com
Zekaj (Trojani) Zhaneta,
Department of Biotechnology,
University of Tirana

CYTOLOGICAL DIVERSITY BETWEEN THREE POPULATIONS OF *SCILLA AUTUMNALIS* L. IN SOUTH ALBANIA

Abstract: In this study, three populations of *S. autumnalis* L. were investigated. The aim of the work is to analyse the cytological variation of this species, examined for the first time in Albania. The technique used for cytological study is the squash technique. Three cytotypes resulted for this species in Vlora area. For population of Portopalermo was realised chromosome formula, karyogram and idiogram.

Keywords: *Scilla autumnalis* L., cytological variation, cytotype, squash technique.

I. Introduction: *Scilla autumnalis* L. is a rather widely distributed and common species in the Mediterranean region and Western Europe. In our country is wide distributed in all territory, but in other countries (Romania) is critically endangered [1]. Is one of the most studied species by many authors. Till now it has been classified as a a single species, mainly based on morphological traits. It is a species with a large variation in the number, type and morphology of the chromosomes. So far, 10 cytologically distinct populations have been detected at the species level [2; 3; 4; 5]. For the populations analyzed in Tunisia and Aegean regions, 8 cytotope was reported [6]. In a study of 31 *Scilla autumnalis* L. populations from Spain and Portugal 4 cytotypes were found [7]. The aim of this study has been to add more information on the cytotypes, realised for the first time for these species in Albania.

II. Materials and methods:

For the cytological analysis of *S. autumnalis* species in the three habitats, the were used root tips. The slides were prepared using the squash technique. The technique of processing the herbal material for the preparation of the chromosome slides passes through several stages: the prefixation of the roots tips in icy water at 2 °C throughout the night [8]. Then were moved to Carnua (absolute ethanol: glacial acetic acid/3:1) for 3–12 hours at 4 °C. After fixation in Karnua root tips were stored in alcohol 70% at 4 °C for several weeks. Then were transferred into acetic orcein 45% [9] for several hours at ambient temperature and then was made double enzymatic treatment with pectinases and cellulase which was left in 4 °C overnight. The next day has been prepared the slides with the squash technique. Observation has been realized with microscope Optika at 100

× magnification. Measurement of chromosomes, chromosomal formula, karyogram and Idiogram was realized with Cromo II software [10]. Photos were realized with Apple iphone at ocular tube.

III. Results and discusion

Scilla autumnalis L. in three considerated habitats shows variation of chromosome number. For *S. autumnalis* L. Portopalermo we were able to define the chromosome number and chromosome morphology. For other two population we defined only chromosome number. Three cytotypes were found during investigation. The population of Dukat results tetraploid with chromosome number 2n = 4 x = 28, while the population of Llogara appears hexaploid with chromosome number 2n = 6 x = 42 (Figure 1).

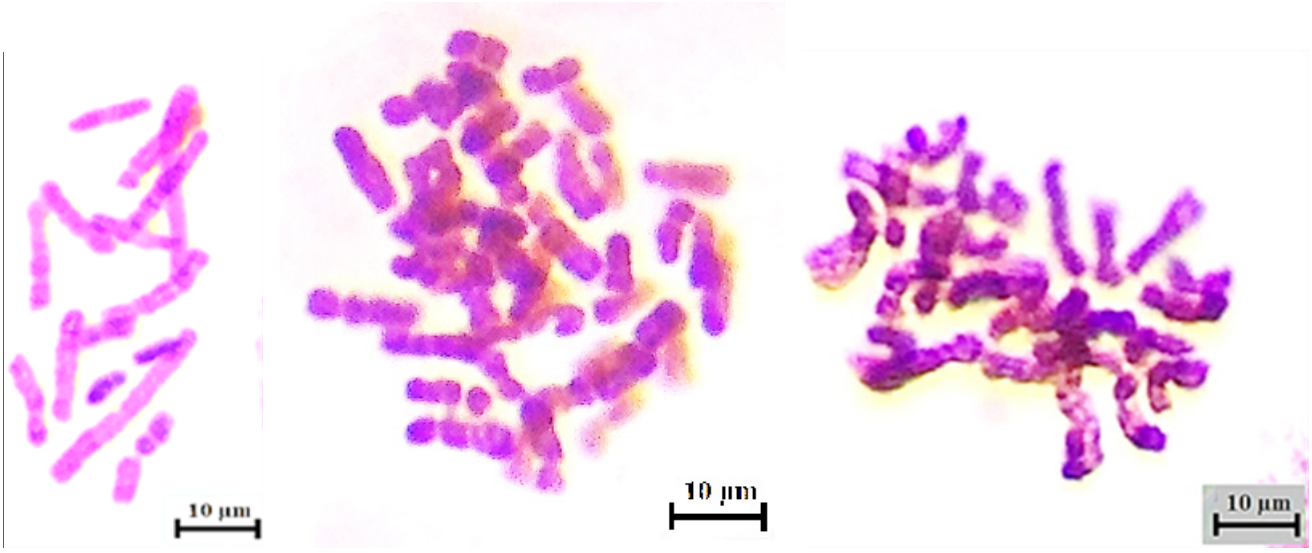

a) b) c)

Figure 1. *S. autumnalis* L. chromosomes: a) Portopalermo; b) Llogara; c) Dukat

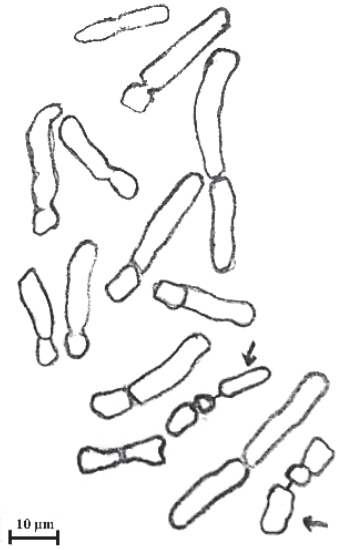

Figure 2. Chromosomes of *S. autumnalis* L. Portopalermo (arrows indicate the presence of satellites)

Chromosome number defined for Portopalermo population was 2n = 2x = 14 and chromosomal formula: 2n = 2x = 5m + $2m^0$ + 3sm + 4st = 14. In this cytotype we encountered a pair of satellites present in the pair of metacentric chromosomes. In the figure 2 appears the chromosome sketch

for population of Portopalermo where arrows indicates the satellites. The (figure 3) shows the karyogram and idiogram of *S. autumnalis* L. Portopalermo. They represent the typology, number and position of satellites in the chromosomal haploid and diploid set.

DATI INSERITI E DATI ELABORATI

Num: 63 **Taxon:** Scilla autumnalis
Scala: 100 **Locus:** Portopalermo
Formula di Levan: 5m + 2m°+3sm + 4st

Id	Lu	Co	Tot	r	S	S1 T1	S2 T2
3	170	120	290	1.42			
13	150	140	290	1.07			
11	150	90	240	1.67			
4	110	80	190	1.38			
10	125	40	165	3.13			
2	125	30	155	4.17			
7	115	35	150	3.29			
9	110	30	140	3.67			
12	65	40	105	1.63		30TC	
14	60	40	100	1.50		30TC	
5	95	40	135	2.38			
6	90	40	130	2.25			
8	80	40	120	2.00			
1	70	45	115	1.56			

A

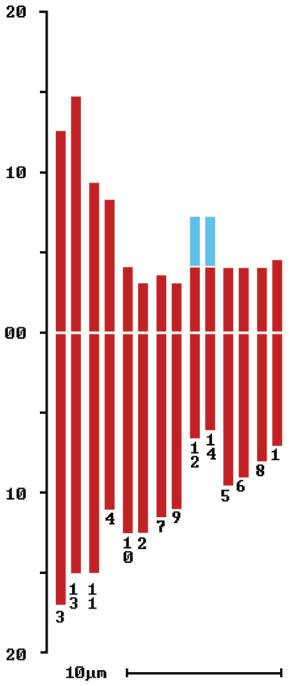

B

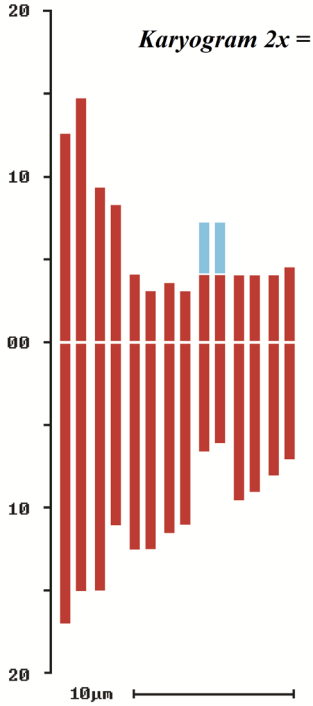

C

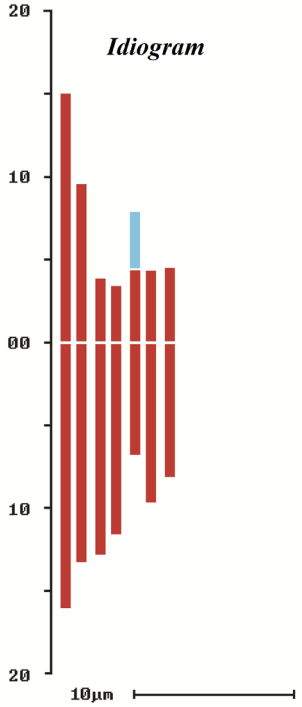

D

Figure 3. *Scilla autumnalis* L. A. Table with data for chromosomes (long arm, short arm, arm ratio, satellite), B. Numerical Karyogram, C. Karyogram, D. Idiogram

During the study, it is noticed that the population of Llogara, which is at higher altitude, has a higher level of ploidy. Many authors reported that elevation increases also the level of ploidy [11; 12]. The phenomenon of chromosome number variability is also related to the resistance of polyploid genotypes to abiotic stress factors (drought and cold) [13], therefore polyploid individuals extend at higher altitudes than diploid individuals. This is in accordance with our results, where individuals of Portopalermo exhibit diploid karyotype, while the populations of Dukat and Llogara located at higher altitudes exhibit poliploid.

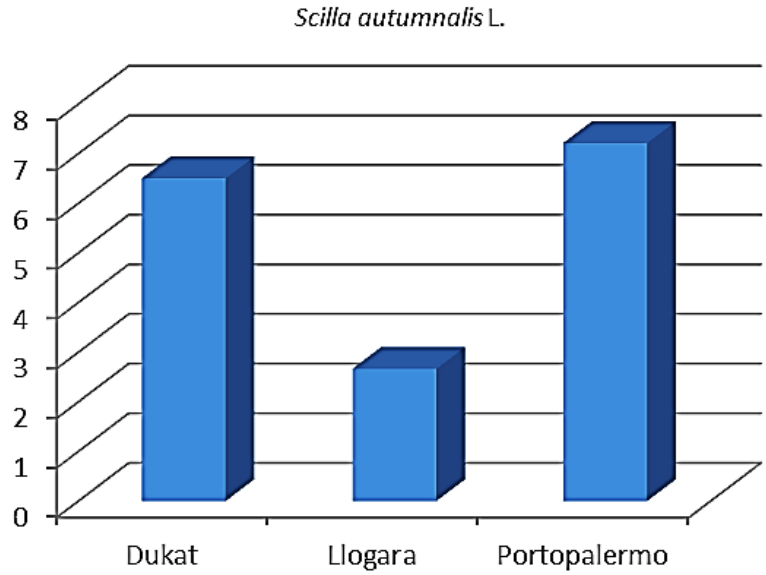

Figure 4. Mitotic index of *S. autumnalis* L. in three habitats

According to the data of other authors, polyploid species exhibit different morphological and physiological traits that allow them to spread in different geographic areas [14; 15; 16]. Usually in many plant species, polyploid individuals are superior to diploid ones in terms of morphological features but in some cases polyploid plants may have slower rates of growth [17] due to slower cell division causing smaller mitotic index. This is in accordance with our results. The population of Llogara with a higher level of ploidy results with a lower mitotic index (Figure 4).

References:

1. Banciu C. M., Mitoi F. Helepcıuc and F. Aldea. In vitro propagation of critically endangered species S. autumnalis biochemical analyses of the regenerants. Fascicula Biol. 2010; 2: 318–323.
2. Battaglia A. Scilla autumnalis L. Biotipi 2n, 4n, 6n e loro distribuzione geografica, Caryologia, 1957; 10, 75–95.
3. Ainsworth C. C., Parker J. S. and Horton D. M. Chromo-some variation and evolution in Scilla autumnalis. KewChrom. Conf, 1983; 11, 26 1–268.
4. Guillen A. and Ruiz Rejon M. Structural variability and chromosome numbers variation in natural populations of Scilla ausumnalis (Liliaceae). Pl. Syst. Evol, 1984; 144, 201–207.
5. Vaughan H. E., Taylor S. & Parker J. S. "The ten cytological races of the Scilla autumnalis species complex."Heredity 79, 1997.– P. 371–379. Doi:10.1038/hdy.1997.170.
6. De-Yuan H. Cytotype variation and polyploidy in Scilla autumnalis L. (Liliaceae) Hereditas 1982; 97: 227–235.

7. Parker S. J, & Lozano Rafael & Taylor S. & Ruiz Rejón,– M. Chromosomal structure of populations of Scilla autumnalis in the Iberian Peninsula. Heredity. (1991). 67. 10.1038/hdy. 1991; 92.
8. Tsuchiya T. Barley genetics newsletter,– Vol. 1. III. Genetic and cytological technique.– P. 71–72.
9. La Cour L. F., Darlington C. D., F. R. S. The Handling Of Chromosomes: 127, London George Allen & Unwin Ltd., 1941.
10. Pavone P. & Salmeri C. Cromo II version 1.1. 1993.
11. Boratynski A. Chronione i godne ochrony drzewa i krzewy polskiej części Sudetów, Pogórza i Przedgórza Sudeckiego. 2. Empetrum nigrum L. s.l. (Protected or deserving protection trees and shrubs from the Polish part of Sudety Mts., Pogórze and Przedgórze Sudeckie region. 2. Empetrum nigrum L. s.l.). Arbor. Kórnickie 1986; 31: 21–37.
12. Xie-Kui C., Ao C. Q., Zhang Q., Chen L. T., Liu J. Q. Diploid and tetraploid distribution of Allium przewalskianum Regel. (Liliaceae) in the Qinghai-Tibetan Plateau and adjacent regions. Caryologia. 2008; 61: 190–198.
13. Yildiz M. Plant Responses at Different Ploidy Levels, Current Progress in Biological Research Marina Silva-Opps, IntechOpen, 2013. DOI: 10.5772/55785.
14. Otto S. P., Whitton J. Polyploid incidence and evolution. Annu. Rev. Genet. 2000; 43: 401–437.
15. Ramsey J., Schemske D. W. Neopolyploidy in flowering plants. Annu. Rev. Ecol. Syst. 33: 2002. 589–693.
16. Borgen L., Hultgard U. Parnassia palustris: a genetically diverse species in Scandinavia. Bot. J. Linn. Soc. 2003; 142: 347–372.
17. Ranney T. G. Polyploidy. From evolution to new plant development. Proceedings of the International Plant Propagator's Society 2006; 56: 604–607.

Section 3. Machinery construction

Vasenin Valery Ivanovitch,
associate professor, candidate of technical sciences,
department of "Materials, technologies and design of machinery"
State National Research Polytechnic University of Perm
E-mail: vaseninvaleriy@mail.ru
Sharov Konstantin Vladimirovitch,
senior teacher

STUDY OF THE GATING SYSTEM OPERATION WITH VERTICAL SLOT GATE

Abstract: The article concentrates on theoretical and experimental study of the gating system (GS) with a vertical slot gate (VSG). This gating system consists of two parts: 1) Pouring basin, sprue, sprue basin and well; 2) VSG and foundry mould. In such system, the liquid is poured from the well into the mould through the VSG. It was found that Bernoulli's equation (BE) is necessary for calculations due to the fact that the time of filling the form with metal is determined by the first system. Calculation technique for such systems has been developed. It was proven that the mould filling time does not depend on the width of the VSG and occurs in the lower section of the VSG at 1/8–1/5 of the gate height. Upwardly extending VSG does not accelerate process of filling the mould with metal.

Keywords: pouring basin, sprue, sprue basin, head, resistance coefficient, flow coefficient, flow velocity, fluid flow rate.

Introduction

Gating systems with VSG have been in used for a long time. However, there are not many studies devoted to the analysis of such systems (examples of such studies are [1–5]). And its main issue has not been addressed: how to calculate the hydraulic characteristics of this system and determine the time when the foundry mould is filled with metal through the VSG. The effect of the width of the gate on the filling time of foundry mould has not been investigated. This article concentrates on the calculated analysis and experimental study of such systems.

Research technique

GS shown in the figure was used for this research. The system consists of a pouring basin, a sprue, a sprue basin, a well, a VSG and foundry moulds. The diameter of the pouring basin is 272 mm, the height of the water in the basin is 103.5 mm. Diameters of the sprue and sprue basin (mm): $d_s = 12.03$, $d_{sb} = 20.08$. The internal diameters of the sprue and sprue basin were adjusted using development drawing. The dimensions of the well are 28 × 47 × 450 mm, the size of the mould is 246 × 254 × 500 mm. The width of VSG varied from 2 to 22 mm; its length and height were 50 and 450 mm. Extending and

tapering upwards slots – 8 × 18 and 17.5 × 8 mm respectively – were also studied. The water level H – the vertical distance from section *1–1* in the basin to section *2–2* (the longitudinal axis of the sprue basin) – was maintained constant by continuously pouring water into the basin and draining its excess through a special slot in the basin: $H = 610$ mm. The filling time in each mould was determined at least 6 times, and the deviation from the average value of the time of filling is ±0.3 s.

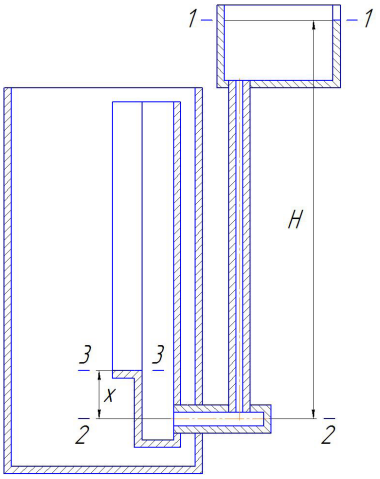

Figure 1. Gating system with a mould and a well

Main body

The table shows that increase in the slot width by 11 times, from 2 mm to 22 mm, had almost no effect on the time of filling the mould with a height of 400 mm. The slots of 2 mm and 4 mm wide differ somewhat, but it must be noted that the entry edges of the slot were not chamfered, and the flow compression in the slots of 2 mm or 4 mm wide is stronger than in other slots.

Table 1.

Slot width, mm	2	4	6	10	14	18	22	8 × 18	17.5 × 8
Filling time, s	154.8	153.9	150.8	150.1	151.6	150.7	150.9	151.6	152.1

Let us analyse the effect of slot height on flow quantity. For example, for a slot of 10 mm width and 10 mm height, the mould filling time is 196.2 s, 20 mm – 170.5 s, 30 mm – 159.6 s, 50 mm – 154.1 s. This means that the filling of the mould happens in the lower 50 mm of the slot – in 1/8 of the height of the slit – and the remaining 9/10 of the height does not affect the filling time. Other sizes of slot have approximately same results, and size of the slot no longer influences the filling time when its area is 250–350 mm^2.

The filling time of mould without a well is 153.7 s. And if the diameter of the sprue is increased from 12.03 to 24.08 mm, then the filling time will decrease by more than 3 times: to 44.4 s.

How can all of this be explained? In fact, there are two hydraulic systems. Flow is determined by the system that consists of a pouring basin, a sprue, a sprue basin, and a well. The second system consists of an VSG and a mould. And the liquid is poured from the well through the VSG into the mould. Liquid surface in the well is affected by atmospheric pressure acts (it is a free surface), and only first hydraulic system can be calculated using BE.

The fluid fills the well up to the filling point. In this case, the BE for section 1–1 and section 3–3 (liquid level at the bottom of the gate) will be in accordance with the recommendations of R. R. Chugaev [6, p. 216]:

$$H - x = h_{1-3}, \qquad (1)$$

x – is the vertical distance between sections 2–2 and 3–3, m; h_{1-3} – is head loss when fluid flows from section 1–1 to section 3–3, m. As seen from (1), the difference in head $H-x$ is consumed on head losses – h_{1-3}. Those head losses can be deduced to the following equation:

$$h_{1-3}=\left(\zeta_s+\lambda\frac{l_s}{d_s}\right)\alpha\frac{v_s^2}{2g}+\left(\zeta_{sb}+\lambda\frac{l_{sb}}{d_{sb}}\right)\alpha\frac{v_{sb}^2}{2g}+$$
$$+\left(\zeta_w+\lambda\frac{x}{d_w}+\zeta_{out}\right)\alpha\frac{v_w^2}{2g}, \qquad (2)$$

ζ_s, ζ_{sb} and ζ_w – are coefficients of local resistances of the metal entrance from the pouring basin to the sprue, on the turn and expansion of the flow from the sprue to the sprue basin, on the turn and expansion of the flow from the sprue basin to the well; λ – is coefficient of friction loss; l_s, l_{sb} – are the length (height) of the sprue and the length of the sprue basin, m; d_s, d_{sb}, d_w – are hydraulic diameters of the sprue, sprue basin and well, m; α – is the coefficient of uneven distribution of velocity over the cross section of the flow (Coriolis coefficient); we consider $\alpha=1.1$ [6, p. 108]; v_s, v_{sb}, v_w – are fluid velocities in the sprue, sprue basin and well, m/s; g – acceleration of gravity, $g=9.81$ m/s^2; ζ_{out} – is the coefficient of local resistant at metal outlet of well into VSG, the shape and section of the well, located above its bottom; $\zeta_{out}=1$ [6, p. 187].

Head losses can be deduced to any of three velocities: velocity in the sprue – v_s, velocity in the sprue basin – v_{sb} or velocity in the well – v_w. It is easier to do this for velocity in the sprue basin – v_{sb}. Flow continuity equation is as follows:

$$Q=v_sS_s=v_{sb}S_{sb}=v_wS_w. \qquad (3)$$

Using the flow continuity equation (3), we obtain the following equation from (1) and (2):

$$H-x=\alpha\frac{v_{sb}^2}{2g}\left[\left(\zeta_s+\lambda\frac{l_s}{d_s}\right)\left(\frac{S_{sb}}{S_s}\right)^2+\zeta_{sb}+\right.$$
$$\left.+\lambda\frac{l_{sb}}{d_{sb}}+\left(\zeta_w+\lambda\frac{l_w}{d_w}+\zeta_{out}\right)\left(\frac{S_{sb}}{S_w}\right)^2\right]. \qquad (4)$$

Let us denote the ratio in square brackets as $\zeta_{1-3(sb)}$ which is the coefficient of resistance of the system from section 1–1 to section 3–3, reduced to the fluid velocity in the sprue basin – v_{sb}. (1) can be deduced to:

$$H-x=\alpha v_{sb}^2\zeta_{1-3(sb)}/2g. \qquad (5)$$

And the flow rate coefficient of the system from section 1–1 to section 3–3, reduced to velocity – v_{sb},

$$\mu_{1-3(sb)}=\zeta_{1-3(sb)}^{-1/2}. \qquad (6)$$

Velocity in the sprue basin with fluid at the level of the cross section of 3–3,

$$v_\kappa=\mu_{1-3(sb)}\sqrt{2g(H-x)/\alpha}. \qquad (7)$$

Flow rate Q is calculated by (3).

When filling the well to a height of 400 mm, the head changes from $H-x$ to $H-x-0.400$. The calculated head is found by the following formula: H $\sqrt{H_c}=\left(\sqrt{H-x}+\sqrt{H-x-0{,}400}\right)/2$. This is an exact formula for calculating the filling of a mould with a constant cross section height. And the velocity is determined by the following formula: $v_{sb}=\mu_{1-3(sb)}\sqrt{\frac{2g}{\alpha}}\frac{\sqrt{H-x}+\sqrt{H-x-0.400}}{2}$.

Length of the sprue basin: $l_{sb}=0.0925$ m, its size $x=0.046$ m. We consider (as in [7; 8]) that the coefficient of friction loss is $\lambda=0.03$. The coefficient of local resistance of the entrance from the basin to the sprue (depending on the chamfering radius of the entry edge) is determined by [9, p. 126]: $\zeta_e=0.12$. And the coefficients of local resistance on the turn and expansion of the flow are found by the formulas of [10]: $\zeta_{sb}=8.156$, $\zeta_w=18.952$. Calculations results: $\sqrt{H_c}=0.578$ m$^{1/2}$, $H_c=0.334$ m, $\zeta_{1-3(sb)}=20.429$, $\mu_{1-3(sb)}=0.221$, $v_{sb}=0.540$ m/s, $Q_{sb}=171.03$ cm^3/s. Mould filling time is 146.29 s; experimental result is 151 seconds. The difference is 3.1%, which is a very satisfying result for a process of such complexity.

Results and discussion

It is evident that the mould filling time does not depend on the width of the VSG and occurs in the lower section of the VSG at 1/8–1/5 of the gate

height. Which is very unexpected and even curious. However, simple experiments with a stopwatch to determine filling time and constant height of mould give us no reason to doubt the results.

Flow is determined by the system that consists of a pouring basin, a sprue, a sprue basin, and a well. The second system consists of a VSG and a mould. And the liquid is poured from the well through the VSG into the mould. Liquid surface in the well is affected by atmospheric pressure acts (it is a free surface), and only first hydraulic system can be calculated using BE. It was found that the mould filling time is determined by the first system and it is crucial to calculate it. Calculation technique for such systems has been developed. We calculate velocity and flow rate of the fluid in the collector when filling the mould through the VSG up to the filling point, given that the head difference is spent on the head loss when the fluid flows from the level in the pouring basin to the bottom of the gate.

It is known from practical experience that sometimes freezing of the metal in the upper section of the slot can occur. And it is necessary to increase the width of the slot, or make an upwardly extending slot. Liquid may freeze due to lack of movement in most parts of the slot. Expansion of the slot can prevent this event, even if it does not affect the filling time.

Conclusion

In summary, research technique for GS with VSG was created and a theory has been developed for system calculation. It has been established that the filling of the mould does not depend on the width of the VSG and it occurs in the lower section of the VSG. Upwardly extending VSG does not accelerate process of filling the mould with metal.

References:

1. Дубицкий Г. М., Токарев Ж. В. Действие вертикально-щелевой и ступенчатой с обратным стояком литниковых систем при истечении жидкости под затопленный уровень // Проблемы литейного производства.– Пермь: изд-во ЦБТИ, 1960.– С. 57–66.
2. Поручиков Ю. П., Топоров В. Д. Вертикально-щелевые литниковые системы с обратным стояком // Литейное производство. 1968.– № 5.– С. 4–6.
3. Василевский П. Ф. Технология стального литья.– М.: изд-во «Машиностроение», 1974.– 408 с.
4. Зарубин А. М., Зарубина О. А. Исследование работы вертикально-щелевой литниковой системы при литье в кокиль // Литейное производство. 2017.– № 10.– С. 27–30.
5. Дудченко А. В. Об оптимизации конструкции щелевого питателя для ускоренной заливки форм // Литейное производство. 2018.– № 4.– С. 19–21.
6. Чугаев Р. Р**.** Гидравлика.– М.: изд-во «Бастет», 2008.– 672 с.
7. Токарев Ж. В. К вопросу о гидравлическом сопротивлении отдельных элементов незамкнутых литниковых систем // Улучшение технологии изготовления отливок.– Свердловск: изд-во УПИ, 1966.– С. 32–40.
8. Jonekura Koji (et al.) Calculation of amount of flow in gating systems for some automotive castings // The Journal of the Japan Foundrymen's Society. 1988.– Vol. 60.– No. 8.– P. 326–331.
9. Идельчик И. Е. Справочник по гидравлическим сопротивлениям.– М.: Машиностроение, 1992.– 672 с.
10. Васенин В. И., Васенин Д. В., Богомягков А. В., Шаров К. В. Исследование местных сопротивлений литниковой системы // Вестник Пермского национального исследовательского политехнического университета. Машиностроение, материаловедение. 2012.– Т. 14.– № 2.– С. 46–53.

Section 4. Medical science

Vashuk Mykola Anatoliiovych,
associate professor of Physiology department, Ph D.,
Kharkiv National Medical University
E-mail: physiologykhnmu@ukr.net
Chesnakova Daria Dmytriivna,
student of 4th year
Kharkiv National Medical University
E-mail: liza-somkina@mail.ru
Somkina Yelizaveta Artemivna,
student of 4th year
Kharkiv National Medical University
E-mail: liza-somkina@mail.ru
Hloba Nataliia Serhiivna,
assistant of physiology department
Kharkiv National Medical University
E-mail: tsarenkons@gmail.com

PECULIARITIES OF SLEEP AS POSSIBLE RISK FACTOR OF OVERWEIGHT IN YOUNG PEOPLE

Abstract: The article features the importance of regimen of sleep and its impact on human organism. The relationship between sleep peculiarities and weight changes were pointed out. The mechanisms providing weight gaining are explained. The original research data on weight changes related to peculiarities of sleep are provided. Importance of sleep and working regimen and further prospects of such studies are shown.

Keywords: sleep and working regimen, overweight, obesity, young people, medical students.

Background. During last years the problem of obesity in people of all ages all around the world not only doesn't diminish, but continues to increase, leading to of worsening of health of world population. According to statistics, about 30% of adult people aged 20 years and more have obesity [4, 166]. Potential risk factors that may cause overweight and obesity include various biological and genetic causes, cultural, social and environmental factors [4, 172–173]. Among such risk factors, especially for children and adolescents, many scientific researches consider sleep disorders [1, 137–138]. Studies showed that the probability of overweight and obesity increases twice in children and adolescents with shorter sleep duration [1, 145]. Results of many researches and cross-sectional studies show that around 30–35% of adults suffer from disorders of sleep,

and at least 10% of the population suffers from a sleep disorder that is clinically significant [3, 63]. Furthermore, many of sleep disorders are greatly underdiagnosed by both patients and their doctors [3, 67]. In last decades studies about biological clock of human organism and its influence on processes of substances exchange increase their popularity and importance, focusing especially on carbohydrates and lipid exchange and trying to reveal the connection between sleep disorders and excessive weight problems [6, 132–133; 8, 26–28; 2, 12472]. As the basis of weight increase lies in energy imbalance, i.e. significant difference between intake and expenditure of energy, that is controlled by circadian rhythms of the body, changes of those rhythms provide appearance of weight variations [1, 146]. Setting of biological rhythms is provided by hormones and biological active substances that have daily dynamics based on duration and phases of sleep. Sleep disorder causes disturbance of production of biologically active substances in hypothalamus and epiphysis that leads to changes of exchange processes in young organism [2, 12472; 7, 17; 8, 27]. As young people, and especially students, have excessive psychic and emotional loads together with improper regimen of work and rest in many cases, the interest to this topic arises. There is also a lack of data regarding sleep habits among students in Ukraine, even though quality and quantity of sleep greatly influences concentration ability and memorization that are necessary for academic achievements of students, thus proving the importance of such studies.

The aim of current research was to study the connection between sleep disorders and increase of body weight in students. The tasks set for that aim included determination of category of student with sleep disorders, estimation of peculiarities of their diet, evaluation of dynamics of student physical development during last 3 years, and determination of interrelation of sleep disorders and possible body mass change.

Materials and methods of research. In current study participated 150 students of Kharkiv National Medical University aged 18–22, including 70% of young woman and 30% of young men, all participants gave written consent to take part in research. The survey was made using a questionnaire that included questions about quality and duration of sleep, availability of insomnia or other sleep disorders, esteem of peculiarities of diet. Big attention was paid to time of falling asleep as one of factors influencing production of hormones.

Research results and their discussion. Analysis of results allowed us to divide all examined students into groups according to established manner of lifestyle and habits. 1st group included 25% of young people with well-determined sleep regimen, i.e. falling asleep before 22.00, sleep duration of 7–8 hours, without night awakening episodes and insomnia. Together with sleep regimen, people of 1st group showed strict dieting habits with last intake of food not later than 3 hours before sleep time. As a result, no significant body weight variations were detected in them during last 3 years. Wholly satisfactory level of physical development in persons of 1st group with stability of body weight can be explained by simultaneous established diet habits and sleep regimen, that leads to maintenance of levels of hormones influencing exchange processes.

The 2nd group consisted of 38% of people with significant changes of sleep and dieting characterized by insomnia, night awakening episodes, late falling asleep time (after 1 AM), food intake at night and directly before sleep. The increase of body weight was determined in that group together with worsening of general health state and decreased working ability. Body weight changes may be related to disruption of biological rhythms as during some particular phases of sleep hormones leptin and ghrelin are produced that have antagonistic effect on centers of hunger and satiety in hypothalamus [6, 132–133; 2, 12472]. In people with sleep disorders the increase of ghrelin level and decreased leptin production is determined

that causes overeating and body weight increase [7, 17]. Moreover, thyroid stimulating hormone (TSH) also obeys circadian rhythms with peak production in the evening between 23.00 and 04.00. Therefore, late falling asleep time causes decreased TSH secretion leading to disorder of basal metabolism, decrease of lipolysis and activation of lipogenesis [5, 13–15; 7, 17]. Sleep disorders and further decrease of hormones secretion together with improper dieting becomes the base of significant body weight increase during examined 3 years.

The other 37% of examined people who have balanced diet, however, disturbed sleeping regimen, constituted 3rd group. Excessive load and time deficiency due to studying process make persons of that group to sleep for 4–5 hours per day and change their falling asleep time to later hour, thus causing feeling of fatigue and sleepiness during the day. Furthermore, even though there is strict control of feeding habits in people of 3rd group, the increase of weight still occurs. That fact proves the theory of direct connection existing between sleep disorders and continuing body mass increase in students. Massive researches of last decade showed that decrease of sleep duration by 1 hour causes increase of body mass index on 0.35 kg/m^2 [8, 30–31]. Therefore, the maintenance of stable normal body weight is possible only in case of combination of healthy diet with adequate regimen of sleep. Moreover, the situation with sleep duration may be even worse as self-reports on sleep usually exceed real sleeping time on 0.3–1.3 hours in average [1, 146].

Conclusions. The significance of sleep and circadian rhythms for human health is hard to overestimate. Many current researches and scientific societies aim at studying of those features, and one of problems that make them so important is that sleep deficiency and sleep disorders work as a stress factor for human organism that increases risk of overweight and obesity development, starting from childhood and adolescence up to old age. Disturbances of different phases of sleep lead to changes of carbohydrates and lipid metabolism and hormonal imbalance of the body. Current study proves the importance of maintenance of balanced diet and rest and the necessity to continue the research of influences of biological rhythms as the cause and the target of body metabolism changes. Further prospects of researches in that area should also be aimed at development of means of correction of sleep and working regimen of young people including students for prevention of possible negative outcomes.

References:

1. Fatima Y., Doi S. A. R., Mamun A. A. Longitudinal impact of sleep on overweight and obesity in children and adolescents: a systematic review and bias-adjusted meta-analysis // Obesity Reviews. 2015.– T. 16.– No. 2.– P. 137–149.
2. Fernández Vázquez G., Reiter R. J., Agil A. Melatonin increases brown adipose tissue mass and function in Zücker diabetic fatty rats: implications for obesity control // Journal of pineal research. 2018.– T. 64.– No. 4.– P. e12472.
3. Ram S. et al. Prevalence and impact of sleep disorders and sleep habits in the United States // Sleep and Breathing. 2010.– T. 14.– No. 1.– P. 63–70.
4. Williams E. P. et al. Overweight and obesity: prevalence, consequences, and causes of a growing public health problem // Current obesity reports. 2015.– T. 4.– No. 3.– P. 363–370.
5. Диханова З. А., Мухаметжанова З. Т., Искакова А. К., Алтаева Б. Ж., Мукашева Б. Г. Влияние климата на организм человека // Гигиена труда и медицинская экология. 2017.– № 1(54).– С. 11–15.
6. Кельмансон И. А. Экологические и клинико-биологические аспекты нарушений циркадианных ритмов сон-бодрствование у детей и подростков // Междисциплинарный научный и прикладной журнал «Биосфера». 2015.– Т. 7.– № 1.– С. 131–142.

7. Мисникова И. В. Нарушения углеводного обмена в рамках метаболического синдрома: диагностика и лечение // Поликлиника. 2016.– № 1–2.– С. 17–20.
8. Струева Н. В., Мельниченко Г. А., Полуэктов М. Г., Савельева Л. В.. Эффективность лечения ожирения у больных с инсомнией и синдромом обструктивного апноэ сна // Ожирение и метаболизм. 2016.– Т. 13.– № 2.– С. 26–32.

Section 5. Food processing industry

Myrtaj Anisa,
Wastewater Treatment PhD., candidate
Department of Chemistry, Faculty of Technical Sciences
University of Vlora, Albania
E-mail: anisarexhepi87@gmail.com
Malollari Ilirjan,
Academic Asoc. Prof. Dr.
Department of Industrial Chemistry,
Faculty of Natural Science, University of Tirana, Albania

PHYSIOCHEMICAL CHARACTERIZATION OF WASTEWATER FROM FRUIT JUICE AND BEVERAGE DRINK INDUSTRY IN ALBANIA

Abstract: One of the main sources of surface water pollution in our country besides urban discharges are industrial ones, which contain organic substances, soluble phosphorous and nitrogen compounds, which favor the eutrophication process. In order to make an accurate assessment of the water quality condition, were determined various physical and chemical parameters of the wastewaters from the fruit juice and beverages industry in Albania. In this sense, the importance of this paper is the assessment of the quality of the discharge waters and the determination of the main pollutants that are discharged into the receiving waters, with the aim of protecting and/or rehabilitating the environment.

Keywords: Biological oxygen demand, suspended solids, nitrogen, phosphorus, wastewater.

I. Introduction: This study provides a review of the physiochemical characterization of the parameters applied to individual wastewater streams or to final effluent to reduce pollutant discharges to surface waters in Albania. Wastewater generated by food industry are typically characterized as having high concentrations of organic pollutants including biochemical oxygen demand, fats, oils, grease, suspended solids, and nutrients such as nitrogen and phosphorus. Other pollutants may be present depending on the specific nature of the raw materials and processing operations [8; 9].

The food-processing sector in Albania includes facilities that process dairy products, meat, poultry, grain, oilseed, fruits, vegetables, and beverages [10]. The majority of these facilities discharge untreated or partially treated wastewater into municipal sewage treatment systems for final treatment before being discharged to the environment.

Wastewater treatment technologies can be broadly categorized as: 1) primary treatment aimed at removal of floating and settleable solids); 2) secondary treatment for removal of organic material and; 3) tertiary treatment for removal of nitrogen, phosphorus

or suspended solids. Primary treatment includes technologies such as screening, flow equalization, gravity separation, and dissolved air flotation. Secondary treatment typically includes various configurations of aerobic or anaerobic biological systems. Tertiary treatment includes both biological and physiochemical treatment technologies [11; 12].

Food processors that discharge to municipal sewer typically employ primary treatment as a minimum level of treatment, whereas facilities that discharge directly to surface waters or land use primary and secondary treatment [10].

A common approach is to regulate direct dischargers in the food industry using legislation and regulations. Criteria used in establishing permit limits and conditions are based on receiving water impacts [1].

The beverage industry consists of four different sectors; soft drink manufacturers, distillers, brewers and wineries. The industries can be considered as operating in non-alcoholic and alcoholic beverages.

II. Materials and methods:

The beverage industry has different wastewater issues for each different product. Wastewater volumes of "soft drink processes" are lower than in other food-processing sectors, but fermentation processes are higher in BOD and overall wastewater volume compared to other food-processing sectors.

Fruit and Vegetable Manufacturing sector typically generates large volumes of wastewater with high organic loads from wash water, skins, rinds, pulp, and other organic waste from fruit and vegetable cleaning, processing, cooking and canning. The wastewater may contain cleansing agents, salt, and suspended solids such as fibres and soil particles.

In this study we provide information that can be used to develop a characterization plan for Albania food processor wastewater discharges. This includes: the nature and impact of contaminants that may be present in food processing wastewater; the selection of wastewater and solid waste parameters for characterization; preservation and storage of samples; analytical methods.

The scope for the study was established by the following objectives, which were to:

- Present an overview of the food wastewater processing industry in terms of its environmental impacts.
- Develop a list of wastewater parameters that may be used to characterize food processor effluent.
- Summarize the characteristics of wastewater discharges from the various food processing industry.

Samples were analyzed for total suspended solids, total dissolved solids content (TDS), nitrogen, and phosphorus content in accordance with the standard method. pH and conductivity are measured with the aid of the digital pH meter, and the digital conductivity meter. Nitrogen determination was performed by standard spectrometric method. The maximum test portion volume is 40 ml. For samples with high nitrogen concentrations, smaller volumes of the test portion are collected and diluted to 40 ml with water.

Definition of phosphorus – E. We use the Ascorbic Acid Method were Ammonium molybdate and potassium antimonyl tartrate react in acidic orthophosphate environment to form acid-phospho-acidic acid heteropoly-reduced in intensive blue molybdenum color in the presence of ascorbic acid.

Determination of the chemical oxygen demand index (ST-COD) – Small scale method with closed tubes (test kits). The method determines the chemical need for oxygen (ST-COD) using the closed tube method (test kit). Testing is empirical and applicable to any wastewater, which includes all contaminated water.

Determination of biochemical oxygen demand after n day (BODn) – Method of allylthiourea. BOD_5 was measured by the photometry method and the Oxi-top measurement system. Incubation times are 5 days – as in ISO 5815.

III. Results and discusion

The increase in the number of production activities in the field of industry and agriculture has significantly contributed to the increase of polluting factors in the environment and in particular to

the level of pollution in surface waters at significant levels as a result of the increase of these untreated discharges [2; 3; 4].

In this sense, it is important to estimate the quality of surface water and determine the main pollutants that are discharged into them.

Table 1.– Results of wastewater discharge from beverage drink and friut juice

Analyzed parameters	Unit	Value Case 1	Value Case 2	Value Case 3	Value Case 4	Allowed value
pH	–	7.89	5.52	8.72	7.41	6–9
Temperature	^{0}C	1.4	0.5	4.21	3.83	+/–3 °C
COD	mg/L	29	13	26	1000	250
BOD_5	mg/L	13	7	16	419	50
Suspended solid	mg/L	6	5.9	2.8	1411	50
N-total	mg/L	1.1	0.79	–	–	10
P-total	mg/L	0.37	0.32	–	–	5
Oil and grease	mg/L	1.13	0.75	–	–	10

(case 1–2 brewers, 3 distillers, 4 fruit juice)

To make an accurate assessment of the water quality status, different parameters were measured and compared with the allowed values.

The goal of this study is to determine the pollutants caused by anthropogenic activity in the aquatic environment, their impact and risk.

Water quality assessment and comparison of levels of chemical parameters with norms presents difficulties. However, some standards for industrial water discharges are still in force, according to the Council of Ministers Decision, no. 177 dt 31.03.2005.

At each sampling point it was measured the water temperature, pH, suspended matter, dissolved oxygen and also the approximate assessment of nitrogen, phosphorus, chemical oxygen demand, and biological oxygen demand. The first three companies exhibit low parameter values as they perform a primary treatment prior to discharge while the fourth company discharge them directly to the receiving water. They are working on the construction of a wastewater treatment impiant. In our study the monitoring objective was academic (academic) and it included the local area of the city of Tirana and its suburbs.

References:

1. Vendimi i Keshillit te Ministrave – No. 177; dt 31.03.2005.
2. Mathur B. S. The pollution of water resources due to rural industrial waste. Chemistry and Chemical Engineering Department of the Indian Institute of Technology, – Delhi, India, 2005.
3. EEA (European Environment Agency). Europe's Environment: The Second Assessment.
4. International Review for Environmental Strategies,– Vol. 4.– No. 2. 2003. ISSN1345–759.
5. APHA, AWWA, WPCF (ed) Standard Methods for the Examination of Water and Wastewater, 16th ed. American Public Health Ass., Washington D. C. 2005.
6. Robert A. Corbitt, Standard Handbook of Environmental Engineering, Second Edition.
7. British Columbia Ministry of Water, Land and Air Protection. Environmental Protection Division. 2004. Waste Discharge Regulation Implementation Guide (Draft). July 26, 2004.

8. Food Manufacturing Coalition for Innovation and Technology Transfer. 1997. Great Falls, VA, State-of-the-Art Report: Biological Oxygen Demand (BOD) and Nutrient Removal From Food Processing Wastewater, March, 1997.
9. Food Manufacturing Coalition for Innovation and Technology Transfer. 1997. Great Falls, VA, State-of-the-Art Report: Wastewater Reduction and Recycling in Food Processing Operations, March 1997.
10. Anisa Myrtaj (Rexhepi), Ilirjan Malollari, Luljeta Pinguli: "Biological treatment and best management practices on food industry wastewater in Albania", 4th International Scientific Conference ERAZ 2018: "Knowledge Based Sustainable Economic Development".
11. Anisa Myrtaj (Rexhepi), Ilirjan Malollari. "Biological Remuval of Nitrogen and Phosphorus using Activated Sludge Treatment in Meat Processing Wastewater", International Journal of Engineering Research and Science,– Vol. 4.– Issue 8.– August, 2018.– P. 38–41. ISSN2395–6992. Impact Factor 5.716.
12. Anisa Myrtaj (Rexhepi), Ilirjan Malollari, Luljeta Pinguli, Dhurata Premti. "Design of a meat Processing wastewater anaerobic digester", Europian Journal of Engineering and Technology,– Vol. 6.– No. 3. 2018.– P. 13–17. ISSN2056–5860.

Section 6. Technical sciences

Bukleshev Dmitry Olegovich,
graduate student of Life Safety department,
Federal State Budgetary
Educational Institution of High Education
"Samara State Technical University"
Sumarchenkova Irina Aleksandrovna,
PhD., candidate in Chemical Sciences,
associate professor of Life Safety department
Federal State Budgetary
Educational Institution of High Education
"Samara State Technical University"
Buzuyev Igor Ivanovich,
PhD., candidate in Technical Sciences,
associate professor of Life Safety department
E-mail: bukleshev_dima@mail.ru

ANALYSIS OF METAL STRESS AND DEFORMATION DISTRIBUTION IN WELD-AFFECTED ZONES AT MAIN GAS PIPELINES

Abstract: Pipeline operational integrity directly depends on the quality of technical diagnosis the scope of which includes accounting and analytical estimation and technical state prediction. Technical diagnosis result mainly depends on analysis completeness and quality obtained in the course of result inspecting. This, in turn, depends on the existing relevant regulations, evaluation techniques and other materials which allow to thoroughly estimate negative influence of all the defects revealed.

Keywords: main pipeline, stress, weld-affected zones, cracking, a stress-corrosion damage.

Introduction

The most important component of the power industry in the Russian Federation is pipeline systems. Their basic goal is to ensure faultless and safe oil and gas transit from supplying countries to import countries and to supply domestic consumers with the products. Main pipelines are the most economic type of hydrocarbon transport. Their total length in Russia is more than 200 thousand km. They are high-risk facilities the accidents at which can lead to irrecoverable losses of a transported product, to pipeline, fitting and equipment damage, farmland, forest destruction owing to the fires and explosions at gas pipelines, thermal injuries for people and excessive pressure of an air shock wave. Accident hazards are defined by the factors accompanying the pumping process and dangerous properties of pumping environment. Dangerous production factors include:

pipeline breakdown or breakdown of its elements which is followed by metal and soil fragment dispersion; product ignition at pipeline breakdown, open flame and fire thermal impact; air-gas mixture explosion; collapse and damage of buildings, constructions, installations; lowered concentration of oxygen; smoke, emission toxicity of product constituents.

The major factor defining freedom from accidents and pipeline operational safety is its technical condition. Monitoring technical condition and timely defect detection is carried out by the line maintenance service.

One of the reasons for pipeline accidents is stress-corrosion failure (SCF). SCF problem at main pipelines entered into the world agenda as one of the main reasons for pipe body breakdown. However, due to essential complexity of SCF emergence, the mentioned phenomenon is insufficiently studied today and therefore not all the factors influencing it are thoroughly considered when determining potentially hazardous areas. Along with general regularities, SCF has considerable number of specific features which are common for a specific pipeline being studied (resistance of a concrete steel type to stress corrosion, chemical characteristics of external pipe environment, pipeline operation regulations and its structural features, stress in pipeline seams and a weld-affected zone).

According to the literature sources and the research results, one of the main conditions for stress corrosion crack formation is stress which occur in a pipe body near concentrators (these include welded seams) and exceed material yield limit. According to the authors, apart from other factors (corrosion environment, relief, assembly conditions, weights, etc.) which are common to all pipes irrespective of the way and place of their production, emergence of rather essential local additional stresses is caused by geometrical form weaknesses of double-seam pipes which are generally laid at the production stage [6].

Failure causes analysis of pipeline welded designs

It is known that sites of metal structure breakdown, including main pipelines, most often occur near the welded joints [1]. Apart from the defects in metal resulting from welding due to various deviations from the set standards and specification requirements and considerable internal stresses which are created in metal in the course of welding near the welded seams, the reason for it is the fact that the metal changes its structure and its physical and mechanical properties accordingly in the course of welding [3].

Stress states and corrosion are the main reasons for accidents at the main and distribution steel pipelines. Eventually, there is a change of remanent magnetization, usually occurring in these sites along with stress state formation in metal [2].Pipeline operation practice shows that the main sources of damage during main pipeline operation are local stress zones – local corrosion, stress-crack corrosion (SCC) and deformation resulting from joint assembly, which are formed under the working loads [4].

Corrosion cracking of pipe steel

Currently, stress-crack corrosion (SCC) is the most common cause of failures at line segments of main pipelines. Corrosive medium influence, temperature, work load fluctuation and stresses gradually change the structure and properties of the operated pipe metal in comparison with initial properties. Repeatedly static loads in case of geometrical (a welded seam, mechanical damages of a pipe surface, corrosion damages) and structure heterogeneity (grain boundaries, nonmetallic inclusions) lead to inevitable metal damages due to accumulation of irreversible microplastic deformations.

Increase in dislocation concentration and damage accumulation is the first stage of failure, the subsequent stages of which are microcrack initiation, their stable growth and spontaneous breakdown. Failure processes are intensified in double plastic deformation zones caused by pipe production technologies (welding crimping and subsequent calibration), cold bending sites, pipelaying with compulsory assembly bending, pipeline deformations caused by geophysical processes [1].

Failure causes analysis of pipeline welded designs at pipeline operation

When loads influence a pipe metal, there is predisposition to accumulate and form stress concentration zones (SCZ) [9]. Stress concentration implies local stress increase in zones of sudden alternation of cross-section of a deformable body. In WAZ, such concentrators include welding production defects, openings, pores, inclusions, cuts and others. Stress concentration in welded joints is defined by the overall structure of joint elements, geometrical form of the pipeline seam welded to basic metal, and by transmission mode and welding energy. Regarding pipelines, such concentrators by all means include ring butt joints. In addition, the peculiar fact is that residual stress exists and is counterbalanced in pipe material without extra external loads. SCZs are caused by the total contribution of all heredity forms accumulated at rolled sheet production, pipe production, assembly welding installation and welding at a pipeline construction and changes in structure and metal properties which gradually accumulate them.

With the raise of stress gradient, as it happens near crack-like defects, separate structural elements, such as subgrains, separate grains which have various focuses in relation to power flow, grain boundaries, etc. begin influencing stress distribution. It leads to the fact that metal inhomogeneity contributes to stress raise. In small volumes of real constructional materials with a crystal structure, material isotropy, uniformity and continuity conditions are violated. Due to various orientations of separate structural components, stress distribution can't be smooth in case of small volumes of a real material. Therefore, structural microinhomogeneity of a real material is shown in the form of its deformation heterogeneity.Nowadays, development of nondestructive methods to define a metal structural condition and assess the changes in stressed-deformed state (SDS) of a product at operational loads is actively carried out, but the majority of these works do not consider the fact that even at the manufacturing stage and when transporting a pipe to the assembly site and at assembling immediately the pipe can be in a state of additional plastic strain.

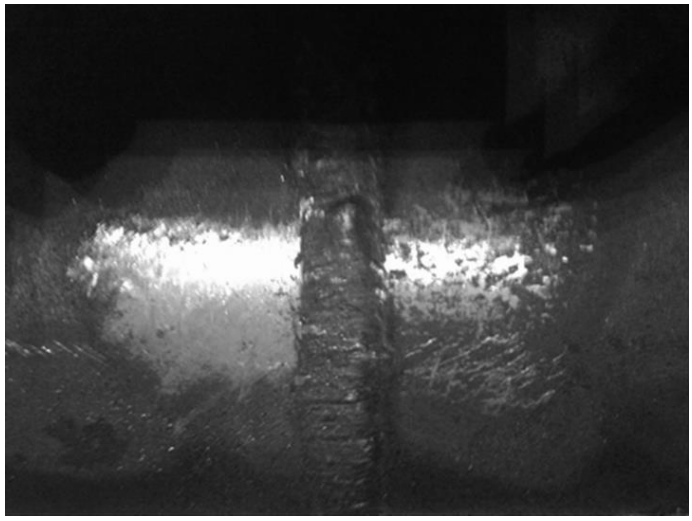

Figure 1. A sample of the main gas pipeline section (a section of welded joints at Central Asia-Center main gas pipeline, 09GSF steel, DN is 1420 mm, Brinnel hardness number, HRB = 110)

Three zones are usually distinguished in welded designs: basic metal, welded seam and weld-affected zone (WAZ). Fig. 2 presents the scheme of a heat-affected zone structure when welding a single-layer butt joint in structural steels [4]. At the same time, as the listed zones differ in structure, physical and mechanical properties and residual stress level, material of various welded design sites will differently react to the applied load effect in the course of production, transporting, assembling and operation.

Respectively, prior plastic deformation will differently affect behavior of metal magnetic characteristics at various sites of a pipe welded joint at their subsequent elastic deformation [4; 5].

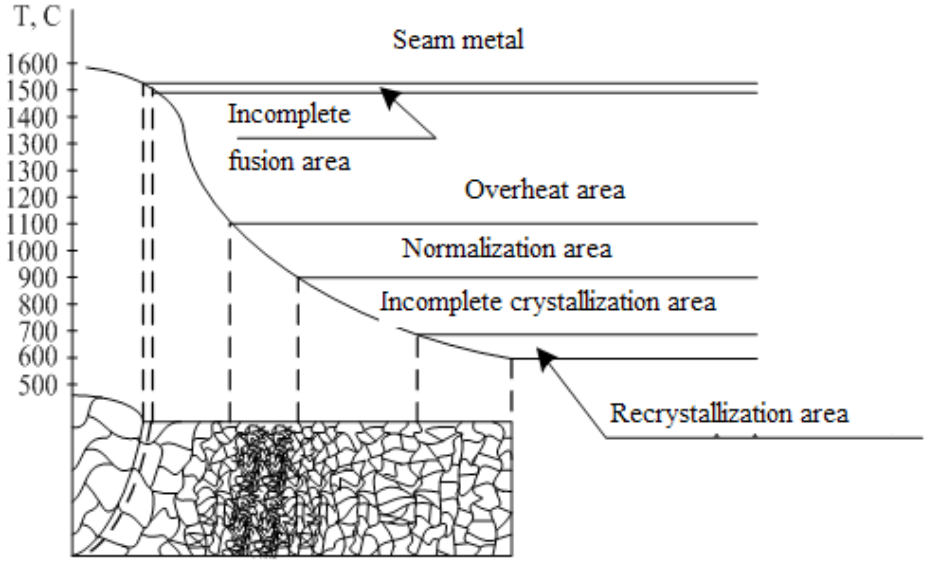

Figure 2. Structure scheme of a weld-affected zone of a welded joint

The cause for stress initiation and growth in pipeline welded elements

It is known that initiation of welding stress and deformations is caused by: 1) temperature contrast in welded joints at a heating stage and subsequent cooling; 2) casting shrinkage of seam metal – reduced volume of molten crater metal when hardening; 3) volume changes of seam metal and a weld-affected zone during the phase transformation at heating and cooling stages [5].

The reasons for internal residual stress to be formed in weld-affected zones include [6; 7]:

1. Local uneven metal heating. All metals are known to extend when heating, and to compress when cooling. In the course of welding, as a result of local metal heating and its subsequent cooling, a contrast temperature field is created in a welded joint. Thus, there is squeezing and (or) stretching thermal internal stress in a welded part. The magnitude of this stress depends mainly on heating temperature, linear expansivity and heat conductivity of the welded metal. When welding a rigidly fixed design, the magnitude of thermal stress can increase owing to the limited free movement in the course of heating and cooling. At the same time, at first there will be squeezing internal stress in a heating-up design due to its expansion, and then when cooling subsequently in the course of its shortening – there will be stretching stress. When the magnitude of internal stress reaches yield limit, plastic deformations leading to form and size changes of the welded product will begin to happen in metal. After welding, there will be residual stress in the areas exposed to uneven plastic deformation.

2. Uneven structural transformations in metal. In the course of main gas pipeline joint welding when heating above critical temperatures there can be stress caused by phase transformations with a crystal lattice change and phase formation of larger specific volume and different linear expansivity. In pipe steel, structure transformation is followed by the formation of the so-called hardening structures (martensite) having larger specific volume, higher hardness, fragility and lower plasticity. Such transformation is followed by the increase in volume; adjoining metal will be exposed to stretches, and sites with martensite structure will have phase yield limit. In nonplastic alloys it may lead to crack formation.

3. Casting shrinkage of weld deposit. When cooling and hardening, metal shrinks at a welded seam and a seam weld-affected zone [7]. This results from the fact that when hardening, metal density increases, and its volume therefore decreases. Owing to indissoluble contact between weld deposit and basic metal, the latter remaining of the invariable volume and counteracting shrinkage, there is longitudinal and cross internal stress in a welded joint resulting in the corresponding welded joint deformations.

Figure 3 presents geometric variables of elastic stress concentration at pipeline pure bending. SCZs initiate in the places with the greatest mechanical heterogeneity of seam properties, which is shown in the form of stress diagram deformations in a heat-affected zone while testing. It should be noted that in case of dynamic loads, ultimate damages start to show in the inner side of a pipe body, forming defective regions. This effect can be explained by pipeline metal tensile and compression while testing.

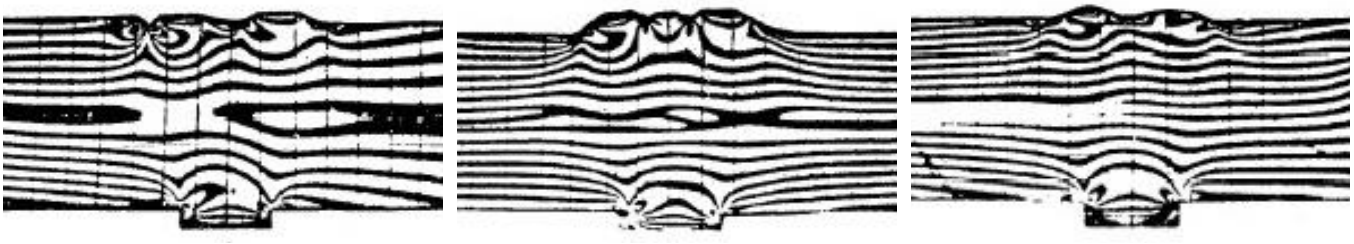

1 2 3

Figure 3. Stress concentration of a sample under dynamic load:
1 – load of 80 kN; 2 – load of 120 kN; 3 – without load

It is important to consider stress and deformations due to thermal and deformation welding cycle when calculating welded design durability. On the basis of approximate calculation used in the theory of welding deformations and stresses, to establish allowances and oversize for elements of bearing and enclosing structures, deformations of welded elements are usually defined. At the same time, it is generally a rather difficult task to calculate residual welding stress and deformations with a certain probability, as it has to consider all reasons causing their emergence and material thermal-physical properties as well.

Conclusion. The main sources of damages at main gas pipeline operation are local stress zones – local corrosion, fractures based on stress corrosion cracking and deformations as a result of joint assembly which are formed under working loads. Pipeline reliable operation can be provided only in case there are no defects of different nature: chemical and structural homogeneity of a pipeline body. In turn, the lack of defects will ensure main pipeline reliability and service life, maintaining operational properties, pipe material qualitative characteristics which will be as close as possible to their theoretical (calculated) values.

Stress in a weld-affected zone is an indicator of a stressed-deformed state, metal stress in a weld-affected zone is a source of defects. These stresses are added to operating stresses, accelerating a crack formation in weld-affected zones of pipe joints, cause continuous corrosion process and contribute to a crack formation before pipeline breakdown. Weld-affected zone stress is a result of internal stress which can be caused by various reasons. Basic reasons for stress include welded seam uneven heating and shrinkage, metal and weld-affected zone structural changes. In addition, the reasons for stress include inappropriate equipment and welding technique use (incorrect electrode diameter, welding condition violation, etc. aren't observed), low welder qualification, violation of welded seam sizes, etc. One of the reasons for weld-affected zone stress also includes the pressure created by a transportation product.

References:

1. Bukleshev D. O., Yagovkin N. G. Mathematical modeling of stress formation in gas pipeline weld-affected zones and their behavior under loads by means of the ANSYS software product. Magazine: Neftegaz territory – No. 10. 2016. of – M.: Camelot Publishing, 2016. – P. 88–92.
2. Gorkunov E. S. Behavioral features of metal magnetic characteristics in separate zones of a big-diameter pipe with various initial stress deformed state at elastic deformation / E. S. Gorkunov, A. M. Polovotskaya, S. M. Zadvorkin, E. A. Putilova // NDT days 2016. – No. 1(187). – P. 3–7.
3. Kasyanov A. N. Performance evaluation of weld-affected zones of main pipeline ring welded joints: Ph.D. thesis in Engineering Science / A. N. Kasyanov. – M., 2012. – 151 p.
4. Makovetskaya-Abramova O. V., Hlopova A. V., Makovetsky V. A. Stress concentration research at pipeline welding / O. V. Makovetskaya-Abramova, A. V. Hlopova, V. A. Makovetsky // Technical and technological service problems. 2014. – No. 2 (28). – P. 25–27.
5. Okhrimchuk S. A., Babelsky R. M., Rudenko S. N. The review of possible reasons for crack formation at MG Urengoy-Pomary-Uzhhorod double-seam pipes / S. A. Okhrimchuk, R. M. Babelsky, S. N. Rudenko // Gas industry. 2011. – No. 814 (appendix). – P. 7–10.
6. Bukleshev D. O. Experimental and metal fractographic study of stress corrosion cracking formation and growth in main pipeline welded elements / D. O. Bukleshev // Energy efficiency as an indicator of scientific, technical and economic capacity of society. – Nizhny Novgorod: NOO "Professional Science", 2018. – P. 88–133.
7. Bukleshev D. O. Defect formation in weld-affected zones of main gas pipeline welded joints under working loads. Magazine: Pipeline Transport. Theory and practice. – No. 2 (54). 2016 – M.: VNIIST, 2016. – P. 31–35.

Vapaev Murodjon Dusummatovich,
doctoral candidate, basic doctoral studies of the department
"Technology of plastics and high-molecular compounds"
of the Tashkent Institute of Chemical Technology Uzbekistan, Tashkent
Akhmadzhonov Sardor Akhmadzhonovich,
master of Tashkent Institute of Chemical Technology Uzbekistan, Tashkent
Teshabaeva Elmira Ubaidullaevna,
doctor of Technical Sciences, professor, envious of the department
"Technology of plastics and high-molecular compounds",
Tashkent Institute of Chemical Technology Uzbekistan, Tashkent
Ibadullayev Akhmadzhon,
doctor of technical sciences, professor, envious of the department
"Chemical technology of oil and gas processing",
Tashkent Institute of Chemical Technology Uzbekistan, Tashkent
E-mail: Ulug85bek77@mail.ru

INVESTIGATION OF MODIFIED ANGREN CAOLINE AS FILLING AND ACTIVATOR OF VULCANIZATION OF SOME ELASTOMERIC COMPOSITIONS

Abstract: This article presents the results of research into the feasibility of using modified kaolin as a filler and activator of rubber compounds based on butadiene nitrile rubbers. It is shown that it is influenced by the kinetics of the vulcanization process of rubber compounds on technological and technical parameters of elastomeric compositions. It was found that the optimum content of the modifier and Angren caolin in the composition of rubber compounds.

Keywords: rubber, rubber compound, of Angren caoline, modification, activator, vulcanizing agent.

Introduction

On the base of analysis of literature of investigation of morden state of technological process of modification elastomers and compozitional materials on their base by filling it was determined that the most perspective direction at development of such compositions at present time is searching of multifunctional filling and elaboration of technology of obtain compositional elastic materials and articles on the base with specifical properties [1].

In accordance with this the aim of this investigation is concluded in modification of Angren caoline by suturated adsorbent of primery processing of oil and gas.

Objects and methods of investigation. For carring out of this investigation copolymer butadiennitryl- acrylic acid was used. Rubber mixtures on the base of this elastomer were prepared on laboratorial at 30–35 °C and then they were vulcanization on press. Modified and reached caoline of Angren deposite was used as vulcanizational agent, activater and filling. Technological properties of rubber mixtures have been investigated according to corresponded GOSTs; kinetics of vulcanization of rubber mixtures was investigated on reometr Mansanto 100–4L.

Discussion of obtained results. It is khown that vulcanization of elastomers with functional groups

$-C\overset{O}{\underset{}{\overset{\|}{}}}-O-$ carring out by action of $Ca(OH)_2$ is characterised by presence in structure of forming rubbers side by side with ionic also cross-linking bonds. Their formation is course by fact that activater of salt vulcanization at the same time is used in by reaction of pereeterification with functional groups of elastomer. It was determined that threeethanolamine is vulcanizational agent of elastomers which were structured by functional groups at temperatures don't lower than 180 °C only in presence of activator – $Fe(OH)_3$.

On the base of carring out investigations [2; 3] and experimental investigations it was determined that Angren caoline with out correspouding physico-chemical modification and treatment can't be used in production of compositional elastomeric materials. Angren caoline contains to 2–3% of Fe_2O_3 (Table 1) what negatively influence on the complexe of properties of rubber compositions and articles from them. The main demand produced to mineral fillings at production of compositional elastomeric and articles from them is that containe of Fe_2O_3 was didn't more than 0.3%.

In result of carring out experimental investigations it was determined the possibility of modification of reached Angren caoline by saturated absorbent of primary processing of oil and gas, which is presented by self suspension of yellow couler with temperature of boiling 541K.

Modification of Angren caoline was carried out by following way: enreached caoline has been modified by liquid modificator and was dried after this at temperature 373 + 5 °C befor constant mass. Carring out investigations have allowed to prepose, that using of modified Angren caoline has allowed to proposed principally new approach for construction of high-filling elastomeric compositions with specifical properties on the base of synthetical butadiennitrile elastomer (rubber).

Table 1.– Chemical composition of Angren caoline

Name of components	Contain, was%
SiO_2	51.20
Al_2O_3	43.40
TiO_2	0.60
CaO	0.21
MgO	0.30
Fe_2O_3	2.22
SO_3	0.21
Cl^-	0.01
SO_4^{-2}	0.05
Water – soluble salts	0.10
Moisture	2.7

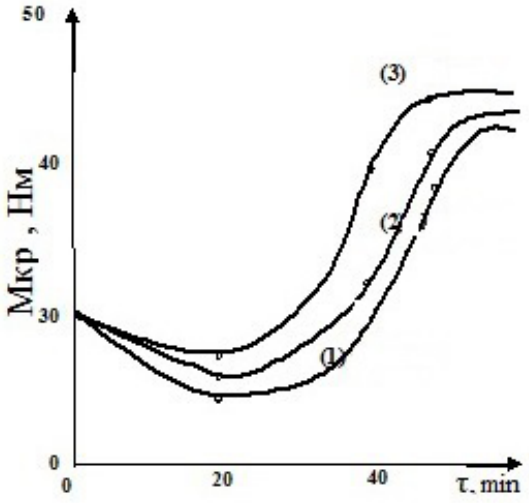

Figure 1. Dependence on kinetics of vulcanization of rubber mixtures on the base rubber CKH-26, containing 40 mass.% by modified Angren caoline (content of modificator (%):1–5%; 2–10%; 3–15%)

For investigation of influence of modified Angren caoline on the complex of properties of compositional elastomer materials some standart aproachers have been choosed which were elaborated on the base of synthetical butadien-styrol rubber. In this aproachers activator, vulcanization agent and technical carbon have been move away.

Kinetical curves of formation of cross – linking bonds have witnessed that vulcanization of rubber mixtures by modified Angren caoline has carried out intensivelly.

It was shown that Angren caoline has promoted to maximal absorbtion of modificator molecules and also has activated by Fe_2O_3 formation of more perfect regulating vulcanizational structures. This effect has shown that modified caoline not only has activated but also has accelerated processes of structuring processes. Very important advantage of modified Angren caoline is the fact it simultaneously has plaied role of filling, vulcanizational agent and activator what has influence on the nature and number of cross-linking bonds and properties of elastomeric compositions (Table 2).

Table 2.– Influence of modified caoline on structure of vulcanizational net of rubbers on the base CKH-26

Contain of filling and modificator	**Type of bonds,%**			
	–C–S_x–C–	**–C–S–S–C–**	**–C–S–C–**	**–C–C–**
40 mass.%. of Angren caoline, modified by 5% of modificator	30	26	25	19
40 mass.%. of Angren caoline, modified by 10% of modificator	20	25	27	36
40 mass.%. of Angren caoline, modified by 15% of modificator	22	26	28	24
20 mass.%. of Angren caoline, modified by 10% of modificator	18	23	25	34

In result of vulcanization of elastomer filling by modified caoline it was determined that it is characterised by number of advantages in comparasion with using vulcanization agent (S+ZnO): increasing stability of undervulcanization; higher mechanical characteristics, residual deformation of pressing, water-stability and also frost-resistance (Table 3).

Table 3.– Technological and physico-mechanical properties of rubbers on the base of elastomer CKH-26 filling by modified Angren caoline

№	**Properties**	**Properties of composition**	
		Initial composition	**Composition filling by modified Angren caoline**
1	***2***	***3***	***4***
1.	Time of begining of undervulcanization at 120 °C, min.	28	45
2.	Strain at elongation 300%, MPa.	21.5	13.9
3.	Conditional stability at tension, Mpa	24.6	29.2
4.	Relative elongation at break,%	386	500
5.	Relative residual deformation,%	13	13

1	*2*	*3*	*4*
6.	Temperature of fragility, °C	–40	–58
7.	Coefficient of frost-resistance ($K_в$) at –25 °C	0.10	0.44
8.	Residual deformation of pressing (24 h. × × 100 °C),%	71	35
9.	Degree of equlibrium swelling,% in: water (70 °C × 24 h.); water (100 °C × 24 h.); mixture of isooctane: tolyol = 70:30 (20 °C × 24 h.)	 6.2 26.0 34.4	 1.5 15.0 33.0

In composition of vulcanizational system can be introduced some additional cross-linking agents including peroxides proving of following improvement of properties of rubber compositions in particular the residual deformation of pressing and water – resistance (table 4).

Table 4. – Technological and some physico-chemical properties of rubbers filling by combinational vulcanization reagen

№	Properties	Properties of composition	
		Initial composition	**Composition filling by modified Angren caoline +peroxide**
1.	Time of begining of undervulcanization at 120 °C, min.	44	44
2.	Time of vulcanization at 180 °C, min.	40	60
3.	Strain at elongation 300%, MPa	18.8	19.8
4.	Relative strain at elongation, MPa	21.4	25.1
5.	Relative elongation at break,%	330	335
6.	Relative residual deformation after break,%	7	6
7.	Temperature at fragility, °C	–57	–61
8.	Residual deformation of pressing(100 °C × × 24 h.),%	31.0	31.7
9.	Degree of equlibrium swelling,% in: water (100 °C × 24 h.): mixture of isooctane: tolyol = 70:30 (20 °C × 24 h.)	 7.56 36	 7.4 33

Resume. Obtained vulcanizating systems can be effectivly used fo manifucture of oil-benzo-stable articles different types by method of vulcanization. At this owing to markedly increasing velosity of vulcanization of rubber articles on the base of syntetical butadiennitrilic elastomers containing modificated Angren caoline this process can be carried out at lower temperatures (150 °C).

References:

1. Тешабаева Э. У., Вапаев М., Ибадуллаев А. Модификация минеральных наполнителей и их влияние на свойства резин. Austrian Journal of Technical and Natural Sciences Austria. 2016. – № 3–4. – С. 125–128.

2. Ибадуллаев А., Негматов С. С., Тешабаева Э. У. Влияние дисперсных наполнителей на вязкоупругие свойства невулканизованных эластомеров // Журнал «Композиционные материалы» – Ташкент, 2003.– № 2.– С. 5–7.
3. Ибадуллаев А., Тешабаева Э. У. Негматов С. С., Таджибаева Г. С. Исследование физико-механических свойств минеральных наполнителей и методы их модификации // Журнал «Композиционные материалы» – Ташкент, 2006.– № 1.– С. 27–29.
4. Ибадуллаев А., Негматов С. С., Тешабаева Э. У. Усиления каучуков общего назначения дисперсными бентонитами Узбекистана. Научно-техническая конф. «Новые технологии рециклинга отходов производства и потребления».– Минск. 2004.– С. 388–391.

Vapaev M. D.,
doctorate student,
Boborazhabov B. N.,
external doctorate student
Teshabayeva E. U.,
doctor of technical sciences, associate professor
Ibadullaev A. S.,
doctor of technical sciences, professor,
Tashkent Chemical-Technological Institute
E-mail: Ulug85bek77@mail.ru

ROAD COMPOSITIONS BASED ON MODIFIED BITUMENS

Abstraact: We examined the possibility of modifying road bitumen BND60/90 and BND90/130 with gas-gas-pyrolysis resin. As a result, compositions of high heat resistance values were obtained.

Keywords: Bitumen, composition, modifier, structure, resin, oxidation, technology.

Introduction. Today, the research in improving the quality and durability of pavement surfacing is focused on modification of bitumens by using various additives to improve the basic properties of asphalt homogeneity, strength, resistance to frost, cracking, moisture and high temperatures [1].

The objective of this research is to modify the BND60/90 and BND90/130 paving bitumen with gas-pyrolysis resin (GPR).

Subjects and methods of research The composition was obtained by mixing BND60/90, BND90/130 bitumen with a modifier on a laboratory paddle mixer by first heating at a temperature of 70–90 °C. Modifier added 2–10 mass% of mass of bitumen.

Research of the properties of modified bitumen was carried out in accordance with the following GOSTs: GOST 4333–2014 "Petroleum products. Methods for determination of flash and fire points in open cup" using TVO-LAB-01 (ТВО-ЛАБ-01) analyzer; GOST 11507–08 "Petroleum bitumen. Method for determination of Fraas break point" using ATH-20 (АТХ-20 – automatic apparatus for determining the breaking point of petroleum bitumen) device; GOST 11505–75 "Petroleum bitumens. Method for determination of ductility" using DB-2M (ДБ-2М) ductilometer; GOST 11506–73 "Petroleum bitumen. The method of the determination of softening point by ring and ball" using KISH-20 (КИШ-20 – automatic apparatus for determining the softening point of petroleum bitumen and bituminous materials); GOST 11501–78 "Petroleum bitumens. Method for determination of depth of needle penetration" using the penetrometer PN-10 (ПН-10).

Results and discussion

The research revealed that the modification of BND90/130 and BND60/90 bitumens, with GPR in the amount of 5–10% of the mass to bitumen changes its dispersion structure, increasing the values of the softening temperature and penetration. The analysis of the values (Table 1) of the adhesion of bitumens modified to 10% of mass by GPR showed that it increases the adhesion properties of bitumens to the mineral material. However, the use of these additives does not always allow obtaining modified bitumens with quality up to the standards of BND60/90.

Table 1.– The quality parameters of paving bitumen modified with GPR

Additive ratio,% mass	Softening temperature, °C	Penetration at 25 °C, 0.1 mm	Penetration at 0 °C, 0.1 mm	Mass loss, % mass	Adhesion std. unit
GPR					
BND60/90	48	89	25	0.270	2.0
2	58	93	15	0.229	1.8
4	67	92	29	0.264	1.8
6	74	100	35	0.292	1.9
8	84	141	36	0.236	1.8
10	93	153	39	0.231	1.7
GPR					
BND90/130	45	117	26	0.417	2.1
2	56	105	27	0.471	1.8
4	65	106	29	0.419	1.9
6	76	115	26	0.472	1.8
8	83	117	29	0.419	1.7
10	94	123	34	0.399	1.7

The acquired results do not meet all the requirements. Figure 1 shows the results of research of the properties of compounded paving bitumens with a softening temperature of 47 °C, obtained by using the modified GPR of deeply oxidized bitumen and tar as the basis.

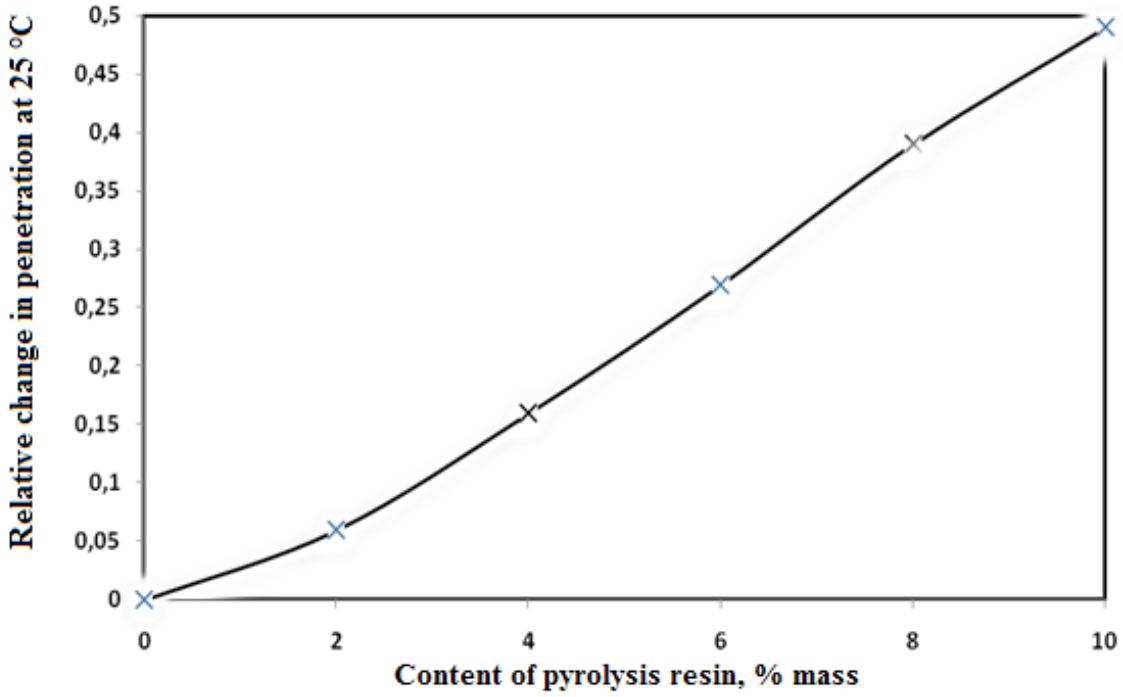

Figure 1. Dependence of the relative change in penetration at 25 °C of bitumen with a softening temperature of 47 °C on the content of gas-pyrolysis resin in bitumen

It is shown that with the introduction of GPR in deep-oxidized bitumen, an increase in its softening temperature occurs. GPR to 5% of the mass slightly change this indicator, and GPR to 10% of the mass affects bitumen heavily. With an increase in the concentration of GPR in bitumen, an increase in penetration occurs at 25 °C and a slight increase in its mass loss after heating, which is probably due to an increase in the tar content in compounded bitumens. With an increase in the density of gas-gas-pyrolysis resins, the values of penetration increase and the adhesion properties improve, the brittleness temperature decreases, and with optimal GPR concentrations in bitumen, its softening temperature values can be significantly reduced after warming up.

According to the values of the relative changes in softening temperature and penetration from the content of GPR, its functional effect on the structure of bitumen can be determined, i.e. to classify the obtained GPR as plasticizing or structuring bitumen modifier.

Therefore, the modification of BND60/90, BND90/130 paving bitumens with addition of GPR leads to an increase in the softening temperature.

To study the properties of samples of asphalt concrete modified with bitumen, made the composition of dense hot fine-grained asphalt concrete type "B" grade II. (Table 2).

Table 2. The number of composite materials in asphalt concrete

No.	Component	Material usage%
1.	Gravel chippings	43.5
2.	Scalpings	10.0
3.	Sand	30.5
4.	Mineral admixtures	10.0
5.	Modified bitumen	7.0
6.	Crumb rubber	7 of modified bitumen mass
7.	Zeolite	2 of crumb rubber mass
8.	Additives	2 of mass

The selection of samples for the road climate zone was carried out on demand. The grain composition of the mineral part of the composition for the manufacture of samples was selected in accordance with GOST. The composition was selected according to the design method for the limiting curves of dense mixtures [2], the optimal amount of modified bitumen was determined experimentally.

The study of the physical and mechanical properties of the composition showed (Table 3) that the bitumen content of 7% is optimal for the studied mineral material, while an improvement in all the physical and mechanical parameters of the composition studied is shown.

Table 3.– The dependence of the physical and mechanical properties of the composition on the bitumen content

No.	Bitumen content	Parameters						
		P_m, g/cm^3	P_m^M, g/cm^3	V^M,%	V^0,%	W,%	R_{cm}, MPa	R_p, MPa
1.	6.0	2.21	2.08	14.02	4.21	3.58	4.13	3.46
2.	6.5	2.22	2.08	14.06	4.19	3.38	4.25	3.23
3.	7.0	2.19	2.05	13.27	4.20	3.62	4.25	3.38
4.	7.5	2.15	2.03	13.20	4.22	3.52	4.20	3.20
5.	8	2.0	2.03	13.19	4.20	3.51	4.15	3.15

On the basis of the research, it was found that modified bitumen of 7% of the mass of the composition is optimal.

Conclusion

It has been established that to obtain BND60/90 and BND90/130 paving bitumens with improved

properties according to the scheme: oxidation of tar to deeply oxidized bitumen – modifying deep-oxidized bitumen by GPR – compounding the obtained bitumen with tar; is 3 to 7% of the mass.

References:

1. Ибадуллаев А. С., Тешабаева Э. У., Жураев В. Н. Создание и применение ингредиентов на основе местных сырьевых ресурсов и отходов производств в эластомерных композиционных материалах // Ж. «Химическая технология» – Тошкент, 2016. – Махсус сон, – С. 66–71.
2. Базарбаев Ф. Н., Комилова М. К., Вапаев М. Д., Ибодуллаев А. Модифицированные гидроизоляционные и кровельные материалы на основе местных сырьевых ресурсов // Композиционные материалы, 2018. – № 2. – С. 11–14.

Kadirov Bakhodir Makhamadjanovich,
deputy dean the faculty of "chemical technology of fuel and organic substances"
Ergasheva Saodat Khasanova,
student of 3rd course,
Kodirov Khasan Ergashevich,
the head of chair "Organic chemistry and technology of the basic organic synthesis
E-mail: Ulug85bek77@mail.ru

RESEARCH OF THE EFFICIENCY OF COMPLEX INHIBITORS OF SALT DEPOSITION, CORROSION AND BIOFOULING

Abstract: The modified process of the synthesis of the copper-zinc complex in the presence of citric acid and phosphoric acid (*Cu: Zn*-OEDP). The effect of the amount of copper and zinc on the degree of protection of metals against corrosion has been studied, and the optimal ratios have been determined. When carbamide is heated in the presence of phosphoric acid extraction and condensation of the obtained product with formaldehyde, carbamide-formaldehyde resin (CFS) is obtained. Prepared compositions based on CFS and Cu: Zn-OEDF. It was established that the degree of protection and the effectiveness of inhibition of the composition due to synergistic avtivnosti, 2–4 times more compared to pure Cu: Zn-OEDF.

Keywords: complexones, copper-zinc complexone, hydroxy ethylidenedi phosphonic acid, GI-PAN, urea-formaldehyde resin, multipurpose inhibitors, corrosion rate, inhibition efficiency, biocides.

At present, global production of polydentate compounds has reached the maximum amount of 2.5–3.5 million tons per year. On average, 40% of these produced reagents, about 1.2 million tons, are used to obtain inhibitors of mineral salt deposition and corrosion. Corrosion inhibitors that are widely used: Dodicor-4543; Dodicor-4712, Danox C1–252, Sepacorrts 3201; K-75w, Danox-CS102 B and inhibitors of mineral salt deposition, such as IMSD-1, OEDP, NTP-3, HELAMIN, etc. The problem of the protection of process equipment from salt deposition, internal corrosion and water treatment remains urgent [1].

Reagents of the new generation are mainly generated on the basis of organophosphonates. The use of phosphorus-containing chelating agents for the stabilization treatment of water started in the 70 s of the 20th century. It has been established that inhibition of the process of salt deposition with the help of phosphonates is based on the phenomenon of a vapor (or substochiometric) effect. Theoccurrence of threshold effect was discovered in the late thirties of the twentieth century for sodium hexametaphosphate: in doses from 1 to 10 ppm (ppm, 10–4%), it is able to delay (inhibit) the release of the solid phase from supersaturated calcium carbonate solutions. Since then, polyphosphates have become widely used as salt deposition inhibitors in industrial water circulation systems. Later, a similar effect was found in phosphonic acids.

However, due to the relatively high cost of such products, at a price they cannot compete with other inhibitors. Therefore, a possible way out of this situation is to create a relatively inexpensive, maximally

effective composition containing organophosphate in an amount of 20–40% of the total mass of the reagent. Many studies have concluded that Zn-OEDPis not an optimally effective metal corrosion inhibitor for heat supply systems. In addition, the increase in the efficiency of Zn-OEDPdue to the increase in concentration is impossible, due to the low MPC for OEDP, which is 0.6 mg / l.

One of the priority areas for solving this problem is the use of a synergistic effect, which occurs when: ethanolamines phosphoric acids [2]; ascorbic acid [3]; dodecyl sulfate [4]; acrylic acid ester, polyphosphates and benztriazole [5]; carbamide-formaldehyde resins [6] and others are added to Zn- OEDP.

The suggested method of obtaining inhibitors of universal action is carried out in the following sequence:

Stage 1. The reaction of condensation of urea with formaldehyde. Condensation of urea with formaldehyde was carried out in a three-necked flask equipped with a reverse water cooler, a drop funnel and a mechanical stirrer. 36.6 g of urea (0.61 mole) were placed in the reactor, and 40 ml of water were added in portions with vigorous stirring. The mixture was stirred for 25–30 minutes at a temperature of 30–40 °C. Then 126 ml (1.55 mole) of 37% formaldehyde was added to the solution, after 1 ml of a 27% solution of extraction phosphoric acid. Then 50 mg of ammonium chloride and 2.5 ml of 25% ammonia water were added to the reaction mixture. The resulting reaction mass was thoroughly stirred at a temperature of 80–84 °C for 1 hour, then the mixture was placed in a flask at a pressure of 10 mm Hg, a temperature of 60 °C, and formaldehyde was distilled off. The code name of the condensation product CFR.

Elemental analysis data.

Found,%: C = 26.52; H = 6.68; N = 31.41

Calculated,%: C = 26.67; H = 6.66; N = 31.11

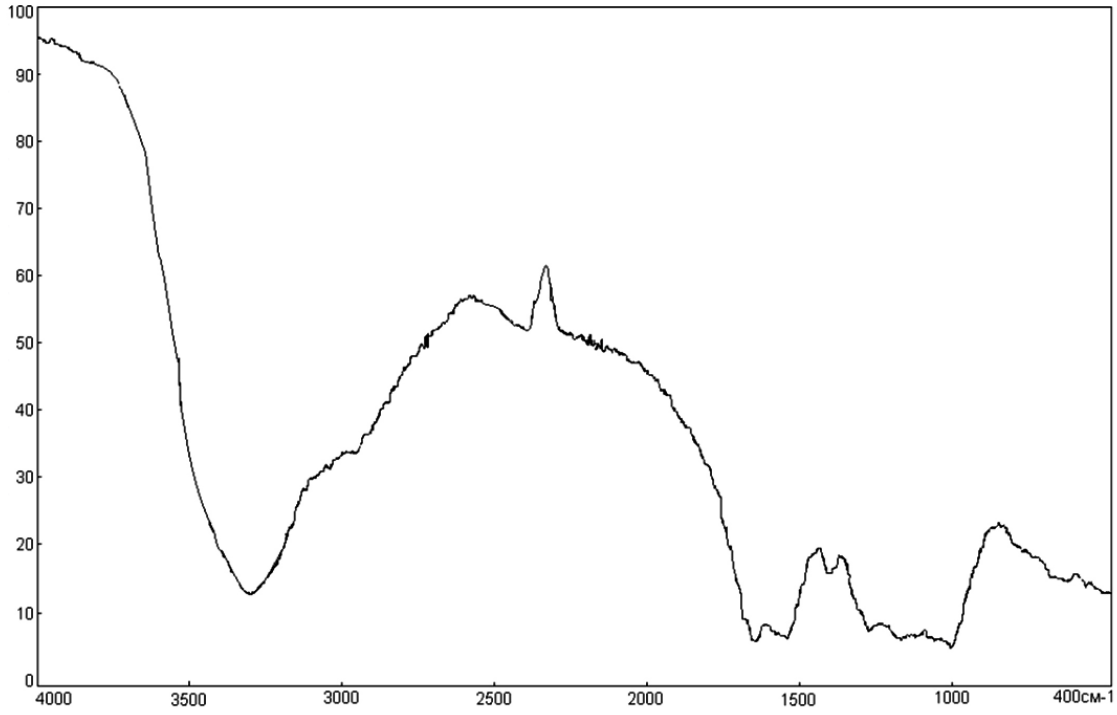

Figure 1. IR spectrum of condensate product of urea with formaldehyde

In the infrared spectrum of condensation products of urea with formaldehyde, intense absorption peaks were found in the regions: 1070–1150 cm^{-1} – stretching vibration – CO-groups, 3200–3400 cm^{-1} – deformation vibration – OH-groups, 650–900 and 1560–1640 cm^{-1} – stretching vibrations of the NH_2 group, 1490–1580 cm^{-1} – stretching vibration of the NH-group.

Stage 2. Obtaining zinc complex of OEDP. A method is suggested for preparing crystalline Cu: Zn- OEDP in the presence of glycerin: a heat-resistant beaker is added to the reactor, water is poured in a calculated amount, and glycerol is added. The mixture is stirred for 5–7 minutes. Then add the calculated amount of OEDP. The temperature at the same time should be 30–35 °C. After that, sodium hydroxide, copper oxide and zinc oxide are sent to the reactor. The mixture is stirred until complete dissolution and a clear liquid is obtained. The finished product is cooled to room temperature.

The composition and structure of the obtained product is established by various physico-chemical methods of analysis.

The aqueous solution of the object was analyzed on chromatography-mass spectrometer "Agilent Technology" GC/MS AT 5973N using the DRUG-SP-SHORT.M method using a 30m × 0.25mm capillary column with 5% phenylmethylsiloxane at an injector temperature of 280 °C, sample size 1 microliter (Figure 2).

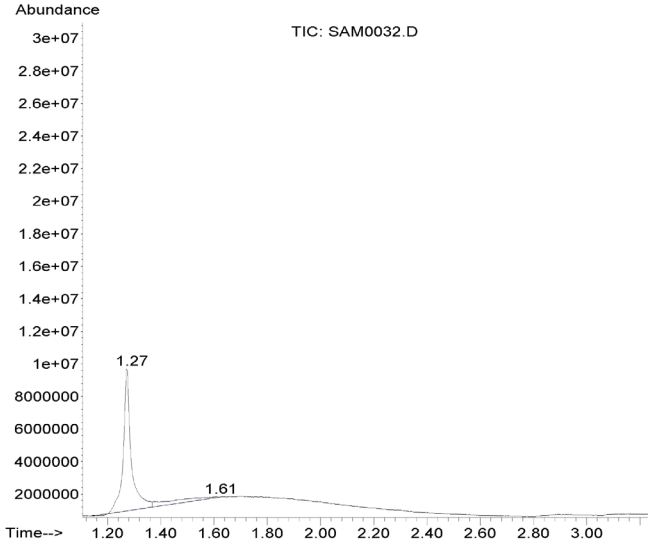

Figure 2. Chromate-mass-spectrum of *Cu: Zn-OEDP*

Conditions of chromate-mass-spectrum: temperature 280 °C, when programming the temperature of the column thermostat from 70 to 280 °C, sample size 1 microliter.

Comparison of the basic data of the device proves that the resulting *Cu: Zn*-OEDP has high purity.

Cu: Zn-OEDP IR – spectrometer (Figure 3) "AgilentTechnologyFTIR-640" under the following analysis conditions: the recording range is 4000––400 cm^{-1}, the number of scans is 12.

In the spectrum of the preparation, there is a band at 1250–1300 cm^{-1}, related to the localized P = O bond; the band at 2500–2700 cm^{-1} refers to the stretching vibrations of the group of the fully deprotonated PO_3 group; there are also bands at 1180–1240 and 2500–2700 cm^{-1} related to the stretching vibrations of the P – O(H) bond of the protonated phosphate groups, which indicates that the complexes are partially protonated; the intense band at 1046–1000 cm^{-1} refers to the stretching vibrations of the Cu – O bond, the band at 650–750 cm^{-1} to the stretching vibrations of the C – P bond, and the intense band at 570–550 cm^{-1} to the stretching vibrations of the Zn – O bond; the absorption bands at 480–460 cm^{-1} to the deformation vibrations – O – P – O. This allows us to conclude that the coordination of the PO_3 group with the Zn atom occurs with the localized π-bond

P = O, the oxygen atoms in the PO_3 group do not equal rights.

Stage 3. The preparation of the composition of the inhibitor is of universal action. To do this, the reactor is a heat-resistant glass, water and extracted phosphoric acid in an amount of 100.0 and 27.0 ml are poured, respectively, and citric acid, the products obtained in the first and second stages in different ratios in turn. The mixture is stirred for 12–15 minutes. This product was provisionally named "IMSD-UNI".

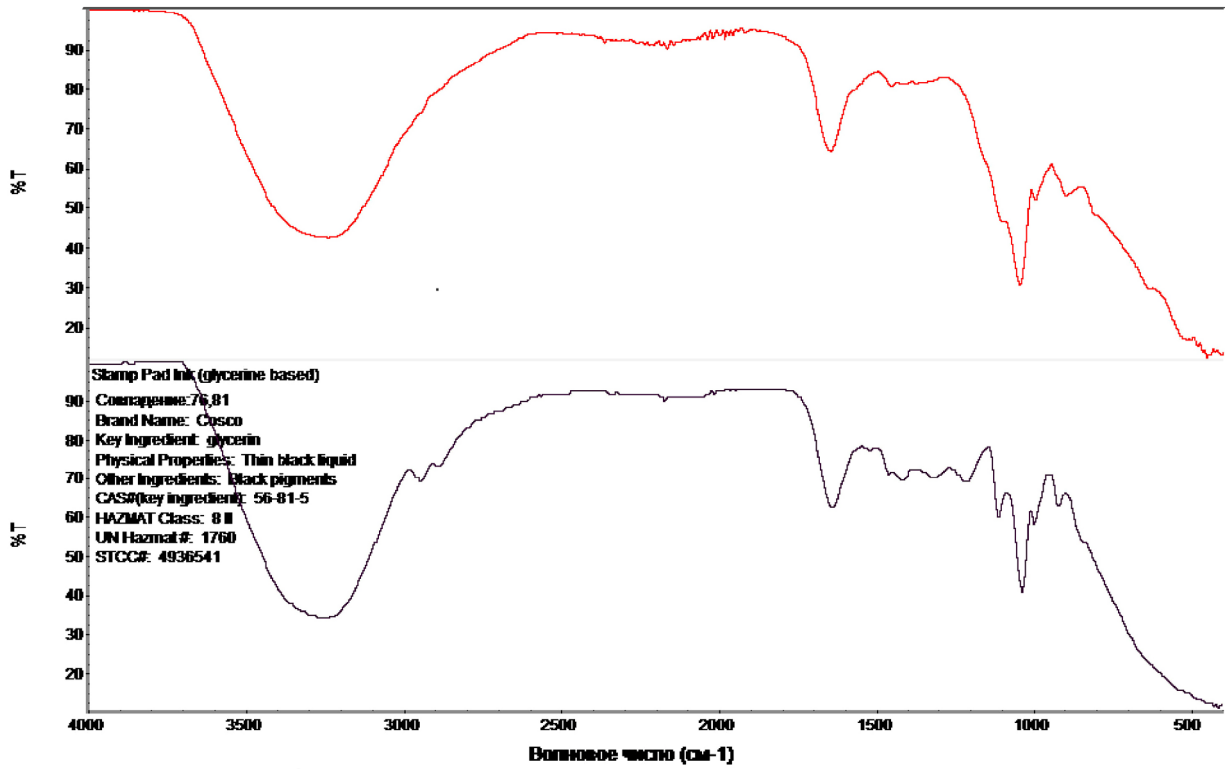

Figure 3. *Cu: Zn*-OEDP IR – spectrometer

To determine the optimal composition of the OEDP: Me, compositions were prepared at ratios of 3:1–2:1. The ratios varied from 0.25: 0.75 to 0.75: 0.25.

Tests of the obtained compositions as corrosion inhibitors were carried out on industrial waters with hardness of 9–10 mg. eq./l. The results are presented in tables 2 and 3 and in figures 5–6.

Table 2.– The influence of complexions based on *Cu: Zn*-OEDPon the corrosion rate of steel grades **in stage 3** (K = 0.240 mm/a year)

Reagent	Mole ratio	Corrosion rate, mm/a year At the reagent concentration, mg/l	
		6	10
Cu: Zn-OEDP	0.5 : 0.5 : 2.0	0.043 ± 0.002	0.024 ± 0.001
Cu: Zn-OEDP	0.33 : 0.66 : 2.0	0.014 ± 0.004	0.007 ± 0.002
Cu: Zn-OEDP	0.66 : 0.33 : 2.0	0.082 ± 0.001	0.065 ± 0.003
Cu: Zn-OEDP	0.75 : 0.25 : 2.0	0.113 ± 0.003	0.106 ± 0.001
Cu: Zn-OEDP	0.66 : 0.33 : 3.0	0.062 ± 0.004	0.053 ± 0.003
Cu: Zn-OEDP	0.33 : 0.66 : 3.0	0.031 ± 0.002	0.022 ± 0.001
Cu: Zn-OEDP	0.75 : 0.25 : 3.0	0.106 ± 0.001	0.096 ± 0.001
Cu: Zn-OEDP	0.25 : 0.75 : 3.0	0.110 ± 0.004	0.106 ± 0.001

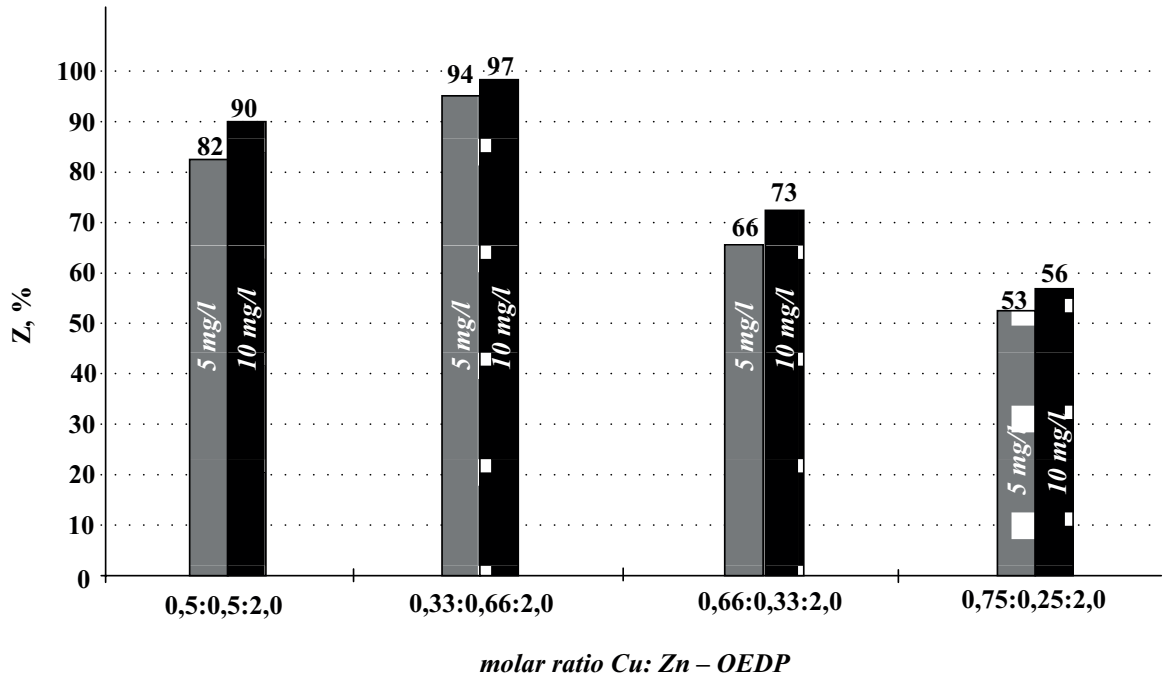

Figure 5. Depenence of the protective effect of corrosion inhibition on the molar ratio *Cu: Zn*-OEDP, with the ratio OEDP: Me = 2 : 1

From the data presented in (Table 2) and in (Figure 5), the following conclusions can be drawn:

a) all investigated *Cu: Zn*-OEDP for the given molar ratios of OEDP: Me reduce the corrosion rate of constructional steel in water with hardness of 9–10 mg eq/l to normal values less than 0.1 mm/a year.

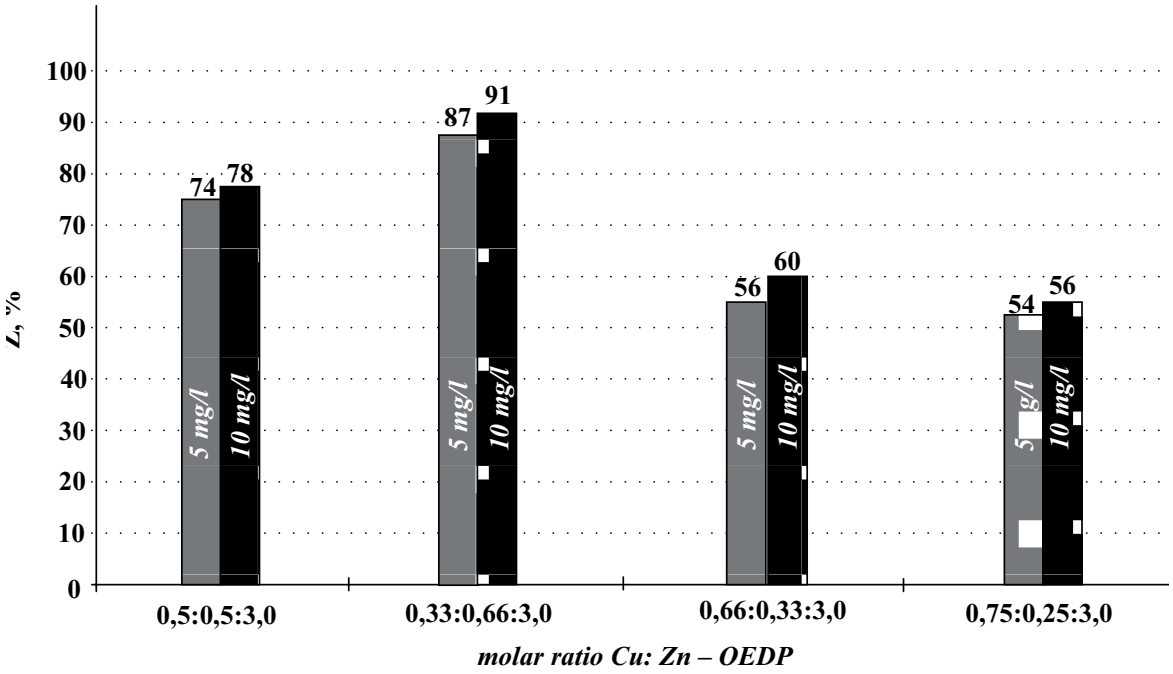

Figure 6. Dependence of the protective effect of corrosion inhibition on the molar ratio of *Cu: Zn*-OEDP, with the ratio of OEDP: Me = 3 : 1

b) compositions with a ratio of OEDP: Me÷2:1 have a greater corrosion inhibiting efficiency than compositions with a ratio of 3:1, due to an increase in the composition of such compositions of zinc complexates. The protective effect of compositions with ratio OEDP: Me is equal to 3:1 does not exceed 78%, while for compositions with ratio OEDP: Me is equal to 2: 1 it reaches 86%.

c) an increase in the composition of the molar fraction of zinc compared to the proportion of copper (compositions with ratios Cu: Zn equal to 0.75: 0.25 and 0.66: 0.33) increases the ability of the compositions to inhibit the corrosion of steel in stage 3, minimum protective effect of such compositions is 57% and increases to 86%.

Table 3.– Influence of compositions on the corrosion rate of steel grades in stage 3 in water hardness 9–10 mg.eq./l (K = 0.240 mm/a year)

Reagent	Corrosion rate, mm/a year at the portion of reagent, mg/l			
	4	6	8	10
CFR	0.163 ± 0.002	0.137 ± 0.002	0.134 ± 0.004	0.134 ± 0.002
Cu: Zn-OEDP	0.053 ± 0.002	0.038 ± 0.004	0.029 ± 0.001	0.024 ± 0.001
IMSD-UNI-1	0.048 ± 0.003	0.031 ± 0.002	0.019 ± 0.002	0.007 ± 0.002
IMSD-UNI-2	0.084 ± 0.001	0.062 ± 0.004	0.048 ± 0.002	0.036 ± 0.001

In order to study the synergistic activity of the CFR and *Cu: Zn*-OEDP, compositions with different compositions were prepared: the inhibiting properties of the products obtained in stages 1 and 2 in pure form were compared; composition consisting of CFR ÷ *Cu: Zn*-OEDP, obtained at a molar ratio of initial reagents of 1:2 (trade name IMSD-UNI-1) and 1:1 (trade name IMSD-UNI-2). The results are presented in (Table 3) and in (Fig. 7) (the corrosion rate in the control experiment was 0.18 mm/a year).

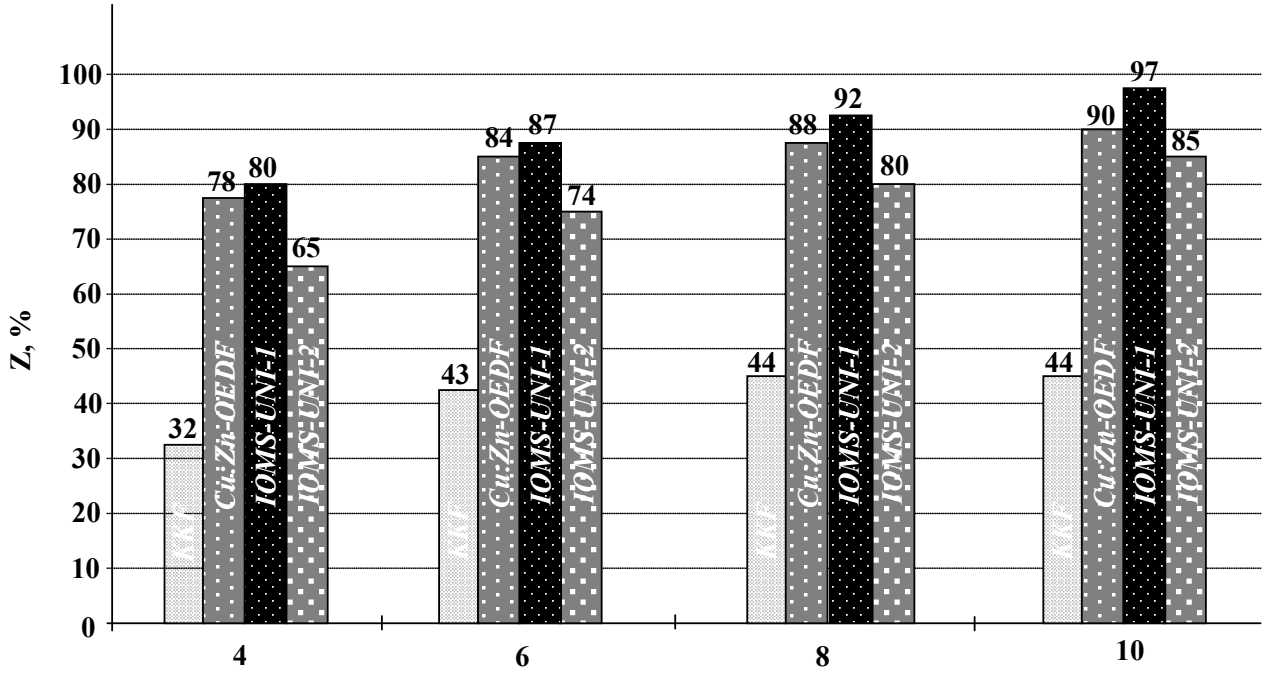

Figure 7. Dependence of the protective effect of inhibiting the corrosion of steel in stage 3 of the concentration and type of reagent

From the data presented in (Table 3) and in (Fig. 7), it can be seen that adding a CFR to the composition can significantly increase the efficiency of the initial *Cu: Zn*-OEDP reagent as a corrosion inhibitor. The protective effect against corrosion of structural steel using IMSD-UNI-1 reagent is more than 80% at all concentrations studied, while using Cu: Zn-OEDP this effect is achieved only at concentrations of more than 6 mg/l. At the same time, the increase in the cost of the modified inhibitor does not exceed 30–50% of the cost of the initial OEDP reagent.

From previous studies, it is known that the IMSD-1 copper-containing complexonates with a molar ratio of IMSD-1 : Cu = 2: and IMSD-1: Cu = 1 : 1, besides inhibiting scaling, exhibit biocidal properties and effectively inhibit vital activity microorganisms, and hence biofouling.

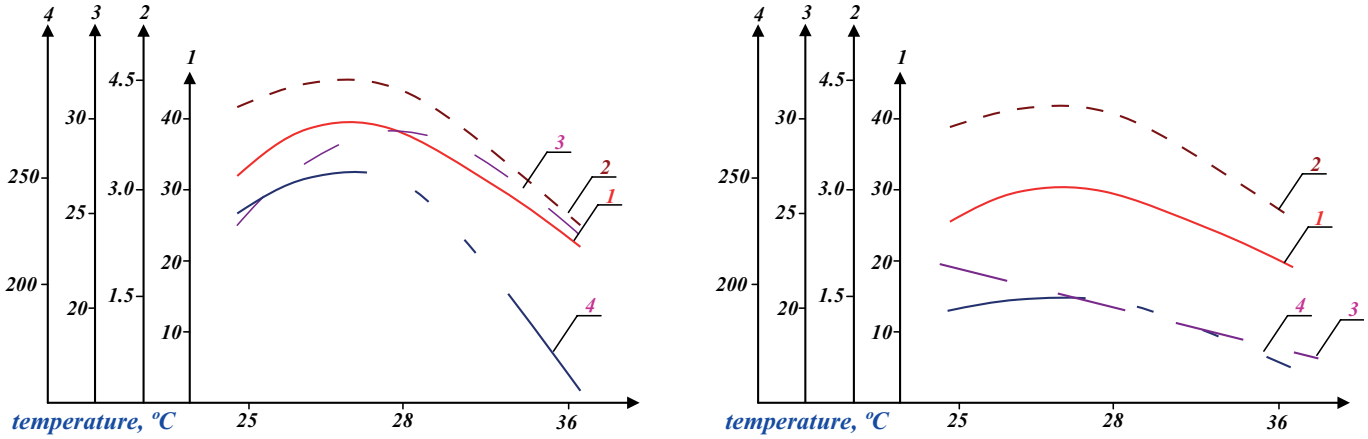

Figure 9. The effect of IMSD-UNI-1 (A) and IMSD-UNI-2 (B) preparations on algae E. claraskuja belonging to the family EuglenaEhr

The experiments were carried out on the basis of standard algological requirements in the following order: objects of experience (or research) were carried out in microalgae: Chlorella, Scenesmus-Chlorellavulgaris, Scenedesmusoblianus and also in E. Clara cultures related to the Euglena Ehr family. Experiments were performed in standard living food conditions for cultures.

Figure 9 shows the results of the experiments carried out in the food media of the E. Clara culture belonging to the Euglena Ehr family.

The result shows that the preparations inhibit the development of algae E. Clara, which is expressed by a decrease in activity in metabolic processes, in particular a sharp decrease in the activity of photosynthesis and breathing processes, the number of living cells, and consequently, the accumulation of biomass cells.

Conclusion. Thus, it was found that in compositions of carbamide-formaldehyde resins (CFS) with copper-zinc complexates of hydroxyethylidenediphosphonic acid, they can increase the effectiveness of salt deposition and corrosion by 2–4 times with the content of the latter up to 40% of end products.

Based on the CFS and Zn: Cu-OEDP reagents, complex inhibitors of salt deposition, corrosion and biofouling have been developed. It has been established that the use of the IMSD-UNI-1 reagent provides both a non-boiling regime and a reduction in the corrosion rate in waters of various chemical compositions and in highly mineralized waters when salts are concentrated in water supply systems.

References:

1. Calcium gluconate as corrosioninhibitor for mild steel in low chloride me- dia Rajendran S., Apparao B. V., Palaniswamy N. // Anti-corros. Methods Mater. 1997.– V. 44.– No. 5.– P. 308–313.
2. Chemistry of organophosphonate scale growth inhibitors: Physicochemical aspects of 2-phosphonobutane-l,2,4-tricarboxylate (PBTC) and its effect on $CaCO_3$ crystal growth / Konstantinos D. Demadis, Panos Lykoudis // Bioinorganic chemistry and applications. 2005.– No. 3–4.– P. 135–149.
3. Choi Dong-Jin et al. // Materials and Engineering, A: Structural Materials: Properties, Microstructure and Processing A 335 (1–2), 2002.– P. 228–235.
4. Corrosion inhibition by carboxymethyl cellulose-1-hydroxyethane- l, ldiphosphonic acid-Zn2+ system / Rajendran S., Joany R. M. et al. // Bulletin of Electrochemistry. 2002.– V. 18.– No. 1.– P. 25–28. 2002.– V. 136. – P. 328–649.
5. Corrosion inhibition of steel in neutral chloride solutions by mixtures of N- phosphono-methylglycine with zinc ions / Pech-Canul M. A., Echeverria M. // Corrosion Engineering, Science and Technology. 2003.– V. 38.– No. 2.– P. 135–138.
6. Кадиров Х. И. Синтез и технология производства ингибиторов солеотложения и коррозии // Дисс … док.техн.наук.– Ташкент. 2017.– 191 с.
7. Козлова О. Г. Рост и морфология кристаллов. 3-е изд., перераб. и доп.– М.: МГУ, 1980.– 357 с.
8. Corrosion inhibitor of carbon steel in open recirculating cooling water systems of petroleum refinery by a multi-component blend containing zinc (II) diethyldithiocarbamate / P. K. Gogoi, B. Barhai // Indian Journal of Chemical Technology. 2010.– Vol. 17.– P. 291–295.

Mehtiyev Rafail Kerim oghlu,
Azerbaijan Technical University,
E-mail: rafail60mehtiyev@mail.ru
Jafarova Saida Allahverdi kizi,
Azerbaijan, Baku

CONTİNİUSİNG SHEAR OF THROUGH CRACKS İN A COMPOSİTE REİNFORCED WİTH UNİDİRECTİONAL ORTHOTROPİC FİBERS

Abstract: The problem of fracture mechanics on the interaction of orthotropic elastic inclusions which surface is equally covered with a material cylindrical slight (layer) is considered. The fiber is weakened by a rectilinear crack of a collinear ordinate axis. The surface is weakened by two doubly periodic systems of rectilinear cracks collinear to the axes of the abscissas and ordinates in the orthotropic plane.

Keywords: doubly periodic lattice, coating thickness, coating fibers, coating–binder, average stresses, linear algebraic equations.

Formulation of the problem

Suppose the issue there is an isotropic elastic binder weakened by a doubly periodic system of circular apertures having radii $\lambda(\lambda<1)$ and centers at points

$$P_{mn}=m\omega_1+n\omega_2;(m,n=0,\pm1,\pm2,\ldots);$$

$$\omega_1=2;\omega_2=\omega_1\cdot he^{i\alpha};h>0;Im\omega_2>0$$

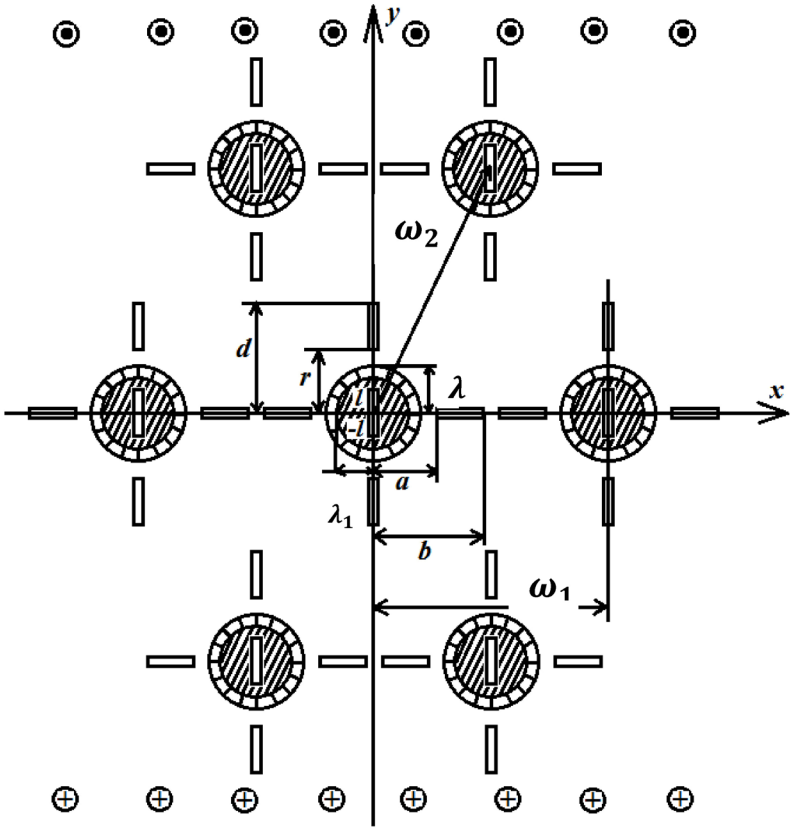

Figure 1.

The plane under consideration is subjected to shea $\tau_y = \tau_y^\infty$, $\tau_x = 0$ (shear at infinity) (Fig. 1). On the basic of the symmetry of the boundary conditions and the geometry of the place D occupied by the stress medium, they are doubly periodic functions with principal periods ω_1 and ω_2.

Expressing voltages and displacement w through an analytic function is like that:

$$u = \upsilon = 0,\ w = w(x, y);\ \sigma_x = \sigma_y = \sigma_z = \tau_{xy} = 0;\ \tau_x = \mu\frac{\partial w}{\partial x},\ \tau_y = \mu\frac{\partial w}{\partial y} \quad (1)$$

$$\tau_x - i\tau_y = f'(z) = F(z),\ \tau_t + i\tau_n = \overline{F(z)}e^{-i\alpha},\ w = \frac{1}{\mu}\operatorname{Re} f(z),\ z = x + iy,$$

(where $\mu -$ is the constant of the medium material; $i = \sqrt{-1}$, t, n are the natural coordinates), we write the boundary conditions of the problem in the form [2]

The operated form for the problem of the interaction of orthotropic elastic inclusions and through cracks

$$\left(1+\frac{\mu_b}{\mu_t}\right)f_b(\tau_1)+\left(1-\frac{\mu_b}{\mu_t}\right)\overline{f_b(\tau_1)} = 2f_t(\tau_1), \quad (2)$$

$$\left(1+\frac{\mu_t}{\mu_s}\right)f_t(\tau)+\left(1-\frac{\mu_t}{\mu_s}\right)\overline{f_t(\tau)} = 2f_s(\tau), \quad (3)$$

$$f_s'(t) - \overline{f_s'(t)} = 0,\ f_b'(t_1) - \overline{f_b'(t_1)} = 0, \quad (4)$$

where $\tau = \lambda e^{i\theta} + m\omega_1 + n\omega_2, \tau_1 = \left(\lambda - h^*\right)e^{i\theta} + m\omega_1 + n\omega_2$, $m, n = 0, \pm 1, \pm 2, \ldots$, h^* – coating thickness; $\theta -$ polar angle; t and t_1 affixes of points of cracks on the abscissa and ordinate axes, simultaneously. The summers related to the coating, the washer and the plane are hereinafter referred to as *t, b* and s, respectively:

Solving a boundary value problem

The solution of the boundary value problem is sought in the form

$$f_s(z) = f_1(z) + f_2(z),\ f_b(z) = f_{1b}(z) + f_{2b}(z), \quad (5)$$

$$f_{1b}(z) = \sum_{k=0}^{\infty} a_{2k}\frac{z^{2k+1}}{2k+1},\ f_t(z) = \sum_{k=-\infty}^{\infty} b_{2k}z^{2k+1}, \quad (6)$$

$$f_1''(z) = \tau_y^\infty + \sum_{k=0}^{\infty}\alpha_{2k+2}\frac{\lambda^{2k+2}\rho^{(2k)}(z)}{(2k+1)!}, \quad (7)$$

$$f_2''(z) = \frac{1}{i\omega}\int_{L_1} g(t)\varsigma(t-z)dt + A,$$

$$f_{2b}''(z) = \frac{1}{i\omega}\int_{L_2} g_1(t_1)\varsigma(it_1 - z)dt_1 + B,\ f_{2b} = \frac{1}{\pi}\int_{-l}^{l}\frac{g(t)dt}{t-z}, \quad (8)$$

where the integrals in (8) are taken along the lines $L_1 = \{[-b,-a]+[a,b]\}$; $L_2 = \{[-d,-r]+[r,d]\}$, $\rho(z) = \left(\frac{\pi}{\omega}\right)^2\frac{1}{\sin^2\frac{\pi z}{\omega}} - \frac{1}{3}\left(\frac{\pi}{\omega}\right)^2$, $g(t)$, $g_1(t_1)$ – the desired functions characterized the shift of the banks of the prefracture zones.

$$g(x) = \frac{\mu_s}{2}\frac{d}{dx}\left[w^+(x,0) - w^-(x,0)\right] \text{ on } L_1;$$

$$g_1(y) = \frac{\mu_s}{2}\frac{d}{dy}\left[w^+(0,y) - w^-(0,y)\right] \text{ on } L_2.$$

Additional conditions are added to the basic concepts (5) – (8), which follow from the physical meaning of the task

$$\int_{-\ell}^{-a} g(t)dt = 0;\ \int_{a}^{\ell} g(t)dt = 0;\ \int_{-r}^{-b} g_1(t_1)dt_1 = 0;\ \int_{b}^{r} g_1(t_1)dt_1 = 0. \quad (9)$$

The unknown functions $g(x)$ and $g_1(y)$, and the coefficients a_{2k}, b_{2k}, α_{2k} must be determined from the boundary conditions (2)–(4). To formulate equations for unknown coefficients, we transform the boundary condition (3) to the form

$$\left(1+\frac{\mu_t}{\mu_s}\right)f_t(\tau)+\left(1-\frac{\mu_t}{\mu_s}\right)\overline{f_t(\tau)} = 2\left[f_t(\tau_1) + if_2(\tau)\right]. \quad (10)$$

Regarding the function $f_2(\tau)$ s and $if_2(\tau)$, we will assume that they decompose on a contour $|\tau| = \lambda$ into Fourier series.

To derive the resolving equations, we substitute the boundary conditions (2) (3) instead of the functions $f_b(z)$, $f_t(z)$, $f_1(z)$ their expansions into Laurent series in the nearly of the zero point, and instead $f_1(z)$ and $if_2(\tau)$ of the – Fourier series on the contour $|\tau| = \lambda$ and equating the coefficients with the same powers $\exp(i\theta)$ in both parts of the boundary conditions, we get after some transformations, the set of infinite systems of linear algebraic equations [6]:

$$b_{2k} = \left(1+\frac{\mu_b}{\mu_t}\right)a_{2k}\frac{\lambda_3^{2k+1}}{2(2k+1)\lambda^{2K+1}}, \quad (11)$$

$$b_{-2k-2}=\left(1+\frac{\mu_b}{\mu_t}\right)\overline{a}_{2k}\frac{(\lambda-h)^{4k+2}\lambda_3^{-2k-1}}{2(2k+1)\lambda^{-2k-2}},$$

$$\frac{\lambda_3 a_0}{4\lambda}\left(g_1+f^2h_1\right)=\tau_y^{\infty}+c_0+\sum_{k=1}^{\infty}\alpha_{2k+2}\lambda^{2k+2}r_{0,k},$$

$$\frac{\lambda_3\overline{a}_0}{4}\left[h_2f^2+g_2\right]=-\alpha_2,$$

$$\frac{\lambda_3^{2k+1}a_{2k}}{4\lambda^{2k+1}}\left(g_1+f^{4k+2}h_1\right)=\alpha_2\lambda^2r_{0,1}+\sum_{p=1}^{\infty}\alpha_{2p+2}\lambda^{2p+2}r_{p,k}+\frac{c_{2k}}{\lambda^{2k}},$$

$$\frac{\lambda_3^{2k+1}\overline{a}_{2k}\lambda^{2k}}{4\lambda^{2k+1}}\left(g_2+f^{4k+2}h_2\right)=-\alpha_{2k+2}.$$

Here

$$g_1=\left(1+\frac{\mu_b}{\mu_t}\right)\left(1+\frac{\mu_t}{\mu_s}\right),\ g_2=\left(1+\frac{\mu_b}{\mu_t}\right)\left(1-\frac{\mu_t}{\mu_s}\right),$$

$$h_1=\left(1-\frac{\mu_t}{\mu_s}\right)\left(1-\frac{\mu_b}{\mu_t}\right),\ h_2=\left(1+\frac{\mu_t}{\mu_s}\right)\left(1-\frac{\mu_b}{\mu_t}\right),$$

$$r_{p,k}=\frac{(2p+2k+1)!\,g^*_{p+k+1}}{(2p)!(2k+1)!2^{2p+2k+1}},\ f=\frac{\lambda-h}{\lambda},\ c_{2k}=c'_{2k}+c''_{2k},$$

$$c'_{2k}=-\frac{1}{\omega i}\int_{L_1}g(t)f_{2k}(t)dt,$$

$$c''_{2k}=-\frac{1}{\omega i}\int_{L_2}g_1(t_1)\phi_{2k}(it_1)dt_1,$$

$$f_{2k}(t)=\frac{\lambda^{2k}}{(2k)!}\gamma^{(2k)}(t)-\frac{\lambda^{2k+2}}{(2k+1)!}\gamma^{(2k+2)}(t),\ \gamma(t)=ctg\frac{\pi}{\omega}t,$$

$$\phi_{2k}(it_1)=\frac{\lambda^{2k}}{(2k)!}\gamma_1^{(2k)}(it_1)-\frac{\lambda^{2k+2}}{(2k+1)!}\gamma_1^{(2k+2)}(it_1),$$

$$\gamma_1(it_1)=ctg\frac{\pi}{\omega}it_1,\ (k=0,\pm1,\pm2,...),$$

$$g^*_{p+k+1}=2\sum_{m=1}^{\infty}\frac{1}{m^{2(p+k+1)}},\ g=\frac{a_{44}}{a_{55}}=\frac{\mu_2}{\mu_1},$$

$$\lambda_3=\frac{\lambda}{\sqrt{2}}\sqrt{\left(\frac{2g}{1+g}\right)^2+\left(\frac{2}{1+g}\right)^2},\ r_{0,0}=0.$$

Now accounting that the functions (5) – (8) satisfy the boundary condition on the banks of the pre–fracture zones, we obtain a system of two singular integral equations with calculation to $g(x)$ and $g_1(y)$:

$$\frac{1}{\pi}\int_{L_1}g(t)\varsigma(t-x)dt-\mathrm{Im}\left[A+f_1'(x)\right]=0\ \text{on}\ L_1,\quad(12)$$

$$\frac{1}{\pi}\int_{L_2}g_1(t_1)\varsigma(t_1-y)dt_1-\mathrm{Im}\left[A+f_1'(x)\right]=0\ \text{on}\ L_2,\quad(13)$$

$$\frac{1}{\pi}\int_{L_1}\int_{-l}^{l}\frac{g(t)}{t-x}dt-\mathrm{Im}\left[f_{1b}'(x)\right]=0.\quad(14)$$

Infinite algebraic systems (11) together with singular integral equations (12) – (14) are the main resolving equations of the problem, allowing to determine $g_1(y), g(x)$ the coefficients $a_{2k}, b_{2k}, \alpha_{2k}$. Algebraic systems (11) and integral equations (12) – (14) turned out to be connected and should be solved together. After determining the complex potentials $f_s(z)$, $f_s(z)$ and $f_t(z)$ it is possible to find the stress–strain–state of a piecewise–homogeneous medium

Algebrization of basic solving equations

Taking advantage of the expansion of the function $\varsigma(z)$ in the main period band, and also taking into account that, $g(x)=-g(-x)$, $g_1(y)=-g_1(-y)$ and applying the change of variables, the integral equations (12) – (14) are reduced to the standard form. The use of quadrature formulas [4, 5, 6] allows replacing the basic resolving equations (12) – (14) with two finite systems of algebraic equations for the approximate values p_k^0, R_v^0 of the desired functions at the nodal points

$$\sum_{k=1}^{n}a_{m,k}p_k^0-\frac{1}{2}\mathrm{Im}\left[A+f_1'(\eta_m)\right]=0,$$
$$(\mathrm{m}=1,2,\ldots,\mathrm{M}-1),\quad(14)$$
$$\sum_{v=1}^{n}a^*_{m,v}R_v^0-\frac{1}{2}\mathrm{Im}\left[f_{1b}'(\eta_m)\right]=0.$$

Здесь

$$a_{m,k}=\frac{1}{2M}\left[\frac{1}{\sin\theta_m}\mathrm{ctg}\frac{\theta_m+(-1)^{|m-k|}\theta_k}{2}+B(\eta_m,\tau_k)\right],$$

$$a^*_{m,v}=\frac{1}{2M}\left[\frac{1}{\sin\theta_m}\mathrm{ctg}\frac{\theta_m+(-1)^{|m-v|}\theta_v}{2}+B_*(\eta_m,\tau_v)\right].$$

To systems (14) it is necessary to add additional conditions (9), which in discrete form take the form

$$\sum_{k=1}^{M}\frac{p_k^0}{\sqrt{1/2\left(1-\lambda_1^2\right)(\tau_k+1)+\lambda_1^2}}=0,$$
$$\sum_{v=1}^{M}\frac{R_v^0}{\sqrt{1/2\left(1-\lambda_2^2\right)(\tau_v+1)+\lambda_2^2}}=0.\quad(15)$$

Systems (14), (1.119) are connected with infinite algebraic systems (11), in which a quadrature relation is substituted for the coefficients.

Since stresses are limited in a composite piecewise homogeneous body, the solution of singular integral equations should be sought in the class of everywhere bounded functions (stresses). Consequently, it is necessary to add the constrained stress conditions at the ends of the pre–fracture zones to the resulting systems. Accounting these conditions, we can get:

$$\sum_{k=1}^{M}(-1)^k p_k^0 ctg\frac{\theta_k}{2}=0,\ \sum_{k=1}^{M}(-1)^{k+M} p_k^0 tg\frac{\theta_k}{2}=0,$$

$$\sum_{\nu=1}^{M}(-1)^{\nu+M} R_\nu^0 tg\frac{\theta_\nu}{2}=0,\ \sum_{\nu=1}^{M}(-1)^{\nu} R_\nu^0 ctg\frac{\theta_\nu}{2}=0.$$

Since the dimensions of the pre–fracture zones are unknown, the combined algebraic system of equations turned out to be nonlinear even with linear–elastic constraints. To solve it, the method of successive approximations was used. In the case of the nonlinear law of deformation of bonds in determining the forces in the bonds, an iterative algorithm similar to the method of elastic solutions was also used [1, 4]. To determine the limiting state at which the growth of cracks occurs, the deformation fracture criterion was used.

$$w^+(x,0)-w^-(x,0)=\delta_{IIIc},\ w^+(0,y)-w^-(0,y)=\delta_{IIIc}.$$

Here δ_{IIIc} – is the characteristic of material resistance to cracking.

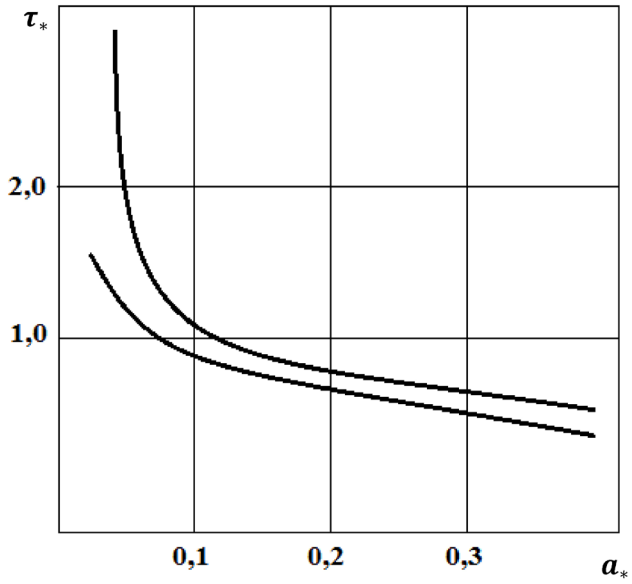

Figure 2. Dependence of the critical load on the distance for both ends of the crack

Based on the results obtained in (Fig. 2) in the case of a hard turn on $\nu_s=0{,}3$, when the graphs of the critical load $\tau_*=\tau_{xy}^{\infty}\sqrt{\omega}\,/K_{IIc}$ as a function of the distance for both ends of the crack are plotted, along the abscissa axis (curve 1 corresponds to the left end) at. In (fig. 3–4) show the dependence of the ultimate load on the crack length. In the calculations it was taken.

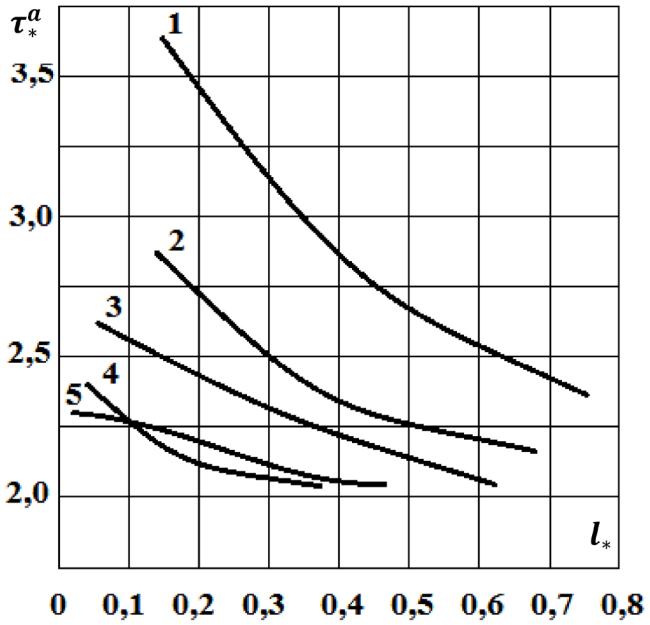

Figure 3. Dependence of maximum load on crack length

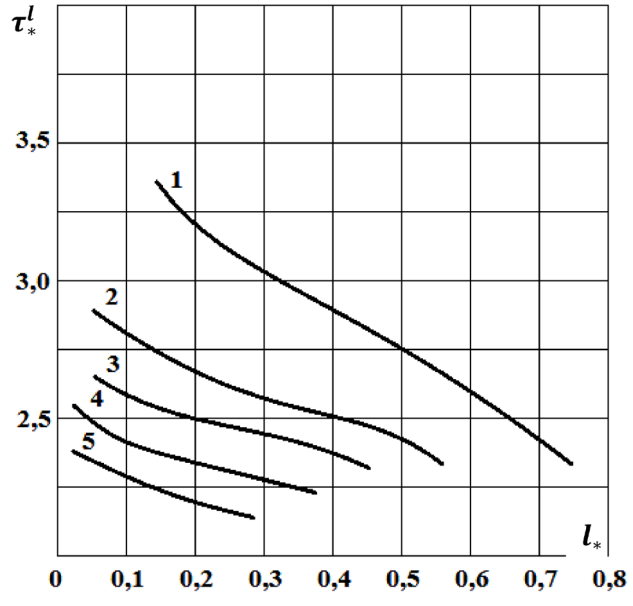

Figure 4. Dependence of maximum load on crack length

Analysis of the critical equilibrium part in a composite with a periodic structure, in which cracks appear, reduces to a parametric laws of the combined algebraic system and the criterion for the appearance of cracks under different laws of bond deformation, elastic constant materials and geometric characteristics of the composite.

The solution of the combined algebraic system allows us to determine the critical value of the external load, the size of the pre–fracture zones and the tangential stresses in the bonds in the state of ultimate equilibrium, during which cracks are formed in the bonding composite.

Straightly from the solution of the obtained algebraic systems, the tangential stresses in the bonds and the shift of the coasts of the pre-fracture zones are determined. The obtained relations allow us to investigate the cracking in the composite body during longitudinal shear.

References:

1. Bolotin V. V. Mechanics of nucleation and initial development of fatigue cracks // Fiz.–chemical chem. Mat. 1986.– Vol. 22.– No. 1.– P. 18–23.
2. Van Fo Fe G. A. Theory of reinforced materials.– Kiev: Sciences. Dumka, 1971.– 230 p.
3. Mustafayev A. B. Crack origin in a uniformly rotating thick–walled cylinder // Mechanics. Mechanical Engineering, 2009.– No. 1.– P. 13–15.
4. Mirsalimov V. M. Destruction of elastic and elastoplastic bodies with cracks.– Bak: Elm, 1984.– 124 p.
5. Mehtiyev R. K. The longitudinal shift of bodies with a complex structure weakened by straight-line cracks // Construction mechanics and the calculation of structures issn 0039–2383 No. 52017.– P. 69–72.
6. Mamedov A. T., Mehtiyev R. K. Simulation of a fibrous composite reinforced with unidirectional orthotropic fibers, weakened by rectilinear cracks during longitudinal shear // Mechanics of composite materials and structures. October-December, 2017.– Vol. 23.– No. 4.– P. 579–591.

Orazimbetova Gulistan Jaksilikovna,
candidate of technical sciences, associate professor,
doctoral candidate, Research and test center "Strom"
Institute of General and inorganic chemistry of the Academy
of sciences of the Republic of Uzbekistan,
E-mail: guli@inbox.ru

Iskandarov Mastura Iskandarovna,
doctor of technical sciences, professor,
head of the Research and test center "Strom"
Institute of General and inorganic chemistry of the Academy
of sciences of the Republic of Uzbekistan,
E-mail: mastura-iskandarova@rambler.ru

Mironyuk Nina Anatolievna,
senior research associate Research and test center "Strom"
Institute of General and inorganic chemistry of the Academy
of sciences of the Republic of Uzbekistan

Kurbanova Aypara Djoldasovna,
candidate of chemical sciences, senior lecturer at the
Tashkent Institute of Engineers and Irrigation
and Melioration of Agriculture

OPTIMIZATION OF RAW MATERIAL MIXTURES FOR BURNING PORTLANDCEMENT CLINKERS at JV LLC "TITANCEMENT"

Abstract: For the purpose of preliminary study of the raw material base of the cement plant of the JV LLC (Joint Venture Limited Liability Company) "Titan cement", the chemical composition of the samples of raw materials selected from various sites of raw materials in the region of the enterprise construction was determined. Technological tests have established that the limestone of the Jamansay-2 deposit, the clayey component of the Severniy Jamansai deposit and the basalt rock of the Berkuttau section of the chemical composition completely meet the requirements of O'zDSt 2950 and are suitable for use as raw materials in the production of portland cement clinkers for cements general construction according to GOST 10178 and sulphate-resistant according to GOST 22266 for compressive strength not less than "400".

Keywords: limestone, clayey component, basalt rock, general construction, sulfate-resistant, technological tests, optimal temperature regime, firing, clinker, milling, cement.

Introduction: After the chemical analysis of the samples, the raw components of the optimal chemical composition are established, which are recommended for selection for use in carrying out technological tests for the production of clinker and cement. Technological tests of the limestone of the Jamansay-2 deposit, the clay component of the Severny Jamansai deposit, the basalt rock

of the Berkuttau site and the gypsum stone of the Severniy Jamansai deposit have been selected for carrying out the technological tests [1]. Taking into account the chemical composition of the selected raw components, mixtures of raw mixtures and clinkers for general construction and sulfate-resistant cements were calculated. The reactivity of raw mixtures is determined and the compositions for laboratory and technological tests are optimized. When using raw mixtures of optimal compositions (two-component: limestone, basaltic rock and three-component: limestone, clayey component, cinder), synthetic batches of clinkers for general and sulfate-resistant cements were synthesized [2]. The chemical-mineralogical composition of the experienced clinkers is determined. The physicomechanical properties of cements based on the experimental clinkers and gypsum stone of the Severny Jamansai deposit have been established. Issued Conclusion on the suitability of the limestone deposit "Jamansay-2", the clay component of the field "Northern Jamansai" and the basalt rock of the site "Berkuttau" for the production of portland cement clinkers for general and sulfate-resistant cements with a compressive strength of at least "400". Gypsum stone of the deposit "Northern Jamansai" is recommended for use in the production of cements as a regulator of the setting time.

Formulation of the problem: The studies were conducted with the aim of establishing the possibility of using local raw materials for the production of general and sulfate-resistant Cement cements at the strength of at least 400 at the Titancement JV.

Methods of materials research, equipment and tools: When carrying out tests to assess the quality of raw components, the chemical analysis of raw materials, raw mixtures and firing products was carried out in accordance with the requirements of GOST 5382–91 "Cements and materials of cement production. Methods of chemical analysis "[3]; the mineralogical composition of the raw materials and firing products was determined on the X-ray unit "DRON-4" with a copper anode at a shooting speed of 2 degrees per minute and the use of *á*-quartz as an external standard; the temperature interval of melting of the basalt rock of the Berkuttau site was established according to the procedure developed at the Strom Research Institute of the Institute of General and Inorganic Chemistry of the Academy of Sciences of Uzbekistan using a high-temperature electric heating furnace; Compositions of raw mixtures and clinkers for general construction and sulfate-resistant cements are calculated according to a special program using SD formulas. Okorokova in accordance with the requirements of O'z DSt 2801: 2013 "Portland cement clinker. Specifications" [4]; the fineness of grinding raw mixes and cements was determined in accordance with the requirements of GOST 310.2–76 "Cement. Test methods "; physical and mechanical tests of experimental cements are made in accordance with GOST 310.1–310.4 "Cement. Test methods " [5]; assessment of the quality of raw materials for clinker production was carried out in accordance with the requirements of O'zDSt 2950: 2015 "Raw materials for the production of portland cement clinker. Technical conditions" [6]; The quality assessment of the gypsum stone used for grinding experienced clinkers on cements was made in accordance with the requirements of O'zDSt 760–96 "Gypsum and gypsum anhydrite stone for the production of binding materials. Technical conditions" [7]; Physical and mechanical properties and chemical composition of test cements were classified according to compliance with the requirements of GOST 10178–85 "Portland cement and slag portland cement. Technical conditions" [8]; GOST 30515–97 "Cements. General technical conditions "and GOST 22266–94 "Sulfate-resistant cements. Technical conditions" [9].

Results and its discussion: Raw materials of optimal mixes No. 2 and No. 16, technological characteristics of which are given in (table 1).

Table 1.– Technological characteristics of the experimental raw materials

No.	Name and the material composition of the raw mix,%	The fineness of grinding on the residue on sieve number 008,%	Bulk mass, t/m^3	Angle of natural slope, degree	Calculated meanings		
					H	n	p
1	**Raw mixture number № 2** – limestone – 83.19 – basalt. breed – 16.81	9.85	0.980	46 ± 2	0.90	2.72	2.31
2	**Raw mixture number № 16** – limestone – 82.72 – clay comp.– 8.90 – cinders of Almalyk Miningand Metallurgical Combine – 8.38	9.40	0.975	46 ± 2	0.87	1.94	0.75

After dosing and homogenization of the components, the raw materials mixtures No. 2 and No. 16 were moistened to (8–10)% and granulated.

Samples-granules after drying at (100–105) °C were fired in a silicon silicate furnace at optimum temperature conditions with a 30 minute exposure:

– an interval for roasting of raw mix No. 2 (1400–1420) °C

– an interval for roasting of raw mix No. 16 (1430–1450) °C

The firing temperature was measured with a TPD thermocouple with the temperature recorded on the secondary device. After firing, the granules were removed from the furnace for rapid air cooling.

The quality of firing products (experimental clinker No. 2 and No. 16) was controlled by the content of free calcium oxide, which was determined by the alcohol-glycerate method according to GOST 5382.

In the averaged samples of experimental clinkers, it was experimentally established: the content of free calcium oxide:

– in clinker No. 2–0.05%; – in clinker number 16–0.10%

content of chlorine ion, determined according to GOST 5382:

– in clinker No. 2–0.05%; – in clinker number 16–0.06%

The averaged samples of clinker No. 2 and No. 16 were studied by X-ray phase and chemical analysis methods. On the roentgenogram of the experienced clinker No. 2 on the general construction cement (Fig. 1), diffraction reflections characteristic of the main clinker phases are noted: C_3S with d/n = (0.298; 0.292; 0.278; 0.272; 0.261; 0.255; 0.214; 0.195; 0.191; 0.181; 0.175; 0.161; 0.156; 0.147 …)nm; C_2S with d/n = (0.288; 0.272; 0.261; 0.230; 0.214; 0.205 …)nm; C3A with d/n = = (0.272; 0.214; 0.191 … 0.153)nm; C_4AF with d/n = (0,261; 0,191; 0,188 …)nm. X-ray diffraction clinker No. 16 on sulphate-resistant cement (Fig. 1) shows diffraction reflections of clinker phases characteristic of normalized mineralogical clinker composition: C_3S with d/n = =(0.298; 0.272; 0.261; 0.255; 0.241; 0.214; 0.195; 0.195; 0.181; 0.175; 0.161; 0.156; 0.147 …)nm; C_2S with d/n = (0.288; 0.272; 0, 0.261; 0.228; 0.214; 0.203 …)nm; C_3A with d/n = (0.272; 0.214; 0.191 … 0.156)nm; C4AF with d/n = (0.277; 0.267; 0.261; 0.203; 0.191 …)nm. The intensity at the background level of diffraction reflections with d/n = =(0.240 and 0.169) nm confirms the data of chemical analysis about low the content of free calcium oxide (0.05–0.10)% in the experimental clinkers No. 2 and No. 16.

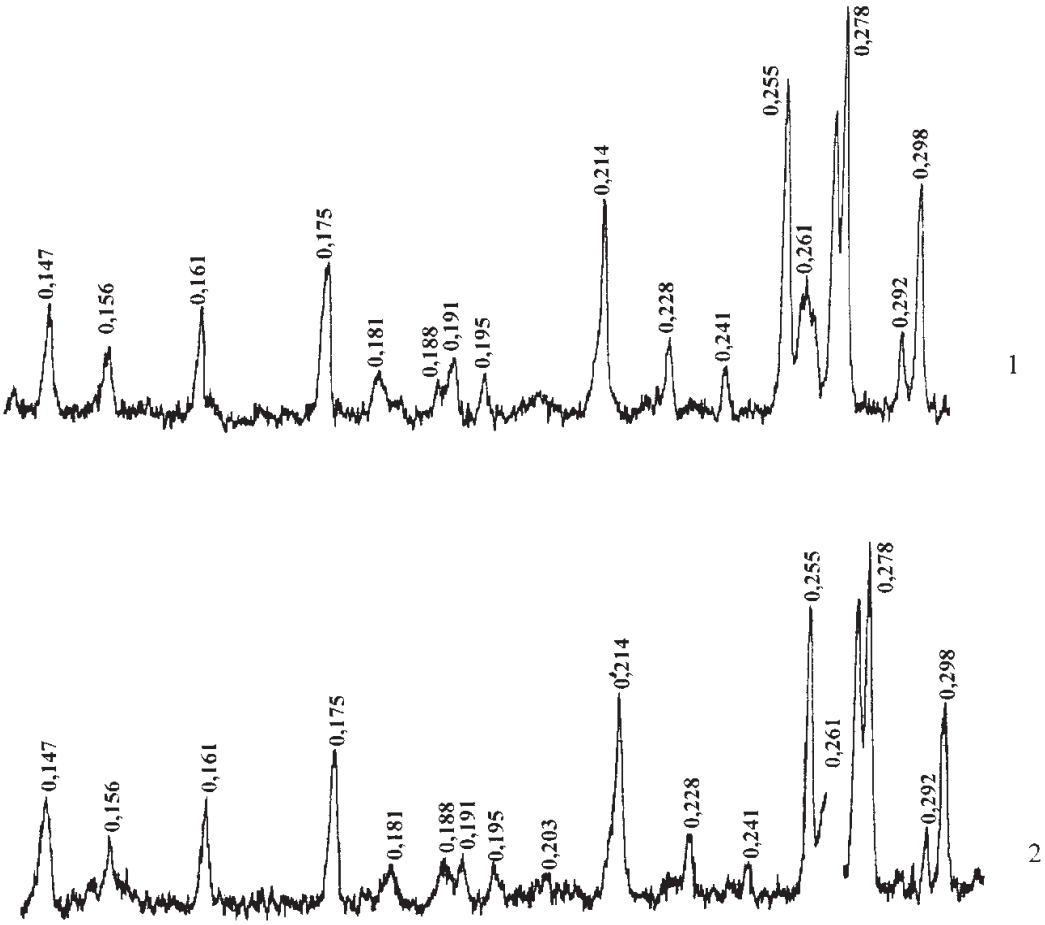

Figure 1. X-ray of experienced clinkers, nm: 1 – experienced clinker number 2; 2 – experienced clinker number 16

The presence of clearly fixed diffraction reflections of the main clinker phases and the absence of intermediate phases on radiographs of the clinkers indicates the complete completion of the processes of mineral formation during the firing of raw mixes.

The chemical and calculated mineralogical compositions of the experimental clinkers No. 2 and No. 16 are listed in (Table 2).

Table 2.– Chemical, computational mineralogical composition and modular characteristics of experimental clinkers

№	Name clinker	oxide content,%									Modular characteristics of experienced clinkers		
		calcination limit	SiO_2	Al_2O_3	Fe_2O_3	CaO	MgO	SO_3	R_2O	TiO_2	H	n	p
1.	Experienced clinker № 2	0.15	22.15	5.80	2.40	65.95	1.05	0.35	1.95	0.20	0.90	2.70	2.42
2.	Experienced clinker № 16	0.10	21.92	4.85	6.27	63.40	0.80	0.55	1.85	0.26	0.87	1.96	0.77

Settlement-mineralogical composition,%: experienced clinker No. 2: C_3S = 58.92; C_2S = 19.05; C_3A = 11.30; C_4AF = 7.30 experienced clinker No. 16: C_3S = 49.96; C_2S = 25.14; C_3A = 2.19; C_4AF = = 19.06 is the content of chlorine ion,% by mass: in clinker No. 2–0.05; in clinker No. 16–0.06 – the content of free calcium oxide,% by weight: in clinker No. 2–0.05; clinker number 16–0.10.

From the data table. 2 it follows that the actual chemical and mineralogical compositions of the experimental clinkers No. 2 and No. 16 are close to the calculated values and meet the requirements imposed by O'zDSt 2801 on the chemical-mineralogical composition and modular characteristics of the clinkers for general construction and sulphate-resistant cements.

Conclusion: Thus, it has been experimentally established that based on local raw materials (limestone from the Jamansay-2 deposit, clay component from the North Jamansai deposit) and basalt rock of the Berkuttau section, it is possible to produce general construction and sulphate-resistant cements, according to the quality indicator that fully complies with the requirements of GOST 10178 and GOST 22266 and of a brand with a strength of at least "400". Raw mixtures are highly reactive. Under optimal firing conditions with the use of the tested raw materials, clinker was synthesized for general construction and sulphate-resistant cements. Experienced clinker in chemical-mineralogical composition and modular characteristics comply with the requirements imposed by O'zDSt 2801 for clinkers for general construction and sulphate-resistant cements. According to the physicomechanical property, cements based on experienced clinkers fully comply with the requirements of GOST 10178 and GOST 22266 and have a strength of at least "400".

References:

1. Butt Yu. M., Timashev V. V. Workshop on chemical technology of binders.– M.: Higher school, 1978.
2. Gorshkov V. S., Timashev V. V., Saveliev V. T. Methods for physico-chemical analysis of binders.– M.: Higher school, 1981.
3. GOST 5382–91. Cements and materials for cement production. Chemicalanalysismethods.
4. O'z DSt 2801: 2013. Portland cement clinker. Technical conditions.
5. GOST 310.1–310.4–81. Cements. Test methods.
6. O'z DSt 2950: 2015. Raw materials for the production of Portland cement clinker. Technical conditions.
7. O'zDSt 760–96. Stone gypsum and gypsum anhydrite for the production of binders.
8. GOST 10178–85. Portland cement and slag Portland cement. Technicalconditions.
9. GOST 22266–94. Sulfate-resistant cements. Technical conditions.

Orumbayev Rakhimzhan Kabievich,
doctor of engineering, professor at
Almaty University of Power Engineering and Telecommunications
Kibarin Andrey Anatolievich,
candidate of engineering, head of Heat Power Units
department at Almaty University
of Power Engineering and Telecommunications
Korobkov Maxim Sergeevich,
Engineer at Almaty University
of Power Engineering and Telecommunications
E-mail: korobkovmax@gmail.com
Khodanova Tatyana Viktorovna,
Senior lecturer at Almaty University
of Power Engineering and Telecommunications

NEW ASEISMIC HORIZONTAL DESIGN KV-GM-55 HOT-WATER BOILERS OPERATIONAL EXPERIENCE

Abstract: This article is dedicated to problems involved in the design of efficient aseismic hot-water boilers. Authors have suggested using the horizontal aseismic design of 35–55 MW capacity KV-GM hot-water boilers in seismically active areas, and to install them inside small boiler houses. According to the extrapolation of experiment data, the temperature of exhaust gases under nominal load equaled to 160 °C, whereas gross efficiency rate of the boiler was about 92.5%.

Keywords: hot-water boiler, heating tests, bi-radiated screen, radiative and convective heat transfer, reliability increase, operational efficiency.

Currently, there is a big number of medium capacity hot-water boilers with outdated design are being used across the whole Republic of Kazakhstan, and which have low efficiency (89–90%) and reliability rates. Main designs of KV-GM and PTVM hot-water boilers were created in the middle of the previous century [1]. New KV-GM-55–150 hot-water boilers with the horizontal design were created by authors due to the technical assignment received from LLP "Almaty teplocommunenergo" (LLP "ATCE"), which wanted to increase the power rates per unit and it was also just about time to substitute outdated PTVM-30MS, PTVM-50 and PTVM-100 boilers as well.

Serial PTVM boilers have tower design and big height of up to 17.6 m. In order to perform the maintenance of tower hot-water boilers, companies had to have a high building to be built next to the boiler, and in the seismically active areas, where the seismic activity reached 9 points of intensity, such boilers were equipped with aseismic supporting structures and that caused sufficient increase of construction costs. That's why authors have suggested KV-GM-55–150 hot-water boiler with an aseismic horizontal design for highly seismic areas, where boilers are to be installed inside the buildings with 9.0 m ceilings or lower.

Hot-water boiler with the new design had it's lower headers (chambers) resting on the basement using special "sliding" supports with convective part of the boiler attached to them.

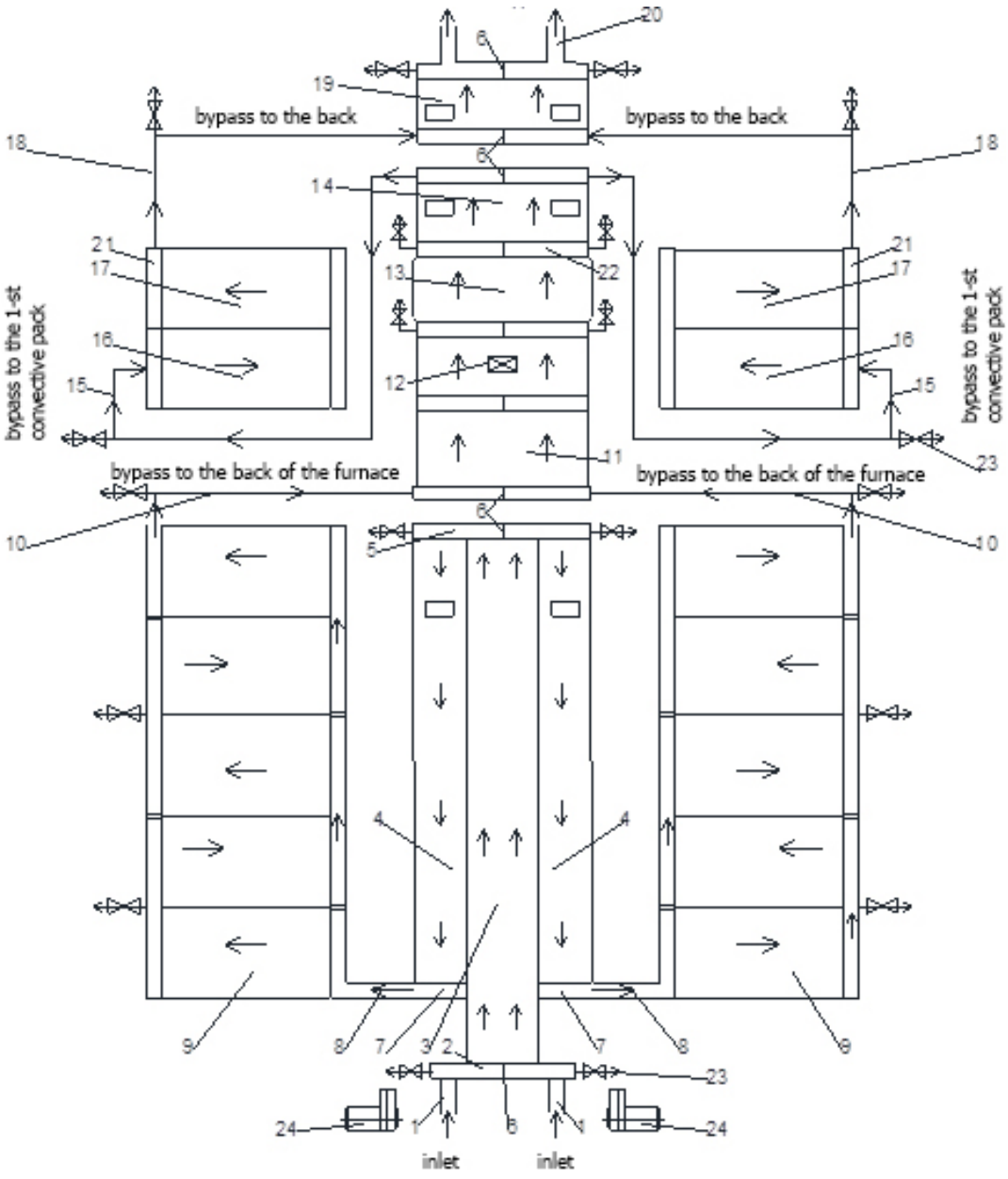

1 – two supplying pipes, Ø327 mm each; 2 – lower front header; 3 – lower Г – shape all-welded screen; 4 – ceiling Г – shape screen; 5 – upper back header of the furnace; 6 – upper separation walls located in the dead middle of the boiler; 7 – two symmetrical Г – shape front headers; 8 – front bypass symmetrical headers; 9 – two symmetrical all-welded side screens; 10 – first upper U – shape symmetrical bypass pipes; 11 – all-welded back screen with lower furnace outlet screen; 12 – lower all-welded screen of the first convective part; 13 – vertical intermediate all-welded screen with upper furnace outlet screen, located between the first and the second convective parts; 14 – upper all-welded screen, located above the first convective part; 15 – second upper U – shape symmetrical bypass pipes; 16 – symmetrical convective packs of U – shaped pipes with checkered placement pattern at the first convective part of the boiler; 17 – symmetrical convective packs of U – shaped pipes with checkered placement pattern at the second convective part of the boiler; 18 – upper third U – shaped symmetrical bypass pipes; 19 – Г – shaped all-welded back screen; 20 – two symmetrical outlet pipes, Ø327 mm each; 21 – upper symmetrical side headers with the upper separation walls that divides the first and the second convective parts in half; 22 – upper header with central separation wall of the vertical intermediate all-welded screen with upper outlet screen; 23 – lower drainage valves; 24 – two symmetrical gas and fuel oil torches

Figure 1. Hydraulic scheme of KV-GM-55 hot-water boiler

Lower headers of side screens are attached to the basement by means of anchor bolts. Expansion of the furnace due to the heating is directed towards the front face, whereas expansion of convective back part is directed towards gas duct. The gas duct of the boiler is equipped with thermal compensator and the second part expands freely towards the back face of the boiler.

General hydraulic scheme of KV-GM-55 hot-water boiler is shown on figure 1 and protected by active Patents of the Republic of Kazakhstan [2; 3]. Water circulation within boiler design in accordance with [2] is performed by means of parallel flows with overall water consumption of up to 658(700) m^3/hour, 329(350m^3/hour) through each symmetrical side of the hot-water boiler, starting at the furnace and going along the whole convective part of the boiler. Coming through the feeding pipes, the water is supplied symmetrically on both sides into the lower front header and then goes through the lower screen, then rotating screen and after that, it is fed towards the front part of the boiler through ceiling screen and then the water falls down through the front screen.

By means of bypass headers of the front screen, the left portion of the flow is supplied into the left side screen, and the right portion of the flow is supplied into the right side screen. Equal water flows circulate 5 times through the left and the right side screens and after that this water is fed into the back outlet screen of the furnace, then, through two symmetrical halves, two flows are falling to the lower outlet header. From the lower outlet header two flows travel through the lower screen of the first convective part and then go up through the intermediate outlet screen to its upper header, and from there the flow comes back to the second upper header of the first convective part via the upper screen. From the second upper header the left portion of water flow goes down through the left convective pack of tubes, and the right portion of water flow goes down through the right convective pack of tubes in the opposite direction to combustion products, and the amount of tubes that go along with the direction of water flow decreases in order to increase its speed in the high-temperature area of furnace gases exhaust. In the lower side convective headers, two flows go through bypass pipes and supplied into the second convective part, where these two flows move up through convective tubes, amount of which decreases in order to increase the speed of water in the opposite-direction pipe in relation to the lowering gas flow. From the side upper convective headers, two water flows travel down into the upper header of the back screen, from where they are then going down into the lower back screen via parallel Г-shaped pipes and extracted beyond the boiler. Fill with new KV-GM-55–150 hot-water boiler with water volume (23.2 m^3) is performed when all air outlet valves are open. Valves are installed between rising and dropping water lines. During the wash of hot-water boiler, all the sludge and slit is being removed from the lowest points via the drainage valves.

There are two PGMG-30 fuel-oil and gas torches installed on the front screen in a parallel manner, which rotate horizontally towards the back of the furnace, washing the tubes of rotating screen in perpendicular motion, then, the gas flow from burners touches the all-welded tubes of back screen and goes through tubes of lower outlet screen coming under the convective pack of tubes of the first convective part. After that, the gas flow rises and through the opposite direction flow line washes convective tubes that are located in the first convective part and have a checkered pattern of placement, then, in the upper part gas flow goes through divided pipes of intermediate outlet screen and travels down flowing around the convective tube arranged in a checkered pattern located in the second convective part, then gas flow travels through gas line that is equipped with thermal compensator, and after that gas is extracted beyond the boiler.

The first KV-GM-55 boiler was put into operation in October 2011 and was adjusted to water consumption rate of G = 658 t/hour, (t_1 =63 °C, t_{2+}= = 128 °C, t_{exh}=154 °C), the hydraulic resistance of this boiler was about 0.23 MPa, and the efficiency rate was

about 92.86% under 49.61 MW heating capacity. According to the demand of micro-districts located around the "Akselkent" (Almaty city) boiler house, the heating load of the boiler was corresponding to design indexes. Testing results and operational indexes appeared to be almost identical to design indexes calculated by engineers, who designed the boiler, and almost identical to project indexes as well.

The new arrangement of two convective parts that have Ø32 × 3 mm tubes and located next to each other, was implemented in similar designs of horizontal hot-water boilers, such as KV-GM-35, KV-GM-40, and KV-GM-50. The front, upper, lower, rotating, back and two side screens allowed to create the symmetrical structure [2; 3]. Screens were made in an all-welded manner, and the membranes (fins) were consequently moved to the opposite sides from the center plane by s/d = 1.4 (d = 57 × 4 mm) in accordance with [4]. All-welded separation panel had eleven or thirteen tubes, and each twelfth or fourteenth tube were interconnected by fins with the asbestos insulating plate between them, and they were not welded. The separation walls (fins) of furnace screens were consequently moved to the opposite sides from the centerline plane in order to provide more uniform heating across the whole perimeter of screen tubes. All-welded screen with separation walls that were consequently moved away from the centerline plane [5] is forming the rigid structure. Being assembled in such a manner screens provide sufficient density in the furnace and strengthen the structure of boiler, also making it almost immune to cracks and pops inside the furnace volume and to changing heating loads.

KV-GM-55 boiler was operating for seven heating season in automatic mode along with the auxiliary equipment (APCS – Automatic Processes Control System) and maintaining the fuel oil handling equipment of the boiler house in operational condition. There were still no changes, deformations, leaks or water condensation on screen tubes surfaces or tube packs or headers observed up to the present.

In order to perform heating tests of the new KV-GM-55–150 hot-water boiler No.5 at the "Akselkent" boiler house, there were preparatory works done to the unit, which included the installation of additional gauges, gas analyzing unit with digital duplication (APCS) of boiler characteristics measured in five modes of heating capacity in accordance with typical testing methods.

During the process of testing, boiler's heating capacity was ranging from 25.18 to 49.6 MW, the consumption rate of the 8289 ccal/m^3 gas was ranging from 2700 m^3/hour to 5566 m^3/hour. The excess of air α in the content of exhaust gases was ranging from 1.36 to 1.16 accordingly. The quality of combustion was constantly controlled by the gas analyzing unit.

Main thermal characteristics of the new KV-GM-55 boiler with a horizontal design, which were obtained during operational testing, are shown in (table 1).

Extrapolation of testing results shows that the temperature of outlet gases under nominal load would be 160 °C, whereas the gross efficiency rate of the boiler would be 92.5%, which is significantly higher than the same parameters of boilers currently used in the JSC "ATCE" system of boiler houses [1; 5].

Table 1 – KV-GM-55 hot-water boiler testing results

Parameter	Mode 1	Mode 2	Mode 3	Mode 4	Mode 5
1	*2*	*3*	*4*	*5*	*6*
Heat production rate, MW,	25.95	36.63	43.5	45.79	49.6
Gas pressure, kgf/cm^2	0.051	0.087	0.126	0.139	0.167
Water consumption of a boiler, t/hour	658	658	658	658	658
Air pressure in torches (mm water column)	125	104.7	158	177	208
Inlet/Outlet water temperature, °C	55/89	63/111	63/120	63/123	63/128

1	*2*	*3*	*4*	*5*	*6*
Gas consumption acc. to gauge, m^3/hour	2915	4023	4803	5076	5566
Boiler's hydraulic resistance, MPa, ($R_{in;}$ R_{out}) kgf/cm^2	0.35 (11; 7)	0.35 (11; 7)	0.35 (11; 7)	0.35 (11; 7)	0.35 (11; 7)
Efficiency rate, natural gas operated,%	93.73	93.69	93.34	93.06	92.86
Outside air temperature, °	15	15	15	15	15
O_2 content in exhaust gases,%	5.3	3.1	3.6	3.5	3.2
Discharge pressure in furnace, Pa	30	30	30	30	30
Temperature of exhaust gases, °C	115	133	140	147	154
Heat losses with exhaust gases q 2,%	5.29	5.61	6.07	6.38	6.63
Heat losses into environment, q 5%	0.98	0.70	0.59	0.56	0.51
Specific consumption rate, kg, spec.t/Gcal	152.42	152.48	153.05	153.81	153.84

Nowadays there are three KV-GM-55 hot-water boilers with a new design and six KV-GM-35 and KV-GM-40 hot-water boilers operating in Almaty city.

Authors and boiler engineers have recently perfected designs of KV-GM-55, KV-GM-35, and KV-GM-40 hot-water boilers, they have considered all features and notices obtained from organizations, which were using these boilers. The furnace chamber was equipped with additional two-row wrapping screen, which plays the role of additional radiative surface and intensifies the ignition of gas torches. The efficiency of using bi-radiated screens in hot-water boilers was thoroughly reviewed in the following works [6; 7; 8]. Technical characteristics of the boiler were raised to the following indexes: radiative heating surface H_{rad} = 286.7 m^2, convective heating surface H_{conv} = 1406 m^2, furnace volume V_{rad} = 313.3 m^3. The installation of the additional two-row wrapping screen before the rotating screen at the end of the furnace caused the significant increase of boiler's heating characteristics due to intensification of heat transfer, and to decrease the temperature of exhaust gases behind the boiler along with the increase of boiler's efficiency rate [3] up to 93–93.5% under nominal load.

Nowadays, within the grant financing by Committee of Science of Ministry of Science of the Republic of Kazakhstan for the project AP№ 05133388, the compilation of experience gained due to the operation of new efficient hot-water boilers with medium and low heating production rates using the KV-GM-40, KV-GM-35, KV-GM-55, KV-GM-7.56, KV-GM-3.65 and KSGn boilers as an example.

Conclusion

New generation hot-water boilers KV-GM-55, KV-GM-40, KV-GM-35 are successfully operating within the system of LLP "ATCE", and if speaking about the main characteristics, these boilers surpass boilers with similar designs.

Results of thermal testing have confirmed main calculated parameters pre-defined by engineers in the design of KV-GM-55 horizontal hot-water boiler. The gross efficiency rate of the boiler under nominal load would be 92.5%. The operational experience has shown that during the process of boiler operation it is possible to maintain a high rate of efficiency and low rates of harmful exhausts and greenhouse gases.

Considering the operational experience, notices and remarks obtained from organizations used these boilers, and thermal tests, the design of hot-water boiler was improved – furnace chamber was equipped with additional two-row wrapping screen, which allows increasing heating characteristics of boiler significantly, and raising the design efficiency rate of the boiler up to 93–93,5% under nominal load.

References:

1. Orumbayev R. K., Orumbayeva Sh. R.– Evaluation of economic and ecological effect due to the substitution of outdated hot-water boilers in the Republic of Kazakhstan // Actual Problems of Economics.– Kiev.– No. 5. 2012.– P. 38–43.
2. Innovative Patent of the Republic of Kazakhstan No. 25337. Hot-water boiler. Orumbayev R. K., Orumbayeva Sh. R. and etc. Published bulletin No. 12. 15/12/2011.
3. Utility patent of the Republic of Kazakhstan. No. 2864. Hot-water boiler. Orumbayev R. K., Orumbayeva Sh. R. and etc. Published bulletin No. 21. 11/06/2018.
4. Patent of the Republic of Kazakhstan. No. 11229. Hot-water boiler. Orumbayev R. K., Chizhov V. E. and etc. Published bulletin No. 2. 15/02/2002.
5. Efficiency and reliability increase of fuel oil hot-water boilers of heating systems. Monograph / Orumbayev R. K., Kibarin A. A., Korobkov M. S., Khodanova T. V. // Almaty: AUPET, 2017.
6. Barabash V. V.– Modification of KV-GM and PTVM hot-water boilers: concerning the implemented technical solutions and new designs // "News of heat supply" No. 04 (152) 2013. URL: http://www.rosteplo.ru/nt/152
7. Compilation of hot-water boilers operational experience by OAO (JSC) "Dorobuzhkotlomash" / V. A. Ovchinnikov, S. A. Petrikov, A. K. Krylov // Heat-power engineering. 2011.– No. 12.– P. 22–46.
8. Design-basis and experimental justification of bi-radiated screens installation in PTVM-125 (KVGM-145) working on fuel oil / R. K. Orumbaev, A. A. Kibarin, M. S. Korobkov, T. V. Khodanova // The Austrian Journal of Technical and Natural Sciences, Premier Publishing s.r.o. – Vienna. 7–8. 2017.– P. 15–20.

Tuxtamushova Anisaxon Ubayevna,
senior teacher,
Tashkent Chemical-Technological Institute
Yunusov Mirjalil Yusupovich,
professor,
Tashkent Chemical-Technological Institute,
Ikramova Zulfiya Adilovna,
PhD., Tashkent Pediatrics Medical Institute
Alimxodjayeva Nazira Tillaxodjayevna,
PhD., Tashkent Pediatrics Medical Institute
Sulaymonova Gulchexra Gaybullayevna,
PhD., Tashkent Pediatrics Medical Institute
E-mail: Ulug85bek77@mail.ru

INFLUENCE CRYSTALISTION ABILITIES OF GLASSES ON FORMATION PYROXENES STRUCTURES

Abstact: The general formula of obtained glasses of pyroxene composition is XYZ_2O_6. By virtue of optimal composition of the glass ($Na_{0.2}Ca_{0.8}Mg_{0.8}Al_{0.2}Si_2O_6$), glass crystalline material was obtained, which was underwent to physical and chemical exploring. It is revealed that upon 2 hours heat treatment with temperature of 850 °C, crystalline phases are energetically precipitated in all the studied objects, which coincide with solid solutions of pyroxene structure.

Keywords: glass, diopside, glass-ceramic materials, pyroxsen, Isomorphic replacement.

Introduction. Currently, the creation of materials based on low-cost raw materials for energy and resource-saving technologies with a set of valuable properties dictated by the conditions of their operation does not lose relevance. Such materials are sitalls – glass-ceramic materials (hereinafter referred to as SCM), obtained on the basis of glasses by directional crystallization. On the example of a systematic integrated study [1, 124–134] in the field of obtaining pyroxene sitalls with desired properties, it is necessary to take into account that, in designing the required crystalline phase in a sitall, there are other factors besides common factors [2], feature of the structure and structure of the original melt and glass. The widespread use of the known phenomenon of zomorphism makes it possible to promptly manage the properties of the cellars in the desired direction.

In pyroxene sitalls, even with the participation of components introduced in small concentrations, solid solutions with somewhat different properties are formed compared to the phase not containing isomorphous impurities.

Objects of study. The objects of study were taken glass pyroxene composition and glass-ceramic materials based on them.

Research methods. Complex studies, such as electron microscopic analysis (EMA), differential thermal analysis (DTA), X-ray phase analysis (XRD), IR spectroscopic (X-ray analysis), as well as physicochemical methods of pyroxene glass samples and SCM, obtained on the basis of the optimal composition according to the standard technique.

Results and its discussion. The purpose of this study is to: obtain crystalline sitalls based on pyrox-

ene glass, by isomorphous substitution; elucidation of the dependence of the technological, physicomechanical, chemical properties and crystallization ability of the melt on the phase composition, as well as the identification of areas of coexistence of these phases in optimal ratios for obtaining SCM with desired properties. The design and selection of glass compositions for the further production of SCM from them predetermines what properties the resulting product of their crystallization should have.

The glass composition under appropriate synthesis conditions and heat treatment modes of the glasses under study determines the type, quantitative and qualitative composition of the formed mineral phases, their ratio, composition, residual glass properties, structure and properties of the resulting glass by directional crystallization, carried out with the aim of partial or complete crystallization of the melt. A characteristic feature of crystallized pyroxene glasses is homogeneous microcrystallinity, the presence of which is a necessary condition for the strength of the material.

In sitalls fine crystals are evenly distributed in the vitreous matrix.

Sitalls containing pyroxene solid solutions based on hedenbergite, diopside, aegirine, augite as the dominant phase have high physicochemical properties. For structural studies and the determination of physicochemical and physicomechanical properties, appropriate samples were made. To study the material composition, phase and structural transformations in the process of melting the raw material mixture and crystallization of the resulting melt, a set of research methods was used, including X-ray phase analysis, diffractometry, microscopy and other analyzes. In terms of their chemical composition, all SCM are silicate materials, which are based on, in addition to silicon oxide SiO_2, a number of other oxides – aluminum Al_2O_3, calcium CaO, magnesium MgO, sodium Na_2O, etc., which provide the specified technological and operational properties.

A feature of these materials is that the vitreous and crystalline phases coexist in their structure, the volume ratio of which can vary within wide limits [3]. Depending on the ratio of these phases, it is possible to obtain SCM of various structures, which are used in the future as intended.The structure of the material, the predominant glass phase, results in glass marble, glass crystal or glass silicon, where the individual crystalline formations are dispersed throughout the volume of the vitreous matrix.

If the amount of the crystalline phase in the structure of the material is more than 50–60%, then the glass phase will act as a cementing layer that holds individual crystals of silicates – pyroxenes, etc. Depending on the chemical composition used by us, you can determine the type of the dominant crystalline phase. The chemical composition of glass includes glass-forming oxides such as SiO_2, $A1_2O_3$, CaO, MgO, FeO + Fe_2O_3, $Na_2O + K_2O$, which under a thermal effect in a certain combination can enter into the pyroxene structure.

In order to obtain SCM based on the classical pyroxene composition, we designed and synthesized 18 glass compositions that meet the general formula: $(Me +, Me^{2+}, Me^{3+})\ 2Si_2O_6$, where $Me^{+} = Na^{+}, K^{+}$;

$Me^{2+} = Ca^{2+}, Mg^{2+}, Sr^{2+}$; $Me^{3+} = Al^{3+}; Fe^{3+}$.

We have chosen glass compositions obtained from chemical reagents of the "chd" brand. In the investigated samples of glasses from chemical reagents, the effects of crystallization initiators were studied. For this purpose, we selected 4 glass compositions:

Na Ca Mg Al Si_2O_6, where the values of a and d range from 0.05 to 0.2; the values of b and c are in the range 1.0 ÷ 0.6.

Glass melting and sample preparation for the study were carried out in the laboratory using the accepted classical glass melting technology.

Selection of an effective crystallization stimulator, to which the requirements of non-volatility, durability and effective stimulating action are presented, as crystallization nucleators, we tested the additives Fe_2O_3–2%, Cr_2O_3–1%, which were introduced into the glass in excess of 100%. The effect of combined stimulants was also studied, in particular, the total effect of Fe_2O_3

+ Cr_2O_3, which provides the bulk crystallization of pyroxene glass compositions, was studied. The choice of the type and concentration of the above additives is due to the fact that the compositions of a number of raw materials and industrial waste such as loess, kaolin, slags and others contain the indicated oxides. Combined combined use of various types of natural materials and metallurgical slags for the synthesis of pyroxene sitalls can be without the introduction of special stimulating components and base materials, which provides significant economic efficiency, since these materials are composed of those elements that act as initiators of crystallization, forming embryos. Glasses of compositions A11 – A18 without stimulants crystallize volumetrically, but their structure is crystalline and porous.

To determine the stimulating role of Fe_2O_3, Cr_2O_3 oxides, as well as the total effect of Fe_2O_3 + + Cr_2O_3 oxides, glasses with the specified additives were welded at temperatures of 1350–145 °C, with an exposure of 1 hour, in oxidizing conditions. According to the results of the research it was established that the introduction of additives in the specified amounts does not have a significant impact on the technological properties of glasses of pyroxene composition. All investigated glasses are boiled, brightened and formed satisfactorily. The results of the gradient crystallization in the temperature range of 600–12000 °C showed that the best catalytic effect of all the crystallization stimulants studied is the combined additive of the total effect of iron and chromium oxides (Fe_2O_3 + + Cr_2O_3), provided that the coadministration of 2 and 1% is observed respectively. A12, A14 glasses (380 and 410 °C, respectively) have the widest range of crystallization. At the same time, the greatest decrease in the temperature of the lower limit of bulk crystallization (at 60–800 °C) and the formation of a dense crystalline structure were noted.Since the most effective stimulant has a combined additive (Fe_2O_3 + Cr_2O_3), in order to clarify the optimal concentration of Cr_2O_3, it was introduced in amounts of 0.5–1.5% through 0.1% at a constant concentration of iron oxide (2%). It is established that an increase in the addition of Cr_2O_3 from 0.5 to 0.9% significantly expands the temperature range of bulk crystallization (from 150 to 3500 °C) and causes the formation of a dense homogeneous crystalline structure. With a further increase in the concentration of Cr_2O_3 from 0.9% to 1.5%, the catalytic efficiency of the crystallization process almost does not change. Thus, the optimal amount of introduced initiator of crystallization of Cr_2O_3 should be considered to be 0.9% – 1%, when the content of Fe_2O_3 is 2%.

To assess the effect of heat treatment on the structural changes of the samples under study, as well as on their properties, a comprehensive study was conducted, including X-ray phase, differential thermal, electron-microscopic, IR – spectroscopic methods of analysis and some properties (density, chemical stability, TCLE and other).

The IR spectra of the original glass are characterized by the presence of two wide absorption bands in the regions of 900^{-1},200 and 400–600 cm^{-1}. The position of the main absorption band in the region of 1060–1100 cm^{-1} indicates the frame structure of the main silica-oxygen groups.The absorption bands in the region of 400–600 cm^{-1} can be caused by both the deformation vibrations of the Si – O – Si bridging bonds and the Me – O bond vibrations characteristic of spinel formations. The infrared absorption spectra of the products of crystallization of glasses at 650–8000 °C are caused by the appearance of absorption bands of 520, 650, 960 cm^{-1}. The absorption bands at 960 cm^{-1} are associated with the formation of groups close to metasilicates, which are characterized by a chained arrangement of silicon-oxygen tetrahedra.

The alignment of tetrahedra in chains, relative to each other, is also confirmed by the appearance of an absorption band in the region of 770–790 cm^{-1}, which, in the absence of diffraction maxima in the diffractograms of the samples, is obviously explained by the processes of structural ordering and chemical differentiation of glasses preceding its crystallization.

Heat treatment affects the properties of the studied samples in the temperature range of 600 – –6500 °C, there is a slight change in the indicators of the properties of the samples. Chemical resistance to 1NHCl is minimal. Heat treatment of glass at 8000 °C leads to a certain decrease in the density values and temperature coefficient of linear expansion of samples. Obviously, such an ability of the character of changing the values of properties can be explained by the intensification of the processes of chemical differentiation of glass by a pronounced segregation.

Since the complex introduction of iron oxides and chromium has a significant effect on the crystallization of the glass A11-A18 synthesized by us. We studied the change of some properties (chemical stability, density, softening temperature) of chromium and iron containing glasses depending on the ratio of Na_2O and CaO.

It was established that the type of catalytic additive does not play a significant role in the change of properties, only acid resistance. Properties vary mainly depending on the ratio of CaO: MgO and Na_2O: Al_2O_3. An analysis of the experimental data showed that the ratio of Na_2O/CaO has a significant effect in the process of forming the glass-ceramic structure. When the ratio of Na_2O/CaO is 1: 4 and 2: 3 mol, there is a slight bend in the change in properties, which is probably explained by the active formation of pyroxene structural groups in the glasses under study at the indicated ratios of Na_2O/CaO, which affect the physicochemical properties.

In the products of crystallization of glasses having the ratio of Na_2O : CaO = 0.1 : 0.9, the pyroxene phase is formed. This is because the indicated ratios of Na_2O/CaO determine the possibility of formation of structural groups close to pyroxene in glasses, which subsequently apparently facilitates the crystallization of the pyroxene phase in the presence of appropriate stimulants.

Based on a comprehensive study of the effects of additives in glasses A11 – A18, in combination with a change in some properties and phase composition of crystallization products, it was found that the most dense homogeneous structure is formed in the process of crystallization of glasses having a stoichiometric composition $0.1Na2O \cdot 0.8 CaO\ 0.8MgO\ 0.1Al_2O_3\ 2SiO_2$ and $0.15Na_2O \cdot \cdot 0.7CaO \cdot 0.7MgO 0.15Al_2O_3 2SiO_2$ with the introduction of a combined additive ($2\% Fe_2O_3 + 1\% Cr_2O_3$), the monomineral pyroxene phase is released in the crystallization products.

Conclusion. It should be noted that the data on the determination of optimal compositions, conditions and modes of heat treatment, as well as phase formation for crystallization of glasses synthesized from chemical reagents is somewhat different from the data and conclusions made by us for similar compositions of glasses from natural materials. Apparently this is due to the impurities contained in the natural raw materials. From the crystal chemical point of view, this phenomenon can be considered an isomorphous substitution, both in the cationic and anionic sublattices of natural pyroxenes.

References:

1. Саркисов П. Д. Направленная кристаллизация стекла основа получения многофункциональных стеклокристаллических материалов.– М.: РХТУ им. Д. И. Менделеева, 1997 г.
2. Тыкачинский И. Д. Исследования процессов катализированной кристаллизации стекол. Разработка и применение ситаллов // Сборник докладов симпозиума «Катализированная кристаллизация». – М.: ГНИИС, 1982 г.
3. URL: http://www.eatu.ru/book-pub/byt/index.pl 05.04.2012 г.

Section 7. Physics

Shukurlu Y. H.,
doctor of philosophy in physics and mathematics,
Sheki Regional Scientific Center of the National Academy
of Sciences of the Republic of Azerbaijan,
Sheki, Azerbaijan
E-mail: yusifsh@hotmail.com; shrem@science.az

KINETIC PARAMETERS OF THE FIRST AND SECOND STAGES OF THE FISETIN MOLECULE DIFFUSION IN THE FIBROIN FIBER

Abstract: Development of new bioengineering structures made of fibroin – a unique natural silk biopolymer – and its use in regenerative medicine and consumer goods manufacturing is often mentioned in literature data. It is related to the fact that fibroin has many important properties such as biocompatibility, biodegradability, high strength, hygroscopicity and elasticity. All applications of fibroin are related to its physical and chemical properties, one of which is the dyeing affinity of this biopolymer. Dyeing is closely related to the process of mass transfer – diffusion. Consequently, when fibroin is dyed, the most significant part of the dyeing process is the diffusion of dye molecules into microfibrils and this very complex process is not insufficiently studied.

Diffusion is a gradual process, which speed or kinetics is a very important scientific and technological attribute that determines the degree of homogeneity of the adsorbate distribution throughout the adsorbent. We studied the penetration of fisetin molecules into the fibrin microfibrils to determine the effect of different temperatures of the dye solution and the concentration of electrolytes in the solution on the diffusion kinetics parameters.

It is an established fact that the diffusion of the dye continues until reaching an equilibrium concentration in the entire volume of the fiber. Let us mentally divide this process into three stages: 1. adsorption of fisetin molecules on the surface of fibroin fibers; 2. moment when the molecules of fisetin reach the center of the fibroin fiber; 3. begins after the completion of the second and continues until the equilibrium concentration is established in the whole fiber. The first stage occurs almost instantaneously making it impossible to separate this stage from the second stage during the actual dyeing process. Therefore, we shall combine the first and second stages of diffusion.

In this article, by using a three-dimensional physical model of the diffusion of dye in the fiber, we established formulas that describe the kinetics of diffusion of the dye from the adsorption layer to the moment when the fisetin molecules reached the center of the fiber.

Keywords: fisetin dye; molecular diffusion of fisetin; natural silk fibroin; microfibrils of fibroin; temperature of dye solution; concentration of dye molecules in solution; diffusion kinetics parameters; second stage of diffusion; third stage of diffusion.

Introduction

Software is developed to design, calculate and visualize ion-exchange technological schemes. This software aim is to be capable of calculating a multistage sorption process, as well as regeneration and cleaning in several columns of a technological scheme [1]. The relevant literature has many examples of the analytical solution to problems of diffusion kinetics, defined by difficulties in certain geometrical and physical conditions and having no general results that can be used. There is also a second type – those that refuse analytical approach and use scaling and modeling of transfer processes and chemical processes [1]. As suggested by the authors of [2], we also used the third method: the quasistationary method (as named by authors) or an equally accessible surface, due to simplified calculation and detection of physically significant limiting cases.

Silk fibroin is an amphiphilic protein – a chemical compound that has both hydrophilic and hydrophobic properties – with a significant predominance of hydrophobicity. Its isoelectric point is *pI* 4.2. Fibroin is insoluble in water for this reason. Diluted solutions of many acids and alkalis, and becomes negatively charged at pH 7 [3]. Due to the structure of protein fibers, including natural silk fibroin, period of diffusion of the dye is about 1.0–2.0 hours at temperature up to 100 °C. The fibroin obtained from the Bombyx mori cocoons has a high specific surface area, and its fiber diameter is 15–20 microns.

The amorphous section of the fibroin is a structured medium with mobile part similar to a viscous liquid, but the possible forms of fluctuation cavities and slots are limited to an elastic frame [4].

Fisetin is a crystalline dark yellow powder, well soluble in methanol and ethanol. UV: $\lambda_{max(ethanol)}$: 258, 267, 321, 370 *nm*; + $AlCl_3$/HCl: 232, 277, 431*nm*; IR(*KBr*): IR spectrum has absorption bands at 3000 and 2850 cm^{-1}, corresponding to stretching vibrations of C-H link, at 1600, 1560 and 1510 cm^{-1}, corresponding to stretching vibrations of -C = C- aromatic system, bands at 1350 and 1260 cm^{-1}, corresponding to stretching vibrations of C-O, 3400 cm^{-1}; corresponding to stretching vibrations of phenolic -OH, 1050, 970, 900 cm^{-1}, bands of deformation vibration -C-*H*- substituted benzene ring and 1640 cm^{-1}, corresponding to stretching vibrations of C = O g-pyrone, 1425 cm^{-1}, corresponding to deformation vibration of $C\text{-}H_2$, 3400–3300 cm^{-1}, corresponding to the stretching vibrations of the hydroxy groups [5]. Water solubility of fisetin is less than 1 *mg/g*.

Dyeing is one of the most complex and important process of natural silk product processing. In order to solve a certain part of this complex problem, we used the physical model of the distribution of the fisetin molecules in natural silk fiber. The key feature of this approach is that its microparameters – the process of the distribution of the molecules of fisetin in the medium of fibrin microfibrils, are subject of the macroparameters of the medium (density, temperature, concentration). To study kinetics of this process, we used the postulate of chemical kinetics – "The limiting stage principle". Seeing that in our case, diffusion process is divided into three successive stages connected in a certain way through the raw materials and intermediate compounds. The speed of entire process is determined by the diffusion rate constant, which is smallest (and limiting) in the third stage. Body of mathematics used in this work is based on a system of differential kinetic equations that determines the distribution functions of particles in a selected medium with selected speeds.

Experiment

To study the kinetic characteristics of fisetin molecules diffusion in microfibril fibrin, 4*g* of fisetin was dissolved in 4 liters of distilled water and the reference solution was prepared in the same volume and at the same temperature from distilled water. Natural silk fibroin (cocoon thread) was thoroughly cleaned and dried to a constant weight of 100*g* and added into the process solution and into the refer-

ence solution. The dyeing process was carried out with constant stirring, so that the entire surface of the adsorbent was available for adsorption and excluded from consideration the uneven distribution of the substance in the volume. Thermostatic control was used to maintain a constant temperature. The experiment was carried out at a temperature of 293, 313, 333, 353, and 373*K* and at *NaCl* electrolyte concentration of 1, 2, 3, 4, 5 and 6*g/l*. Every 150 seconds, 20 ml samples were taken from the process solution and reference solution and distilled water was immediately added at an appropriate temperature to keep the solution volume constant. The concentration of fisetin in the solution was measured by spectrophotometer at a wavelength of $\lambda = 313.3nm$.

Results and discussion

Figure 1 shows the relation between the diffusion magnitude of fisetin in fibroin fiber and the duration of the treatment of fibroin with a dye at different temperatures, i.e. absorption isotherms: 1–293*K*; 2–313*K*; 3–333*K*; 4–353*K* and 5–373*K*. As is seen from this, the adsorption isotherms are at first form a straight line and can be characterized by their saturation.

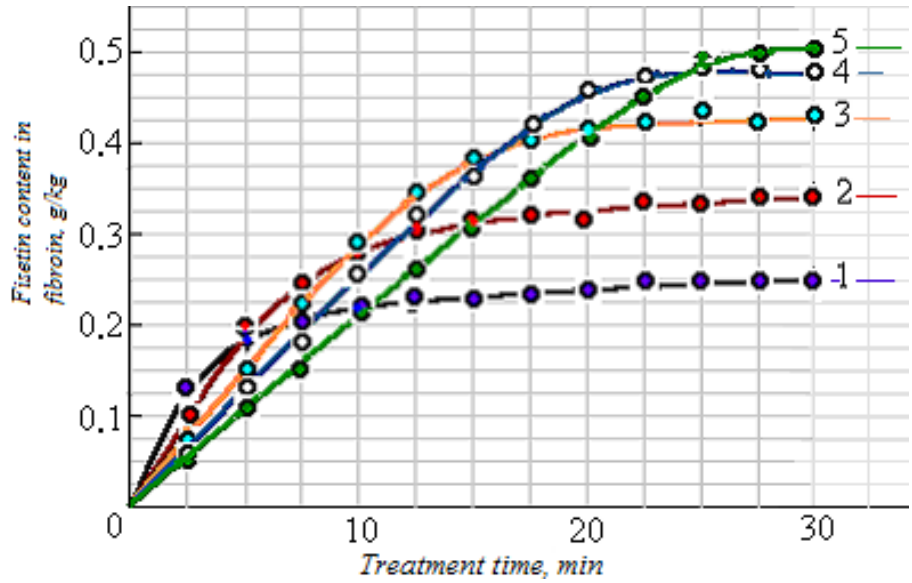

Figure 1. The relation between the diffusion magnitudes of fisetin in fibroin fiber and the duration of the treatment of fibroin with a dye at different temperatures: 1–293 *K*; 2–313 *K*; 3–333 *K*; 4–353 *K* and 5–373 *K*

The introduction of neutral electrolyte *NaCl* into the fisetin dye solution drastically reduces the potential barrier, which makes the dye anions approach the microfibrils to a mutual attraction distance, and the dye is adsorbed by fibroin fiber. *NaCl solution was used as a neutral electrolyte.*

The obtained result (Fig. 2) show that fibroin molecules are bound to Na^+ and Cl^- ions. Therefore neutral electrolytes not only reduce the potential barrier, but also compensate the electric charge, which results in better fiber adsorption. Figure 2 show that the concentration ofin the fisetin solution has an optimal value of – 5 *g/l*.

Experiments have shown that an excess of neutral electrolyte causes aggregation of fisetin anions, preventing their further diffusion into fibroin microfibrils. In summary, it was confirmed that the presence of neutral electrolytes helps to increase the adsorption of the dye fibers.

The adsorption process of fisetin by fibroin occurs almost instantaneously, and the diffusion of dye molecules into the inner fiber is interconnected with this process. In the process of actual dyeing, they cannot be separated. Therefore, the first and second stages of diffusion were studied by us as one, and the third stage was studied separately.

Number of specific dyeing issues were solved by using the physical model of the diffusion of the dye in the fibers and mathematical formulas (Fig. 3), that describe the kinetics of diffusion of the dye from the adsorption layer to the establishment of an equilibrium concentration in the entire volume of the fiber.

Mixing of substances that helps to balance the concentration occurs when there is a concentration gradient in solution. This is three-dimensional diffusion process. We use theoretical assumptions [6] to find a solution suggesting that if the concentration gradient exists only in one direction, then the diffusion issue can be perceived as a one-dimensional problem.

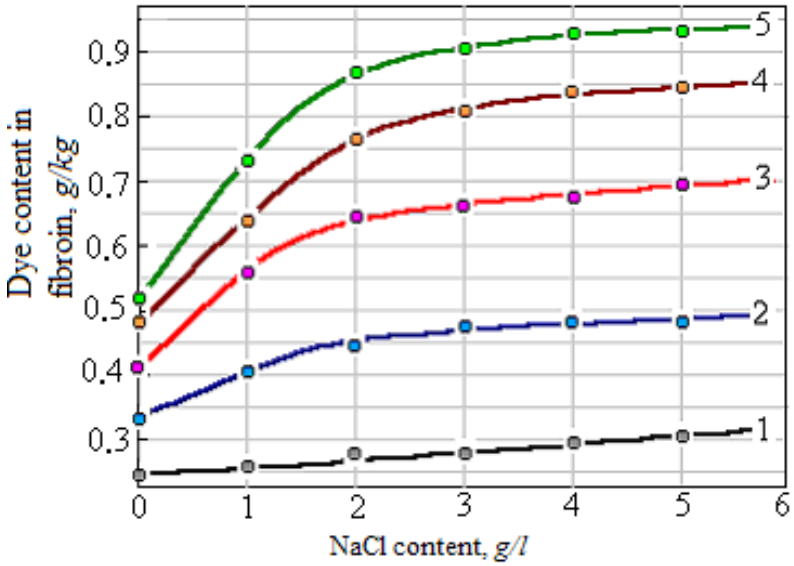

Figure 2. The relation between the content of fisetin molecules and the concentration of *NaCl* in fibroin at different temperatures:
1–293 *K*; 2–313 *K*; 3–333 *K*; 4–353 *K*; 5–373 *K*

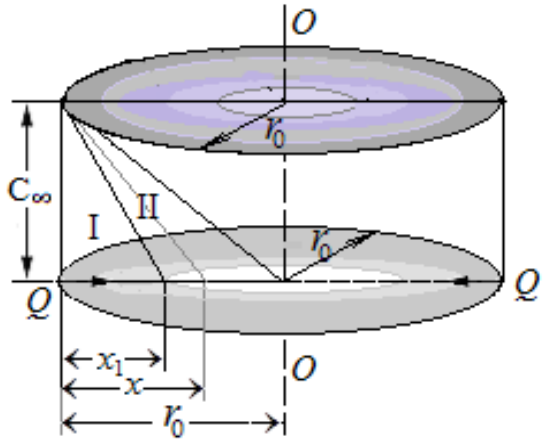

Figure 3. Three-dimensional physical model of the dye distribution in the fiber at the second stage of dyeing

As a part of diffusion process, an amount (or mass) of the substance Δn (or Δm) in a definite time Δt, passes through area ΔS, located along the normal axis, along which the change in substance concentration occurs, and this amount (or mass) is proportional to the concentration gradient dC/dx, area ΔS and time Δt:

$$\Delta m = -\mathrm{D}\left(\frac{dC}{dx}\right)_T \Delta S \Delta t\,, \qquad (1)$$

where D – is the diffusion coefficient, $-D\left(\frac{dC}{dx}\right)_T$ – is the flux density of a penetrating substance (this means the amount of a substance passing through a unit of area per unit of time). With D directly proportional to $\bar{u}$ – the average molecules velocity, and $\bar{\lambda}$ – the average path of molecules:

$$\mathrm{D} = \frac{\bar{\mathrm{u}}}{3}\bar{\lambda}\,. \qquad (2)$$

Where dC/dx – is the concentration gradient of the solute (fisetin in our case) directed to x – center of the fiber.

It should be noted, that concentration C – is means a quantity that is numerically equal to the amount (or mass) of a given substance Δn (or Δm) to the volume V of the mixture and C is expressed in any suitable units, such as mol/cm^3 and g/cm^3. In our case: SI – [n] = 1/m^3{\displaystyle [n]=1/m^{3}}; CGS {\displaystyle [n]=1/cm^{3}}– [n] = 1/cm^3.

Equation (1) formalizes Fick's first law and according to this Fick empirical equation, diffusion flux (J) of penetrant passing through sectional area is determined by the following equation:

$$J = -\mathrm{D}\left(\frac{dC}{dx}\right)_T, \qquad (3)$$

where{\displaystyle n={\frac {N}{V}}} J – is the diffusion flux is in the following units – $mol/(cm^3 \times s)$ [7]. The negative sign in equation (4) appears due to the fact that the particles move in the direction of decreasing concentration.

By plugging (2) in the equation (3), we acquire the following (4):

$$J = -\frac{\bar{u} \cdot \bar{\lambda}}{3}\left(\frac{dC}{dx}\right)_T. \qquad (4)$$

The amount of dQ_x dye (fisetin), diffusing into the fiber (fibroin fiber) through the outer surface S, in a lengthwise direction of fiber for an infinitely small period of time dt, can be reduced to the following equation:

$$dQ_x = JSm_0 dt, \qquad (5)$$

where m_0 – is the mass of fisetin molecules. From (3) and (5) we determine the following:

$$dQ = -\mathrm{D}\left(\frac{dC}{dx}\right)Sm_0 dt. \qquad (6)$$

Using equation (6), we studied the diffusion of fisetin in fibrin fibers. It was assumed that the distribution of the dye concentration over the depth of the fiber is linear, and this makes it possible to compose the following equation:

$$\frac{dC}{dx} = \frac{C_\infty}{x}, \qquad (7)$$

where C_∞ – is the equilibrium concentration of the dye until its fiber moves. This is the end of the first stage (the process of absorption) and beginning of second stage.

The equilibrium is concentration of the dye until its fiber moves. This is the end of the first stage (the process of absorption) and beginning of second stage.

To study the diffusion of the molecules of fisetin in the inner fibroin fiber a three-dimensional physical model of the dye distribution in the fiber at the second stage of dyeing was used (Fig. 3). It shows a cross section of fiber with unit length and the diffusion process reflected in the concentration scale. Therefore, fiber section with unit length has volume: $V = \pi r_0^2$ and side area: $S = 2\pi r_0$.

Considering that the change in concentration during the transfer of dye through the side area over a period of time dt will be equal dC_t^{II} and in the second stage the amount of penetrating dye in the direction x equals

$$dQ_x = \pi r_0^2 m_0 dC_t^{II}. \qquad (7a)$$

Adding (7a) to (6) the following equation is obtained:

$$\pi r_0^2 m_0\, dC_t^{II} = -\mathrm{D}\left(\frac{dC}{dx}\right)Sm_0 dt, \text{ или}$$

$$\pi r_0^2 m_0\, dC_t^{II} = -\mathrm{D}\left(\frac{dC}{dx}\right)2\pi r_0 m_0 dt \qquad (7b)$$

Equation (7) is written after the assumption that the dependence of the concentration of the dye from x is linear. Taking into account the fact that the direction of the fibroin fiber $\vec{r}_0$ and the direction of diffusion $\vec{x}$ are opposite, instead of dC/dx gradient, we can add C_∞ / x and compose (7b) as follows:

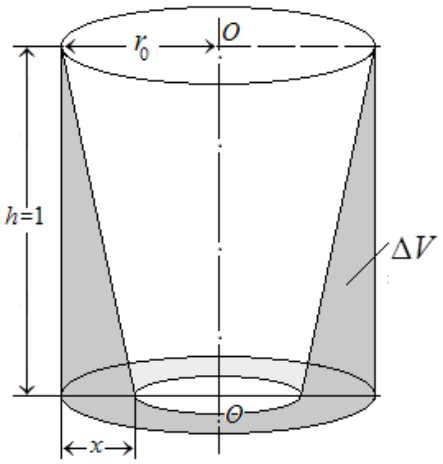

Figure 4. Model of changes in the volume concentration of dye directed to the center of the fiber

$$\frac{dC_t^{II}}{C_\infty} = \frac{2}{x}\cdot\frac{\mathrm{D}}{r_0}dt\,. \qquad (8)$$

The resulting last expression (8) is the **differential equation of the dyeing kinetics** in the second stage of the process. To solve this equation, we first integrate the expression *(7a)*:

$$Q_x = \pi r_0^2 m_0 C_t^{II} + c_1,$$

where c_1 – is the integral constant.

As the initial conditions, we assume that at the initial moment of dye contact with the fiber $(t = 0)$, the fiber has no dye: $Q_x = 0$ and, consequently, $c_1 = 0$. Therefore:

$$Q_x = \pi r_0^2 m_0 C_t^{II}\,. \qquad (9)$$

As shown in figure 4, we use the model of the second stage of fiber dyeing. This model represents the magnitude of the change in ΔV – the volume concentration of dye directed to the center of the fiber, depending on the size of x (dark areas). It is evident that:

$$\Delta V = V_{cylindэу} - V_{ty.conв} = \pi\cdot C_\infty\left(r_0 x - \frac{x^2}{3}\right).$$

By multiplying ΔV by m_0 (the molecular weight of the dyes in this volume) and we find the amount Q_x (mass) of the dye that has already penetrated into the inner part of the fiber:

$$Q_x = \pi\cdot C_\infty m_0\left(r_0 x - \frac{x^2}{3}\right). \qquad (9a)$$

According to the expression (9) and (9a) we can conclude that:

$$r_0^2 C_t^{II} = C_\infty\left(r_0 x - \frac{x^2}{3}\right) \text{ or } C_\infty x^2 - 3C_\infty r_0 x + 3C_t^{II} r_0^2 = 0. \qquad (10)$$

Equation (10) is a quadratic equation in x and since $C_\infty \geq C_t^{II}$, it has two real solutions: $x = 1.5r_0\left(1 \pm \sqrt{1 - \frac{4}{3}\cdot\frac{C_t^{II}}{C_\infty}}\right)$. But $x \leq r_0$. Therefore, we choose the following solution:

$$x = 1.5r_0\left(1 - \sqrt{1 - \frac{4}{3}\cdot\frac{C_t^{II}}{C_\infty}}\right). \qquad (11)$$

By plugging (11) into equation (8), we get the following equation:

$$\left(1 - \sqrt{1 - \frac{4}{3}\cdot\frac{C_t^{II}}{C_\infty}}\right)\frac{dC_t^{II}}{C_\infty} = \frac{4}{3}\cdot\frac{D}{r_0^2}dt\,. \qquad (12)$$

After integrating the differential equation (12), as integrals of irrational functions, the following equation is acquired:

$$\sqrt{\left(1 - \frac{4}{3}\cdot\frac{C_t^{II}}{C_\infty}\right)^3} + 2\frac{C_t^{II}}{C_\infty} = \frac{8}{3}\frac{\mathrm{D}}{r_0^2}t + \mathrm{c}_2\,. \qquad (13)$$

To determine the integration constant c_2, the initial time of the second stage of the diffusion process c_2 is combined with the point of the corresponding end of the first stage t_I. Therefore at $t_{II} = 0$, the ratio $\frac{C_t^{II}}{C_\infty}$ can be reduced to $\frac{C_t^{I}}{C_\infty}$, which means:

$$\frac{C_t^{II}}{C_\infty} = \frac{C_t^{I}}{C_\infty}\,. \qquad (13\,a)$$

By putting equality (13a) into equation (13), we get the following equation:

$$\mathrm{c}_2 = \sqrt{\left(1 - \frac{4}{3}\cdot\frac{C_t^{I}}{C_\infty}\right)^3} + 2\frac{C_t^{I}}{C_\infty},$$

where C_t^I – is the concentration of the dye inside the fiber at the end of the first stage of the diffusion process. If we plug the expression c_2 into (13) we get the following equation:

$$\sqrt{\left(1 - \frac{4}{3}\cdot\frac{C_t^{II}}{C_\infty}\right)^3} + 2\frac{C_t^{II}}{C_\infty} = \frac{8}{3}\frac{\mathrm{D}}{r_0^2}t + \sqrt{\left(1 - \frac{4}{3}\cdot\frac{C_t^{I}}{C_\infty}\right)^3} + 2\frac{C_t^{I}}{C_\infty}. \qquad (14)$$

After simplification:

$$\frac{C_t^{II}}{C_\infty} = \alpha\,;\ \frac{\mathrm{D}}{r_0^2}t = \beta\,;\ \left(\sqrt{\left(1 - \frac{4}{3}\cdot\frac{C_t^{I}}{C_\infty}\right)^3} + 2\frac{C_t^{I}}{C_\infty}\right) = \chi, \qquad (14\,a)$$

and by plugging them into (14), we get the following equation:

$$\sqrt{\left(1 - \frac{4}{3}\cdot\alpha\right)^3} + 2\alpha = \frac{8}{3}\beta + \chi\,. \qquad (15)$$

In its canonical form (13), in relation to α, we get the following equation:

$$\alpha^3 - \frac{9}{16}\alpha^2 + \frac{27}{16}\left(1 - \frac{8}{3}\beta - \chi\right)\alpha + \left(3\beta^2 + \frac{9}{4}\beta\chi + \frac{27}{64}\chi^2 - \frac{27}{64}\right) = 0\,. \qquad (16)$$

And (16) is reduced to:

$$a\alpha^3 + b\alpha^2 + c\alpha + d = 0\,, \qquad (16\,a)$$

where $a=1,\quad b=-\frac{9}{16},\quad c=\frac{27}{16}\left(1-\frac{8}{3}\beta-\chi\right),$ $d=3\beta^2+\frac{9}{4}\beta\chi+\frac{27}{64}\chi^2-\frac{27}{64}$.

The cubic equation (16a) can be reduced to a canonical form by replacing the variable {\displaystyle x=y-{\tfrac {b}{3a}},} $\alpha=y-\frac{b}{3a}$ that changes the equation form to:

$$y^3+py+q=0, \qquad (17)$$

where: $p=\frac{c}{a}-\frac{b^2}{3a^2}=\frac{3ac-b^2}{3a^2}$; $q=\frac{2b^3}{27a^3}-\frac{bc}{3a^2}+\frac{d}{a}=$ $=\frac{2b^3-9abc+27a^2d}{27a^3}$.

It is to be recalled that during the adsorption process, the equilibrium concentration in the adsorption layer is reached almost instantly: $t_1\cong 0$, $C_t^I=0$ (the concentration of the dye in the fiber at the end of the first stage of the diffusion process is zero). From (14 a) we determine $\chi=1$. Given this: $a=1$; $b=-\frac{9}{16}$; $c=-\frac{9}{2}\beta$ and $d=3\beta^2+\frac{9}{4}\beta$. Given that:

$$p=\frac{3c-b^2}{3}=-4.5\beta-0.10547 \text{ and}$$

$q=\frac{2b^3-9bc+27d}{27}=3\beta^2+1.40625\beta-0.0132$. From this, we calculate the discriminant of the cubic equation:

$$\Delta=\left(\frac{p}{3}\right)^3+\left(\frac{q}{2}\right)^2=2.25\beta^4-1.2657\beta^3+ \qquad (18)$$
$$+0.317\beta^2-0.0148\beta$$

Considering $\beta=\frac{\mathrm{D}}{r_0^2}t$, $\beta>0$, (18) determines that $\Delta>0$. If $\Delta>0$, then the cubic equation will have one real root and two conjugate complex roots [8]. We are only interested in the real root. The roots of the reduced cubic equation (17) can be found by the Cardano formula:

$$y_1=A+B,\ y_{2,3}=-\frac{A+B}{2}\pm i\frac{A-B}{2}\sqrt{3}, \qquad (19)$$

Where $A=\sqrt[3]{-\frac{q}{2}+\sqrt{\Delta}}$; $B=\sqrt[3]{-\frac{q}{2}-\sqrt{\Delta}}$ and the real root of the canonical equation (17) is $y_1=A+B$. By plugging it into $\alpha=y-\frac{b}{3a}$, we find α for (16 a):

$$\frac{C_t^{II}}{C_\infty}=y_1-\frac{b}{3}=\sqrt[3]{-\frac{q}{2}+\sqrt{\Delta}}+\sqrt[3]{-\frac{q}{2}-\sqrt{\Delta}}-\frac{b}{3}. \qquad (20)$$

The resulting mathematical relationship (20) is a **kinetic equation that describes the first and second stages of the fiber dyeing process**.

Considering that $a=1$; $b=-\frac{9}{16}$; $c=-\frac{9}{2}\beta$ и $d=3\beta^2+\frac{9}{4}\beta$ is same for numerical calculation:

$$p=\frac{3c-b^2}{3}=-4.5\beta-0.1055 \text{ и}$$

$$q=\frac{2b^3-9bc+27d}{27}=3\beta^2+1.406\beta-0.0264. \qquad (21)$$

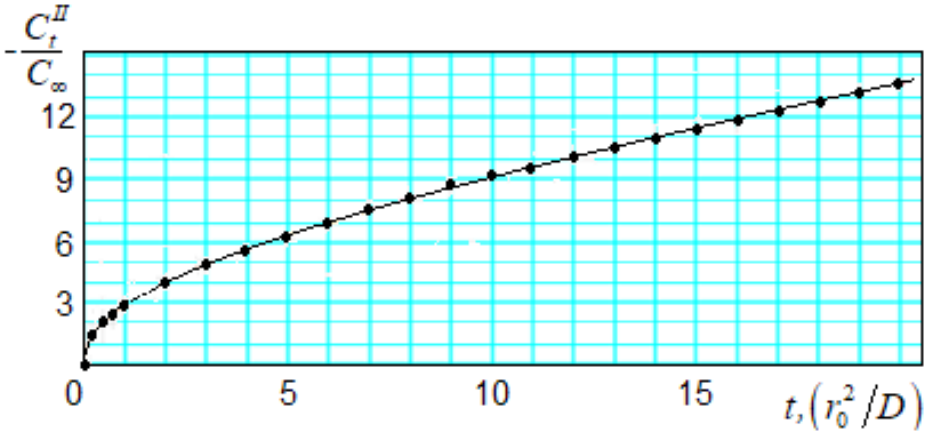

Figure 5. Dependency graph of C_t^{II}/C_∞ concentration of dye molecules on time in r_0^2/D unit of measurement

Figure 5 depicts graph of the kinetic dependence of $C_t^{II}/C_\circ$ on t – in a unit of r_0^2/D, constructed using equation (20) and formulas (21) (the minus sign is placed before the relative concentration, since the gradient of the dye concentration is negative). As graph shows, in the second stage of diffusion, the dependence of the relative concentration in time is parabolic, i.e. the process proceeds in accordance with the diffusion kinetics. This once again proofs the effectiveness of the chosen body of mathematics.

Conclusion. The kinetic equation of the first and second stages of the dyeing fibroin fibers dyeing process with fisetin using a physical model allows us to directly solve the problem of diffusion using numerical calculation. This approach has an advantage – the problem of diffusion does not require additional conditions when solving. This method allows you to fully describe the kinetic equation in both the first and second stages as one, as well as the third stage of the dyeing process, which is described in the next article.

References:

1. Прудковский А. Г. Алгоритм моделирования двухкомпонентной динамики сорбции в случае смешанной диффузионной кинетики / Сорбционные и хроматографические процессы. 2017.– Т. 17.– № 6.– С. 927–934.
2. Франк-Каменецкий Д. А. Диффузия и теплопередача в химической кинетике.– М., Наука, 1987.– 502 с.
3. Франк-Каменецкий Д. А. К диффузионной теории гетерогенных реакций // Журнал физической химии. 1939.– Т. 13.– № 6.– С. 756–758.
4. Архипова А. Ю., Котлярова М. С., Новичкова С. Г. и др. Новые биорезорбируемые микроносители на основе фиброина шелка / Архипова [и др.] // Бюллетень экспериментальной биологии и медицины, 2015.– No. 10.– С. 497–501.
5. Шайтан К. В., Упоров И. Б., Рубин А. Б. К теории миграции лигандов в биомакромолекулах // Молекуляр. биология. 1985.– Т. 19.– С. 742–750.
6. Хасанова С. Р. Экспериментально-теоретическое обоснование создания и стандартизация лекарственных растительных препаратов с антиоксидантной активностью / Диссертация на соискание ученой степени доктора фармацевтических наук, – Уфа, 2016.– С. 173–174.
7. Бекман И. Н. Высшая математика: математический аппарат диффузии: учебник для бакалавриата и магистратуры / И. Н. Бекман.– 2-е изд., испр. и доп.– М.: Издательство Юрайт, 2017.– 459 с.– Серия: Университеты России.
8. Sherwood Th. K., Pigford R. L., Wilke Ch. R. Mass transfer. McGraw-Hill Book Company, Warren L. McCabe, 1975.– 677 p.
9. Гюнтер Н. М., Кузьмин Р. О. Сборник задач по высшей математике. Учебное пособие для вузов. – Санкт-Петербург: Лань, 2003.– 816 с.

Section 8. Chemistry

Islamova Yulduz Urolovna,
The basic doktorant student
of Tashkent Chemical Technological Institute
Republic of Uzbekistan, Tashkent
E-mail: islomova_yulduz@mail.ru
Maksumova Oytura Sitdikovna,
doktor of Chemical Sciences, professor,
Tashkent Institute of Chemistry and Technology
epublic of Uzbekistan, Tashkent
Tadjieva SHaxnoza Abduvalievna,
senior lecturer of Tashkent Chemical Technological Institute
Republic of Uzbekistan, Tashkent

SYNTHESIS OF N-ACRYLOILOCARBAZOLE AND ITS MODIFICATION TO POLYPROPYLENE

Abstract: Interaction with carbazole and acrylic acid has been studied. Polypropylene modification of synthesized N-acryloylcarbazole has been carried out. The ratio of the initial reagents to the reaction was investigated and the optimum conditions of the reaction were determined. N-acryloylocarbazole and its structure were studied using IR, PMR-spectral analysis.

Keywords: carbazole, acrylic acid, hydroxynone, dimethyl formamide, decalene, N-acryloylcarbazole.

Introduction. Carbazole derivatives, such as heterocyclic compounds, are used as medicaments in medicine, as diodes in electrotechnics, as well as raw materials for the production of high molecular compounds. Also, carbazole-derived salts increase the activity of peptide bonds in the human body, and carbazole-derivatives polymers serve as charge collector in capacitors. Carbazole derivative polyepoxypropylcarbazole polymer is a good conductor so, it is used as a light-emitting layer in photoconductor [1, 780–785]. Carbazole derivative homopolycyanurate was synthesized by the authors [2, 1731–1740]. It was observed that the interphase condensation process goes in two steps based on the Shotten-Bauman reaction. The reaction of the linear polymer in the composition of the initial reagents was influenced by the reaction of Cl and NH group and the yield of production was from 56% to 78%.

In another study, the photosophysical properties of indolo [3, 2-b] carbazole derivatives were studied [3, 1629–1635]. Synthesized indolo [3, 2-b] carbazole compounds exhibit high levels of photoluminescence property. These obtained data allowed to use indolo carbazole compounds to be applied in electrolyumination devices. Indolo [3, 2-b] carbazole was used in transistors as an light sensitive electronic material. According to the data, the modification of polypropylene wastes with basic chemical compounds was studied at the temperature of 70–90 °C. Here polypropylene and

polyacrylic acid waste were used [4, 227–232]. Carbazole and acrylic acid reactions were investigated by modifying the ratio of initial reagents based on the above mentioned data. Based on the results of the experiment, it was determined that the reaction carbazole with acrylic acid would proceed without catalysts and catalysts.

Experimental part. Carbazole(dibenzopyrrole) $C_{12}H_9N$ – light yellowish crystalline with sharp odor. $T_{boiling}$ = 245–246 °C, T_{liquid} = 245–246 °C dissolves in acetone, alcohol, toluene. Acryl acid (propene acid) CH_2 = CHCOOH. $T_{boiling}$ = 141.6 °C, d = 1.0511^{20}_{4}, dissolves in acetone, ethanol, ether. In the case of polypropylene colorless granules, the brand J = 150, d = 0.92–93g/sm^3, T_{liquid}=185.2 r, T_{liquid}= 47.7g, is dissolved in the deethylather dekaline. DAA(dinitrile-azo-bisizooil acid) $C_8H_{12}N_4$ colorless white crystalline substance. T_{liquid}=103–105°C. Solvent acetone, benzene, alcohol [5, 392]. IQ-Fure spectrophotometer SISTEM-200, PMR-spectrophotometer Varian UNITY – 400.

N-Acryloylcarbazole synthesis. Dina-Starta, a rectangular tube, a reverse refrigerator, an electric plug, a water separator were used for N-Acryloylcarbazole synthesis. 0.1 ml of carbazole was dissolved in the solvent DMFA and 0.5 mol of acrylic acid with hydroxinone was added. The reaction was carried out at a temperature close to the solvent boil degree for 3 hours and the yield of the product was 72%. The purity of the synthesized compounds was determined by thin-layer chromatography using Silofol plates. System: eluent-benzene-acetone, iodine vapors were used. R_f = 0.8 and R_f = 0.67.

Modification of N-acryloylcarbazole to polypropylene. The modification of acryloylocarbazole to polypropylene was carried out at DMFA and dekaline at room temperature and at 80 °C. DAA was used as aa initiator. The process was carried out for 3 hours in a water bath.

Analysis of results obtained. The reaction of Carbazole and acrylic acid was performed without the use of catalysts in this study. The concentration of the initial reagents without the addition of the catalyst was adjusted to the reaction.

In this study, there was observed the formation of quaternary ammonium (bases) when the ratio of carbazole and acrylic acid to 1: 3 in the reaction. When the same reaction reagent ratio was changed to 1:5 N-(vinylcarbinol) carbazole product was obtained. In this reaction, demethylformamide was used as a solvent. In the experiment, the reaction mechanism can go through the S_N2 mechanism because the reaction can be carried out without catalysts and catalysts. When the catalyst is present in the reaction, the catalyst is the aprotone catalyst and allows the reaction to proceed with the S_N1 mechanism. The solvents make it easier for the reaction to undergo in the S_N2 mechanism. As a result of the experimental results, it can be said that the electrophilic reaction goes according to the S_N1 mechanism. The total appearance of carbazole and acrylic acid reaction can be summarized as follows:

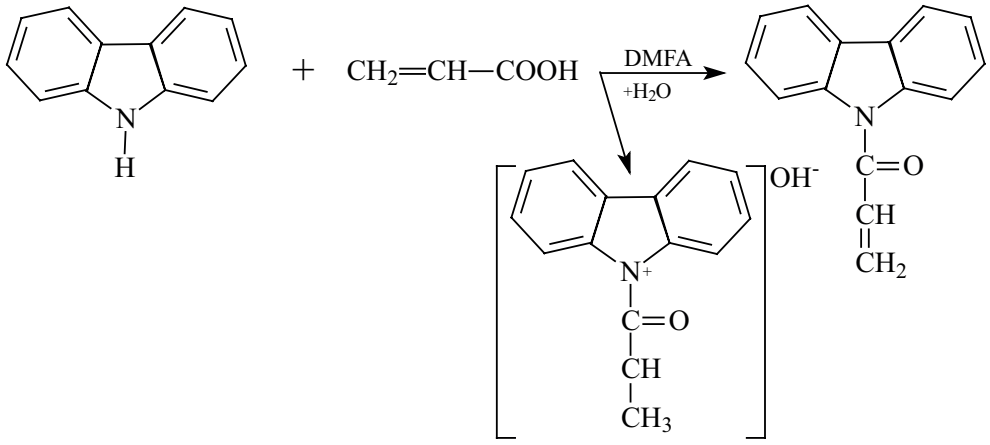

The synthesized N-acryloylcarbazole (AC) and quaternary ammonium salt can be found in the following table.

The structure of the synthesized N-aryloylocarbazole was determined using the IQ and YMR1N spectra. The initial reagents and the IQ-spectrum of the obtained product were obtained (fig. 1).

Table 1.

Carbazole: Ac	The yield of products,%		Liquefaction Temperature, °C		Thin Layer Chromatography, Rf	
	AC	Ammonium salt	AC	Nitric ammonium salt	AC	Clastic ammonium salt
1:1	22	–	–	–	–	–
1:3	25	52	200	220	0.32	0.67
1:5	72	22	200	220	0.80	0.28

In the IQ-spectrum of N-acryloylcarbazole obtained by comparison with them, the formation of carbazole primary structures has been observed to have a new absorption potential in the field of double and single bonds. Valence vibrations of the C = O group in 1717 cm^{-1} and corresponding absorption areas of the valley vibration of the N-C bond in 1282–1306 cm^{-1} were observed.

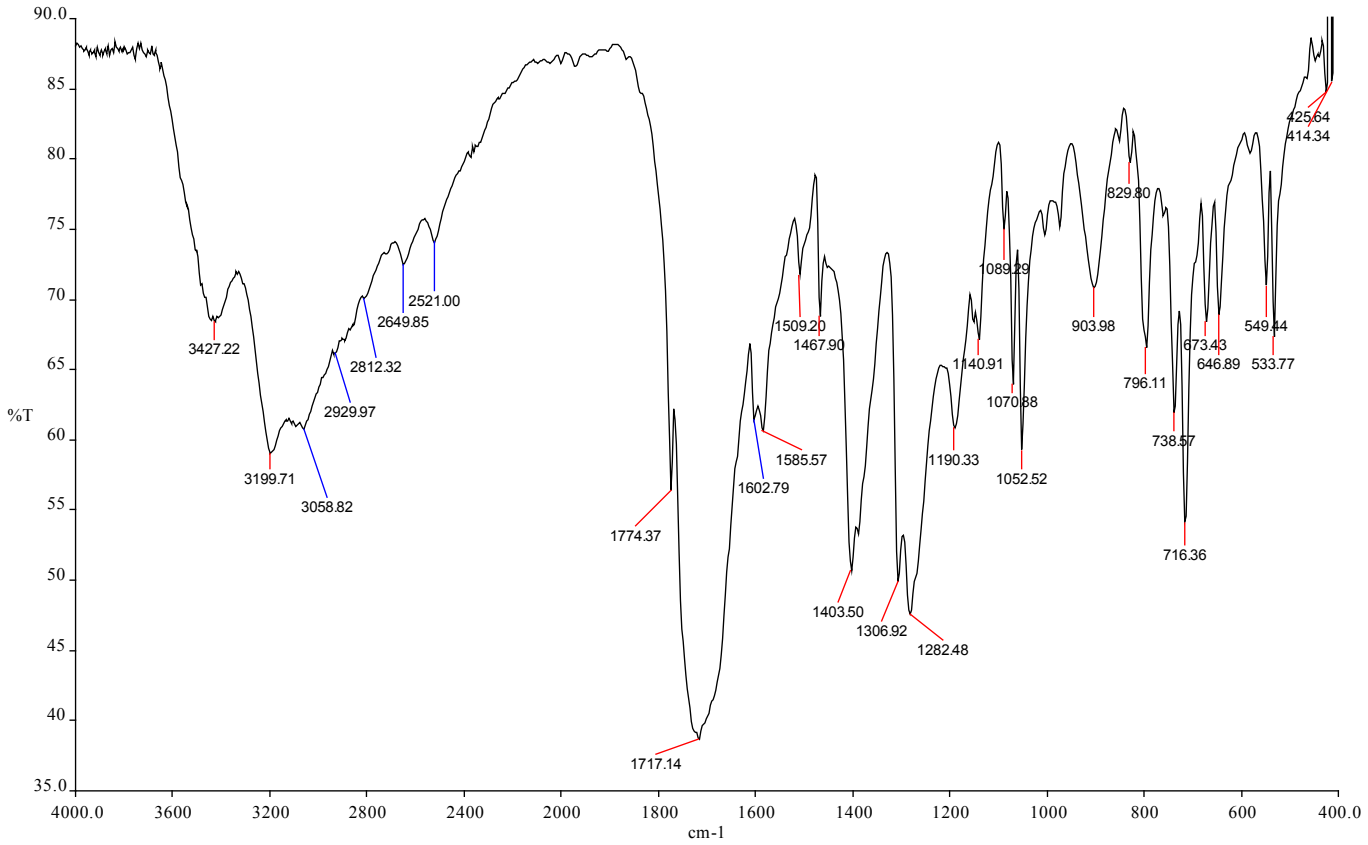

Figure 1. IQ-spectral analysis of N-acryloylocarbazolyl

Additionally, valence vibrations of the CH_2 group were observed in the 1403–1446 cm^{-1}, deformational vibrations of 716 cm^{-1}.

In the PMR1N spectrum of the N-Acryloyl carbazole, doublet-doublet signals of protons in the first and eighth carbon atoms of the aromatic nucleus in 8.22 m.u.field, double-triplet-triplep signals of protons in the second and seventh carbon atoms in 7.43 m.u. field, doublet-doublet-doublet signals of protons in the fourth and fifth carbon atoms in 8.05, and singlet signals of CH group in 3.52 m.u., doublet signals of CH_2 in 4.3 m.u. were determined (fig. 2). PMR spectra were obtained by Varian UNITY – 400.

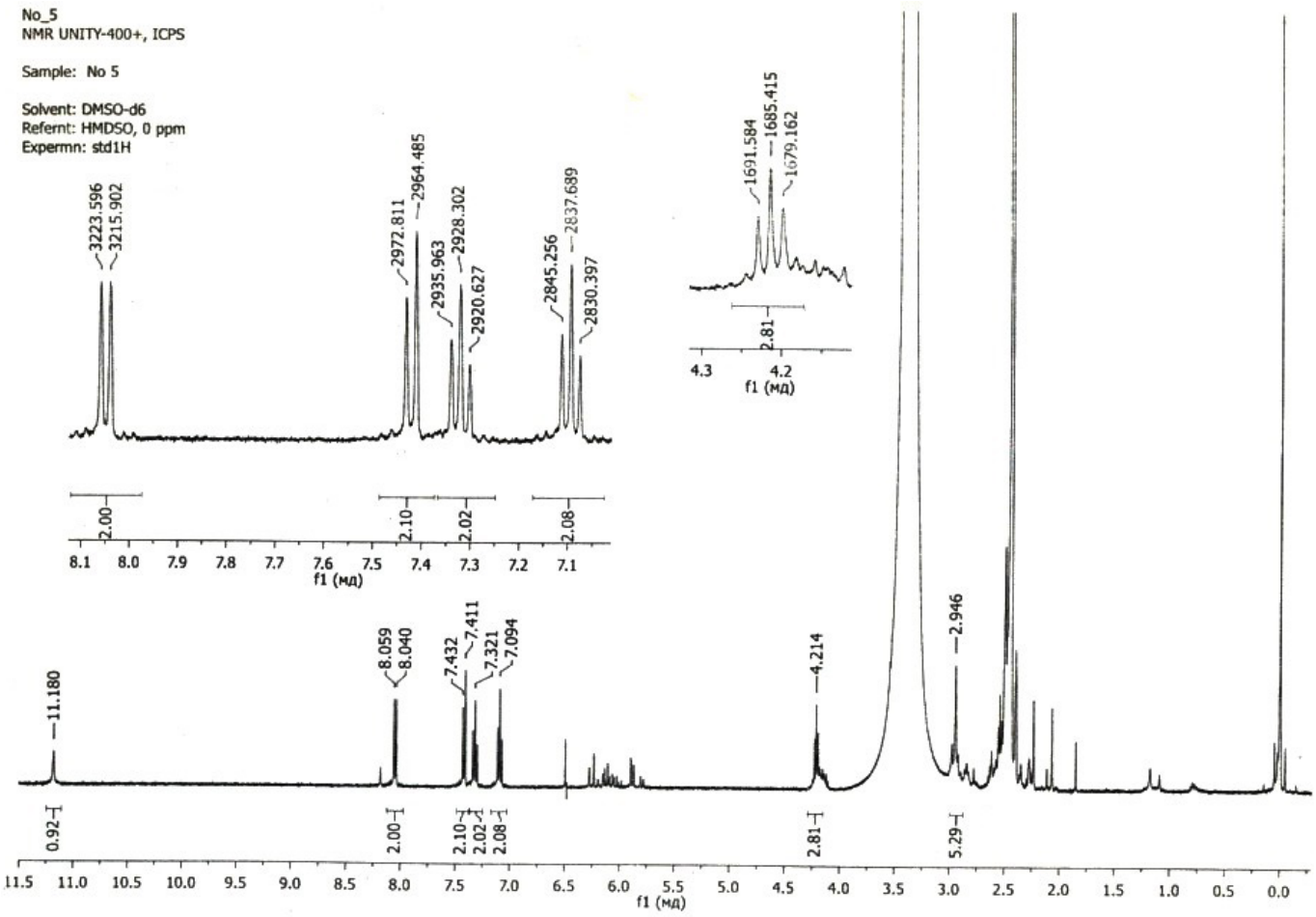

Fig. 2. PMR-spectral analysis of N-acryloylocarbazolyl

Polypropylene is thermoplastic polymer that possesses the density of 0.92–0.93 g/cm^3 and softening temperature of 185 °C, does not dissolve in any solvent at room temperature. Polypropylene is resistant to concentrated acids and alkalis. Polypropylene is used as a variety of electrostatic material and as a coating for various purposes. Linear polymers are obtained on the base of polypropylene, and we have studied the modification of acryloylcarbazole to polypropylene. Polypropylene and acryloylcarbazole modification reaction is shown as below:

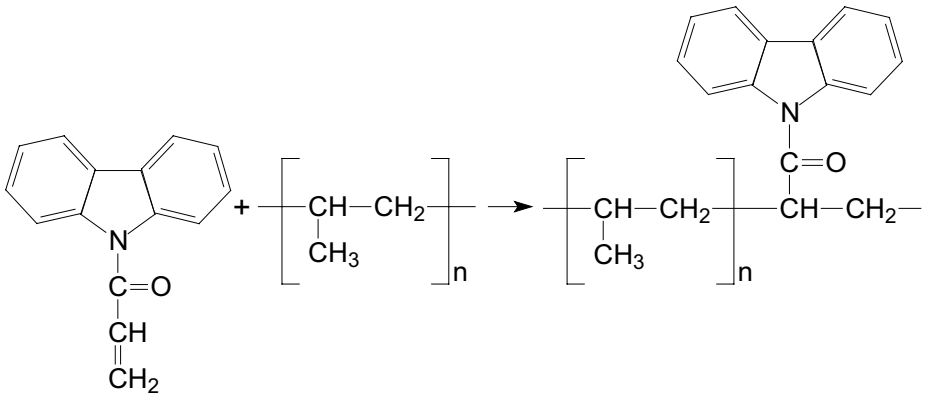

Conclusion

N-acryloylcarbazole has been synthesized by the interaction of carbazole and acryl acid. The structure of N-acryloylcarbazole has been tested through IR-, PMR-spectral analyses methods. The modification reaction of polypropylene and N-acryloylcarbazole has been conducted. The optimal condition of reaction has been determined.

References:

1. Ахмедов Х. М., Каримов Х. С. Фотоэлементы, солнечные элементы и фотоконденсаторы на основе полимеров карбазола //Доклады академии наук республики Таджикистан.2006.–Т. 49.– № 8.– С. 780–785.
2. Асундариа Ш. Т., Патель В. Б., Патель К. С. Синтез и изучение гомополицианураторов на основе 2-карбазол-4,6-дихлор-s-триазина // Журнал общей химии.2011.– Т. 81.–Вып. 10.– С. 1731–1740.
3. Светлечный М., Александрова Е. Л., Мягкова Л. А., Матюшина Н. В., Некрасова Т. Н., Тамаеев А. Р., Степаненко С. Н., Ванников А. В., Кудряцев В. В. Фотофизические свойства индоло [3,2-b] карбазолов – перспективного класса материалов для оптоэлектроники // Физика и техника полупроводников.2010.–Т. 44.–Вып.12.– С. 1629–1635.
4. Базунова В., Мустакимов Р. А., Гимаева Ф. Р. Получение ионитов на основе продуктов химической модификации отходов полипропилена // Химическая безопасность.2017.–Т. 1.– № 2.–С. 227–232.
5. Рабинович В. А., Хавин З. Я. Краткий химический справочник. Изд.: Химия, 1978.–392 с.

Klyuchnikova Natalya Valentinovna,
Belgorod State Technological
University. V. G. Shukhov
Genov Ivan,
Foundation of Science and Education
Bulgaria, Burgas
Piskareva Anastasia Olegovna,
Belgorod State Technological
University. V. G. Shukhov
E-mail: a.burdasova@inbox.ru

INITIATION OF POLYMERIZATION BY THERMO-ACTIVATED CALCIUM OXIDE

Abstract: This work is devoted to the verification of using calcium oxide obtained by thermal decomposition from chalk as an initiator and a filler for the copolymer of vinyl benzene and methyl methacrylate. Methods for the obtaining of a highly active form and for the synthesis of a filled copolymer are presented. The decomposition temperature of the obtained filled copolymer is established. (The temperature is significantly higher than the mechanical mixture of polyvinylbenzene and polymethylmethacrylate). The possible copolymerization reaction mechanism is described (from chain initiation to chain development and chain transfer).

Keywords: methacrylate, styrene, calcium oxide, copolymer, free-radical polymerization.

Calcium oxide from ancient times is widely used in various industries. One of his first uses was found in construction as a binder. Now it is used in agriculture, medicine, food and chemical industries. It is also used to remove sulfur dioxide from flue gases (in the form of hydroxide) and in the so-called "self-heating" dishes [1]. Such widespread use of calcium oxide contributes to its availability, low cost and its specific properties (the ability to absorb water, turning into hydroxide, the ability to change its ligands, turning into other compounds).

However, some properties of calcium oxide have not yet found such widespread use. It is about its ability to initiate polymerization by the radical mechanism of vinyl monomers [2].

To test the possibility of using thermolysis calcium oxide, equimolar mixtures of vinyl benzene and methyl methacrylate were taken as the initiator of copolymerization. As a source of thermolysis calcium oxide, chalk was used that was decarbonated at 600 °C for 4 hours. When the chalk was calcined, its external form and volume did not change. The volume that occupied the volatile product, passed into the pore volume. The copolymerization reaction was carried out in a closed laboratory reactor at 60 °C. For the synthesis, 70% of equimolar monomers (vinyl benzene and methyl methacrylate) and 30% of thermolysis calcium oxide were taken. After mixing the components, the formation of a copolymer of vinylbenzene and methyl methacrylate filled with calcium oxide occurred.

In order to determine the structure of the obtained copolymer, an experiment was carried out on its dissolution in an organic solvent (acetone). A sample weighing 5 g was dispersed into powder, mixed with acetone in a cylinder with a lapped cap, and stirred for 4 days. About 31% of the copolymer dissolved in acetone. It can be assumed that this is a pure copoly-

mer not bound to calcium oxide (see reactions 1, 2). The undissolved part was a filled copolymer of vinyl benzene and methyl methacrylate (reactions 3, 4) [4].

The most likely reaction mechanism:

Chain transfer:

$$-[A-(B-A)n-Ca-O-(B-A)n-B]- + A+B \rightarrow -[A-(B-A)n-Ca-O-(B-A)n-B]- + -[A-B]- \quad (1)$$

$$-[A-B]- + A + B \rightarrow -[B-A-B-A]- \text{ and so on.} \quad (2)$$

Chain origin:

$$Ca{=}O + CH_2{=}C(CH_3)\,COOCH_3 \rightarrow -[Ca-O-CH_2-\underset{\displaystyle COOCH_3}{\underset{|}{C}}(CH_3)]- \quad (3)$$

$$Ca{=}O + CH_2{=}CH(C_6H_5) \rightarrow -[Ca-O-CH_2-\underset{\displaystyle C_6H_5}{\underset{|}{CH}}]- \quad (4)$$

In total:

$$-[Ca-O-\underset{\displaystyle COOCH_3}{\underset{|}{CH_2}}-C(CH_3)]- + CH_2{=}CH(C_6H_5) \rightarrow -[CH_2-\underset{\displaystyle C_6H_5}{\underset{|}{CH}}-Ca-O-\underset{\displaystyle COOCH_3}{\underset{|}{CH_2}}-C(CH_3)]-$$

Chain development:

$$-[B-Ca-O-A]- + A + B \rightarrow -[A-B-Ca-O-A-B]-$$

$$-[A-B-Ca-O-A-B]- + A + B \rightarrow -[B-A-B-Ca-O-A-B-A] - \text{and so on,}$$

where A is methyl methacrylate; B is vinylbenzene.

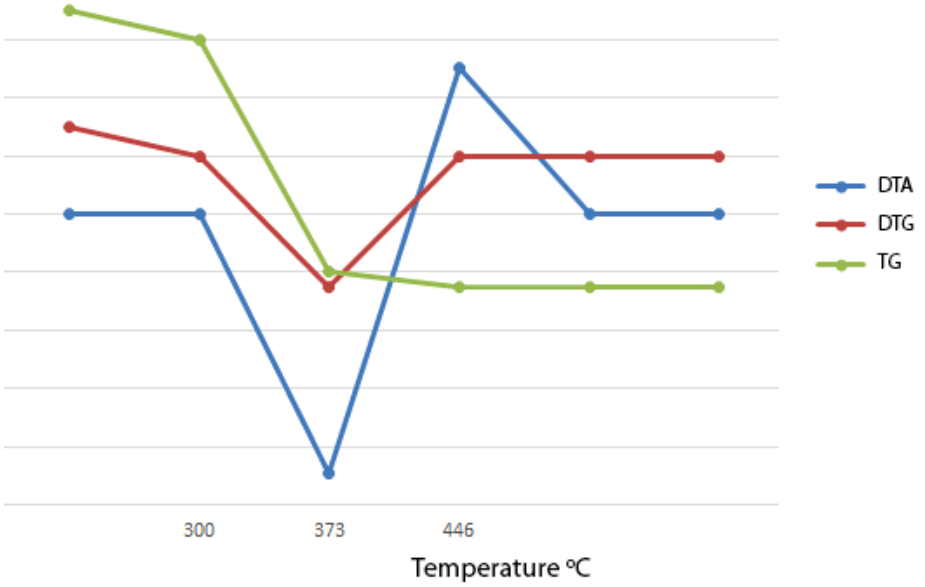

Figure 1. Differential-thermal analysis of the obtained copolymer

Temperature The degradation temperatures of the resulting filled copolymer were determined by the DTA method. As can be seen (Fig. 1), the destruction begins at 608 K, and ends at 642 °C. The destruction of the mechanical mixture of unfilled polyvinyl benzene and polymethyl methacrylate occurs in the range of 490–550 K. This increase in the temperature of destruction is due to the formation of strong chemical bonds between the copolymer and the filler. Estimated destruction of the copolymer occurs through a thermal free radical reaction by the mechanism of unfastening or anti-polymerization.

Using the method of IR spectroscopy to study the obtained copolymer seems to be very useful.

As we can see, the most intense absorption bands of the esters are in the 1732 cm^{-1} region – the stretching vibrations of the carbonyl group C = O. In this region, a series of four absorption bands is observed in the spectrum, which, together with the band at 754 cm^{-1}, are characteristic of the methacrylate structure –CO – O – CH_3. Proof of the presence of the methyl group are the absorption bands at 1388 and 2952 cm^{-1}. The presence of absorption bands of 700 cm^{-1} indicates the presence of polyvinylbenzene. The absence of a peak at 1645CM^{-1} is due to the fact that there is no double bond between CC. This all speaks about the presence of PMMA and PS. The absorption bands listed above indicate that the copolymerization was successful [5].

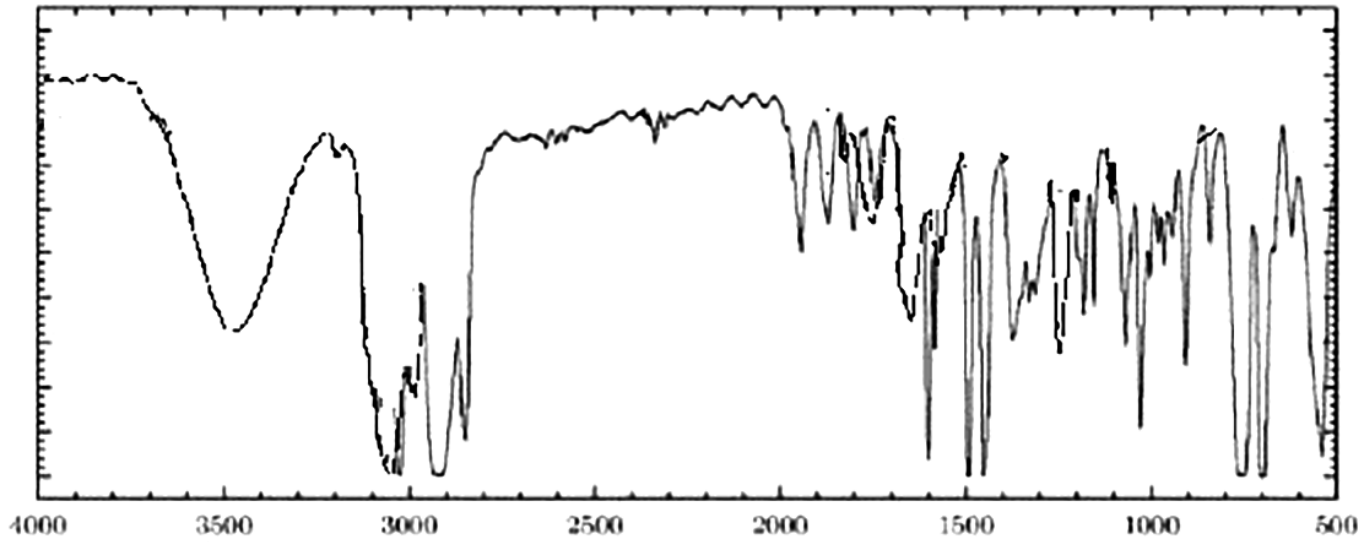

Figure 2. 2 IR-spectrum of the copolymer obtained

Findings: In the work done, the method of using thermolysis calcium oxide as a filler and at the same time an initiator for methylmetracrylate copolymer and vinylbenzene was considered. It has been proven that thermally activated calcium oxide can be used as an initiator for the joint polymerization of methyl methacrylate and styrene. It is established that the obtained copolymer has a high heat resistance.

References:

1. Ershova O. V., Mullina E. R., Chuprova L. V., Mishurina O. A., Bodian L. A. Study of the effect of the composition of the inorganic filler on the physico-chemical properties of the polymer composite material // Fundamental Research. 2014.– No. 12–3.– P. 487–491.
2. Klyuchnikova N. V. The study of the processes of thermolysis of natural calcium carbonates. URL: Perspektywyrozwojunaukiwewspolczesnymswiecie / – Krakow. 2012.– No. 3.– P. 92–96.
3. Kryzhanovsky V. K. Technical properties of polymeric materials: studies.– right. Manual / V. K. Kryzhanovsky – SPb.: Profession, 2005.– 240 p.
4. Klyuchnikova N. V., Piskareva A. O. Receiving polymer wax from waste production of polyethylene pipes / Bulletin of Belgorod State Technological University. V. G. Shukhov. 2017.– No. 11.– P. 106–109.
5. Klyuchnikova N. V., Gordeev S. A., Gordienko M. D. Polymer composite material based on thermoplastic polyimide / Bulletin of Belgorod State Technological University. V. G. Shukhov. 2017.– No. 12.– P. 126–129.

Usmonov Rasul Muratovich,
aspirant (PhD) of Institute of General and Inorganic Chemistry
of the Academy of Sciences of Uzbekistan
Uzbekistan, Tashkent
Salikhanova Dilnoza,
doctor of technical sciences, senior head Scientist
of Institute of General and Inorganic Chemistry
of the Academy of Sciences of Uzbekistan
Uzbekistan, Tashkent
Kuldasheva Shaxnoza Abdulazizovna,
doctor of Chemical sciences, senior head Scientist
of Institute of General and Inorganic Chemistry
of the Academy of Sciences of Uzbekistan
Uzbekistan, Tashkent
Eshmetov Izzat,
head of laboratory of Institute
of General and Inorganic Chemistry
of the Academy of Sciences of Uzbekistan
Uzbekistan, Tashkent
Abdurakhimov Saidakbar,
doctor of technical sciences, professor,
Tashkent Chemical-Technological Institute,
Uzbekistan, Tashkent

CLEANING OF WASTE WATER FOR FATTY PRODUCTION BY WASTE OF SUGAR PRODUCTION-DEFECATE

Abstract: This article the possibility of using a waste of sugar production - defecate for the neutralization of waste water in the fat and oil industry is proved. The optimum amount of introduced defecate is determined, which is 1.2-1.6% depending on pH. Comparative data of defecate and cul-cated soda used to date in enterprises have been compiled. It is established that the use of defecate as a reagent to neutralize acid waste water leads to the prevention of its accumulation in the form of waste in large quantities, to eliminate the negative impacts of it and acid waste water on the environment and equipment.

Keywords: defecate, waste, acid waste water, calcined soda, neutralization, purification, indicator, pH.

The Oil and fat industry (O&FI) is the leading branch of the food industry in Uzbekistan, where large quantities of purified water are used to flush vegetable oils, salmons, etc. Wastewater is formed, which contains fats, fatty acids, phosphatides and different surfactants. Purification of such waters by traditional methods entails considerable losses of both material and energy resources.

It is known that the waste water of the Oil and fat industry (O&FI) contains mainly organic com-

pounds in the form of emulsified fat-containing substances (vegetable oils, free fatty acids, phosphatides, soaps, etc.) and are characterized by a low concentration of the dispersed phase in the dispersion medium, so that they are relatively stable.

Therefore, for effective cleaning them is necessary to know the composition and the amount of pollution and the sources of their formation. As seen wastewater treatment of enterprises of fat and oil industry requires the use of different methods.

At the same time, the waste treatment of fat-containing and fat-free drains is mandatory in the purification scheme. Moreover, preliminary cleaning is mandatory before discharge of sewage into the sewage system. It consists in the allocation and removal of fat by means of greasers arranged in the type of oil traps [1].

In practice, the formed wastewater, containing mineral acids is neutralized and adjusted to pH 6.5 ÷ 8.5. Neutralization with the use of NaOH, KOH, Na_2CO_3, $CaCO_3$, $MgCO_3$, $CaCO_3$ and etc. are considered the most common method. At the same time, calcium hydroxide with an active lime content of 5-10% is considered the cheapest neutralizer of acid waters. It should be noted that during the preparation of lime milk, quenching, lime is associated with significant energy costs. In addition, hydrated lime has a corrosive property and leads to rapid deterioration of the equipment. Therefore, in most cases, calcined soda is used as a reagent to neutralize acidic waters [2]. The disadvantage of the latter is its high cost.

Consequently, the replacement of expensive imported reagents with cheaper and more affordable is considered an urgent task. To this end, we proposed a defect – a waste of sugar production to neutralize the acid waste water of calcined soda (O&FI).

Table 1. – The main physical properties of the defecate obtained from the sugar plant in Uzbekistan

humidity, %	Density, kg/m^3	Specific volume kg/m^3	pH	Oil absorption
18.0÷24.02	912.1–910.8	1030÷1180	8.5–8.7	19.00÷21.4

From (Table 1). It can be seen that the humidity, specific volume and Oil absorption of defecate varies within wide limits, which is related to the quality of processed raw materials, deviations in processing technology, etc. As seen from (Table 1) pH, and other indicators greatly exceed the maximum allowable concentration (MAC) limit. This once again proves that such water must be neutralized and cleaned of related substances.

Therefore, when using a defecate in the treatment of sewage water O&FI it is necessary to use averaging capacity, where the above-mentioned indicators are stabilized.

We have studied this process with the use of the recommended defecate in neutralizing the acid waste water generated at "Urgench yog-moy" when decomposing sopstok with sulfuric acid. Table 2 presents the results of analyzes of the chemical composition of sewage collected in the soap processing workshop.

It can be seen from (Table 2) that in the sewage water of the "Urgench-yog-moy" corporation, the greatest number of cations of the type Ca^{2+} and Mg^{2+}, and anions of the SO_4^{2-} and Cl^- type. This suggests that this wastewater has a complex chemical composition, for the purification of which it is necessary to use a polyfunctional sorbent.

Table 2. – Chemical composition of waste water of "Urgench yog-moy" corporation

The content of the wastewater			
Cations	**mg/l**	**mg – eq/l**	**% – eq/l**
1	***2***	***3***	***4***
Na^+	21	0.91	17

1	*2*	*3*	*4*
K^+	2	0.05	1
NH_4^+	5	0.28	5
Ca^{2+}	41	2.05	38
Mg^{2+}	24	2.0	38
Fe^{3+}	1	0.05	1
Fe^{2+}	0.2	0.01	–
Total:	94.2	5.35	100
Anions	mg/l	mg–eq/l	%–eq/l
Cl^-	87	2.5	16
SO_4^{2-}	638	13.30	83
NO_2^-	< 0.01	–	–
NO_3^-	3	0.05	–
CO_3^{2-}	no	–	–
HCO_3^-	11	0.18	1
Total:	**739**	**16.03**	**100**

We have studied other standardized water quality indicators, the data of which are presented in Table 3.

Table 3. – Standardized indicators of waste water of "Urgench yog-moy"corporation

Indicators of water	**unit measurement**	**values**
Rigidity:	mg-eq/l	
Overall		4.3
Carbonate		1.75
Non-Carbonate		2.55
pH Free CO_2	mg/l	11.0
Oxidizing properties O_2	mg/l	not found
Content:		
SiO_2	mg/l	2.0
H_2S	mg/l	is absent

From (Table 3) it can be seen that the sewage water of the "Urgench yog-moy" corporation is strongly rigid with a high content of non-carbonate compounds. This is confirmed by a pH of 1.8. Although this wastewater is apparently colorless transparent, with a taste of fresh water and a pungent odor.

We neutralized the acid waste water with the defecate by a dry process [6]. Defecate was added to the stock with the above composition in an amount of 1.2-1.6%, depending on the pH. During its addition, a rapid evolution of carbon dioxide was observed to form a stable foam. The neutralization process, with the release of the flocculent sediment, was continued for 15 minutes. After neutralization, the wastewater had a pH of 6.8 ÷ 7.2, which is close to a neutral medium.

It is known that sewage effluents, when neutralized with lime, give abundant and strong gypsum deposits, which are separated by the method [4]. There are also works on the prevention of gypsum deposits, stabilization of the solution by increasing the solubility of gypsum with the addition of acetone and lower alcohols [5].

In our case, after neutralization, turbidity is observed in the mixture and after 1 hour from the moment of addition of defecate a slight flocculent deposit appears, which does not clog the pipes. $CaSO_4$ could be formed in a sufficient amount, capable of producing gypsum deposits, since the main reaction of neutralization proceeds according to the scheme:

$$CaCO_3+H_2SO_4 \rightarrow CaSO_4\downarrow+CO_2\uparrow+H_2O$$

Here precipitation in large quantities is likely prevented by strong foaming of the mixture due to the formation of CO_2 bubbles ↑. On the other hand, the presence of pectic and other organic substances in the mixture improves the solubility of gypsum and prevents the precipitation of $CaSO_4$ [4]. After neutralization, the runoff has the following chemical composition, given in (Table 4).

As can be seen from Table 4. After neutralization with the use of a deficiency, the pH is 6.6–6.9, and SO_4^{2-} is reduced by a factor of 10. up to 62 mg/l. These data confirm the expediency of using the waste of sugar production-defecate as a reagent to neutralize wastewater.

Table 4. – Indicators wastewater after neutralization defecate wastes of sugar production

Parameters, mg/l							
pH	**Na^+**	**Ca^{2+}**	**Mg^{2+}**	**Cl^-**	**SO_4^{2-}**	**HCO_3^-**	**Organic impurity**
6.6–6.9	28	64	22	82	62	36	14.56

For comparison, we conducted studies of the effect of calcined soda in the neutralization of sewage of the (O&FI) corporation. "Urgench yog-moy", where the neutralization reaction proceeds according to the following scheme:

$$Na_2CO_3+H_2SO_4 \rightarrow Na_2SO_4+CO_2\uparrow+H_2O$$

As can be seen from the equation, when a sodium sulfate is used, no precipitate is formed in comparison with the defecate, and the sodium sulfate itself remains dissolved in the waste water. It has been established that the optimum amount of soda ash to be introduced, which is between 0.8–1.2%, depending on the pH. The data obtained are shown in (Table 5).

Table 5. – Main indicators of sewage after neutralization of Na_2CO_3

Parameters, mg/l							
pH	**Na^+**	**Ca^{2+}**	**Mg^{2+}**	**Cl^-**	**SO_4^{2-}**	**HCO_3^-**	**Organic impurity**
6,8-7,1	3493	44	19	87	646	213	8.2

As can be seen from table 5, the pH is lowered to 6.8–7.1, but the amount of sodium ions is increased by several hundred times. In addition, HCO_3 also increases by 20 times. If such water enters the soil, it becomes very saline, which will lead to an environmental problem. Therefore, it is not advisable to use it to neutralize waste water.

On the contrary, the use of a defecate to neutralize acidic wastewater has a significant economic effect due to substitution of expensive reagents, environmental protection, and also to an increase in the service life of equipment, water treatment plant systems, and etc.

Thus, the use of defecate as a reagent to neutralize the acid waste water of the Oil and fat industry (O&FI) leads to the prevention of its accumulation in the form of waste in large quantities, to eliminate the negative impacts of it and acid waste water on the environment and equipment.

References:

1. Yakovlev S. V., Karelin Ya. A. Drainage systems of industrial enterprises. – M., – Stroyizdat, 1990.

2. Komarova L. F. Technology of industrial and sewage treatment: physical and chemical, chemical and biochemical cleaning methods: Textbook / Altai Polytechnic Institute. – Barnaul, 1983.
3. Sapronov A. R. Technology of sugar production. – M.: Kolos, 1998. – 432 p.
4. Yakovlev S. V., Laskov Yu. M. Sewage system – M.: Stroiizdat, 1987. – P. 279–283.
5. Ac. USSR, IPC 02S5 / 02. Vaulin VE-437720 / 25-08; Declared 23.11.70; Opubl. 30.03.71. Bul. 12. – 2 p.
6. Brook-Levinson T. L etc. Use of natural and waste water. – Minsk, 1975. – P. 105–109.

Ruzmetova Dildora Tulibaevna,
doctorate (PhD) of Urgench State University,
Uzbekistan, Urgench
E-mail: ruzmetova.dildora@mail.ru ruzmetovadildora2018@gmail.com
Salikhanova Dilnoza Saidakbarovna,
doctor of technical sciences,
senior head Scientist of Institute of General and Inorganic Chemistry
of the Academy of Sciences of Uzbekistan
Uzbekistan, Tashkent
Abdurakhimov Saidakbar Abdurakhmanovich,
doctor of technical sciences, professor,
Tashkent Chemical-Technological Institute,
Uzbekistan, Tashkent
Eshmetov Izzat Dusimbatovich,
head of laboratory of Institute of General
and Inorganic Chemistry of the Academy of Sciences of Uzbekistan
Uzbekistan, Tashkent

DEVELOPMENT OF EFFECTIVE CLAY ADSORBENTS FOR CLEANING FATTY ACIDS OBTAINED FROM COTTON

Abstract: This article shows the possibility of purification of fatty acids by local clay adsorbents. The physicochemical properties of local clays have been studied.

The carried out researches show that the sorbent obtained from the methods of sulfuric acid activation of Navbakhar alkaline bentonite, which mainly consists of montmorillonite mineral, is the most effective of the considered clay adsorbents.Its high sorption ability is provided by sulfuric acid activation, which develops internal pore volumes, especially with micro-sizes. It was found that the thermal activation of Angren kaolin does not give the desired degree of purification of fatty acids from the above impurities. The regularities of the processes of clarification and removal of residual metals from fatty acids on selected adsorbents have been established, and the optimal conditions for their implementation have been determined.

Keywords: fatty acids, adsorbent, calcinations, activation, clay minerals, bleaching, sulfuric acid.

At present, fatty acids and their individual fractions (stearin, palmitin, olein, etc.) are widely used in the production of rubber, medicines and detergents, surfactants, paints, etc.

At the same time, the quality requirements are increased taking into account the field of their application.

The known technologies for the separation and purification of raw fatty acids, depending on the type of feedstock (oils, salomas, etc.) do not completely satisfy the requirements of consumers. they contain a significant amount of impurities (residues of soap, coloring substances – gossypol, chlorophyll and their derivatives, surface-active substances – phospholipids, etc.)

One of the promising ways of upgrading fatty acids is the adsorption method for their purification using polyfunctional adsorbents, including clay ones [1]. The advantage of clay adsorbents is their availability, cheapness and simplicity of activation with the use of mineral acids, alkalis, etc.

In Uzbekistan there are large bentonite, palygorskite and kaolin clay deposits, which can be used in the production of adsorbents, etc. It should be noted that fatty acids obtained on the basis of cottonseed oil processing are more dark, contain more coloring pigments, phospholipid residues, catalyst metals (Ni, Cu, etc.). Therefore, adsorption purification is considered to be a necessary technological stage of improving their quality.

The use of local minerals in the preparation of clay adsorbents allows several times to reduce the cost of production and use.

Taking this into account, we studied the mineralogical and chemical compositions of clays obtained from promising deposits in Uzbekistan. Analyzes of these samples were carried out according to the standardized methods described in [2; 3].

The results are shown in (Table 1).

Table 1.– Mineralogical and chemical compositions of selected local clays of Uzbekistan for obtaining polyfunctional adsorbents

Name clayey deposits	**Main type of mineral's**	**Chemical composition of clay,%**											
		SiO_2	**TiO_2**	**Al_2O_3**	**Fe_2O_3**	**FeO**	**MgO**	**CaO**	**Na_2O**	**K_2O**	**SO_3**	**H_2O**	**п.п.п**
Navbakhar alkaline bentonite (Navaiya region)	Montmorillonite	57.91	0.35	13.69	5.1	–	1.84	0.48	1.53	1.75	0.75	0.2	16.17
Tul-Sokh carbonate palygorskite (Fergana region)	palygorskite	46.8	–	8.71	0.3	3.5	2.76	10.07	–	1.55		0.5	24.3
Angren kaolin (Tashkent region)	Kaolinite	65.3	0.45	25.28	1.5	0.1	0.35	0.30	0.4	0.94	0.16	0.2	5.12
Askan ascanite (Republic of Georgia) (control)	Ascanite -mont-morilonite	54.14	0.38	18.74	4.98	0.22	4.64	2.41	2.82	0.64	0.07	0.2	10.94

From (Table 1) it can be seen that in the republic there are different types of clay minerals, of which minerals, from which it is possible to produce adsorbents for various purposes. To do this, it is necessary to develop optimal activation conditions taking into account their chemical composition.

It is known that montmorillonite (bentonite and palygorskite clays should be activated by chemical methods (acidic, alkaline or combined methods), and kaolinite by thermal calcination under optimal conditions [4].

The selected clays of Uzbekistan have polymineralogical compositions, so the method and conditions for their activation require a series of analyzes.

We carried out a differential-thermal analysis of the selected local clays in order to determine the optimum calcination temperatures. The experiments were carried out at the request of DTA on the Erba-Erba (Germany).

The results of the analyzes are presented in (Table 2).

Table 2. – Indicators of thermal "effects" of selected local clays

Name clayey deposits	Temperature «effects», °C		
	first	second	third
Navbahar alkaline bentonite (Navoi region)	200–235	550–700	800–900
Tul-Sokh carbonate palygorsk (Fergana region)	250–300	650–750	900–950
Angren kaolin (Tashkent region)	500–700	900–1000[x)]	1200–1250[xx)]
Askan Asconite (Republic of Georgia) (control)	200–250	500–700	850–900

Note: [x)] and [xx)] in these temperature ranges in kaolin, exothermic effects

From (Table 2) it can be seen that with a change in the type and chemical composition of the clay, the temperature values of the first, second and third thermal "effect" vary significantly. If, at the first "effect", moisture and other volatile substances are removed from the surface of the clay, in the second, the removal of the above from their internal part occurs. With the third "effect", the structure of clays is destroyed and their state is changed to a new state [5].

Therefore, taking into account and observing the given temperature values of the calcination allows us to correctly select the activation conditions for the selected clays.

The chemical composition of montmorillonites and hydromica shows the need for their acid (or alkaline) activation by leaching of unnecessary chemical components, and kaolinites – thermal activation under the conditions identified by their DTA.

In laboratory conditions, we carried out the acid activation of Navbakhar alkaline bentonite, Tulsokho carbonate palygorskite at 50 °C using an aqueous solution of 20 and 15% acid (H_2SO_4) for 6 hours, and thermal calcination of Angren kaolin in a muffle furnace at a temperature of 900–1000 °C for 1 hour cooled to room temperature, the adsorbents obtained were stored in glass beads prior to their use in the purification of fatty acids in a special installation [6].

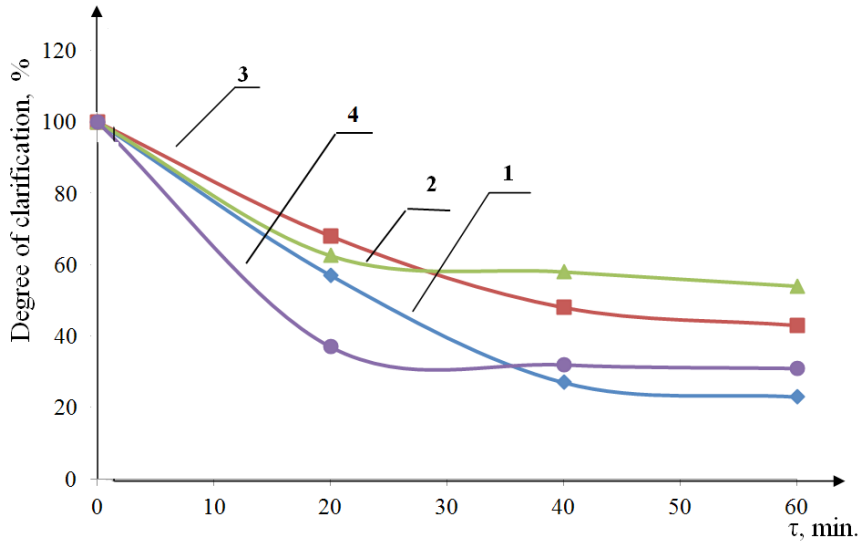

Figure 1. Kinetics of the clarification of fatty acids, depending on the type of adsorbent: 1 – Navbakhar alkaline bentonite (NAB); 2 – Tulsokho carbonate palygorskite (TCP); 3 – Angren kaolin (AK); 4 – Askan Ascanite (AA) (control)

To determine the effective adsorbent, we conducted experiments on the sorption of coloring substances (gossypol, chlorophyll and their derivatives) from fatty acids obtained from the products of processing cottonseed oil. Adsorption purification was carried out with vigorous stirring and 60–70 °C for 1 hour. At

the same time, the amount of adsorbent introduced was 2.0% of the weight of the fatty acids to be tested.

Figure 1 shows the kinetics of the clarification of fatty acids by the developed adsorbents.

Figure 1 it can be seen that when using adsorbents obtained from Navbakhar alkaline bentonite (curve 1), Tulsokh carbonate palygorskite (curve 2), and Angren kaolin (curve 3), the clarification of fatty acids proceeds smoothly according to the exponential law, and the Askan ascanite (curve 4) the initial stage of the process (for up to 20 minutes). At the same time, the greatest clarification of fatty acids is observed when using an adsorbent obtained from Navbakhar alkaline bentonite (curve 1) and vice versa, the smallest when using Angren kaolin (curve 3).

It is known that distilled fatty acids contain up to 95% of unsaturated fatty acids (linolenic, linoleic, oleic, etc.), which are oxidized by air oxygen during storage and thermal processing. This process is accelerated by the presence of metal debris (Ni, Cu, etc.) in them. Therefore, before the purification of fatty acids, it is advisable to use adsorbents that sorb the metals (or their ions) as much as possible.

Taking this into account, we have studied the sorption of these metals in the purification of fatty acids on selected adsorbents. The experiments were performed under the conditions described above, and analyzes of the residual content of nickel and copper were carried out according to the procedures approved in [7]. Figure 2 shows the results of the analyzes

From (Fig. 2) that the greatest sorption of nickel is observed when Navbakhar alkaline bentonite is used and, on the contrary, the lowest – Askan ascanite (control), which in 20 minutes loses its sorption ability and further, practically does not change the residual nickel content in fatty acid. The same pattern is observed when copper is removed from fatty acids, which confirms the selective ability of adsorbents to adsorbate metal and nickel residues.

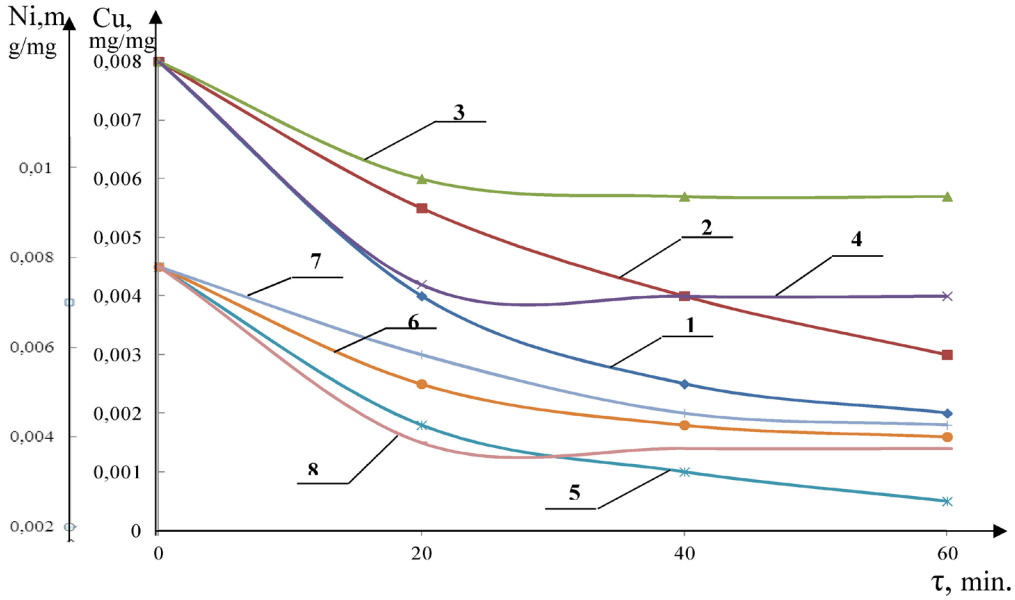

Figure 2. Change in the residual content of nickel (curves 1–4) and copper (curves 5–8), depending on the type of adsorbents and the cleaning time (τ, min): 1-Navbakhar alkaline bentonite (NAB); 2-Tulsokho carbonate palygorskite (TCP); 3-Angren kaolin (AK); 4-Askan ascanite (AA) (control)

On the basis of the studies carried out, the adsorbents chosen are arranged in the following sequence of a series of decreases; on clarifying ability:

Navbakhar alkaline bentonite> Askan ascanite (control)> Tulsokho carbonate palygorskite> Angren kaolin.

Removal of residual metals:

by sorption of nickel:

Navbakhar alkaline bentonite> Tulsokho carbonate palygorskite> Askan ascanite (control)> Angren kaolin.

on copper sorption:

Navbakhar alkaline bentonite> Ascan ascanite (control)> Tulsokho carbonate palygorskite> Angren kaolin.

Thus, the conducted studies show that the sorbent obtained from the methods of sulfuric acid activation of Navbakhar alkaline bentonite, which mainly consists of montmorillonite mineral, is the most effective of the considered clay adsorbents. Its high sorption ability is provided by sulfuric acid activation, which develops internal pore volumes, especially with micro-sizes. It was found that the thermal activation of Angren kaolin does not give the desired degree of purification of fatty acids from the above impurities. The regularities of the processes of clarification and removal of residual metals from fatty acids on selected adsorbents have been established, and the optimal conditions for their realization.

References:

1. Salikhanova D. S., Pardaev G. E., Eshmetov I. D., Agzamkhodzhaev A. A., Complex cleaning of cotton oils on coal and argillaceous adsorbents,– T: Navruz, 2016.– 160 p.
2. Taran N. G. Adsorbents and ion exchangers in the food industry. – M.: Light and Food Industry, 1983.– P. 205–215.
3. Komarov V. S. Adsorbents and their properties [Text] / Komarov V. S. // Science and technology.– Minsk, 1977.– 248 p.
4. Salikhanova D. S., Sobirov B. T., Agzamkhodzhaev A. A. Thermoactivated clay adsorbents for bleaching cotton oils // Journal of Chemical Industry, Russia., 2014.–T. 91.– No. 4.– P. 211–214.
5. Ovcharenko F. D. Investigation of adsorption on dispersed minerals, In collection. "Adsorbents, their receipt, properties and application.– L.: Science, 1971.– P. 13–17.
6. Dubinin M. M., Plachenov T. G. Adsorbents, their receipt, properties and application – L.: Nauka, 1971.– P. 203–208.
7. Alosmanov R. M. Investigation of the kinetics of sorption of lead and zinc ions by a phosphorus-containing cation [Text] / R. M. Alosmanov // Bulletin of the Moscow University. Series 2. Chemistry 2011.– Vol. 52.– No. 2.– P. 145–1.

Sultonov Shavkat Abdullayevich,
Amonov Muxtor Raxmatovich,
Bukhara State University
E-mail: ximiya@mail.ru

THE STUDY OF THE RHEOLOGICAL PROPERTIES OF THE THICKENING POLYMER COMPOSITIONS AND INK-BASE PRINTING

Abstract: The article describes the research results about the dependence of the viscosity of the concentration system of bentonite and it was found that bentonite K-4: HAE = 1 : 0.05 : 0.2 provides stable structures with the required dynamic viscosity in case of having optimal components. The influence of the concentration of the alkaline agent and the holdup time of the active dyes on the degree of fixation was revealed during the research. Along with this it was found that the degree of fixation of active dyes when printing using a thickener has not been reduced and in contrast it was higher by 10–25% than when using existing thickeners. The structural-mechanical and rheological properties of the developed polymer systems were carefully studied and revealed a deeper penetration of printing inks into the fabric, compared with printed inks thickened with sodium alginate.

Keywords: Viscosity, concentration, bentonite, degree of fixation, thickener, component, packing, porosity, polymer composition, rheological properties.

The urgency of the issue. Significant progress has been made in the artistic and coloristic design of textile materials, and printed textiles are becoming more and more essential all over the world, and the competition in the field of textile printing is taking on a global scale.

In these conditions, the basic problem of the domestic textile industry has been the increase in the competitiveness of its products, the solution of which requires not only improving the quality of textile materials, but also reducing production costs, as well as providing ecological requirements in accordance with world standards.

In the converters all over the world, pigments and active dyes are mainly utilized for printing cellulose-containing textile materials. In both cases, the effectiveness of the printing process depends to a large extent on the correct choice of the thickener, which is manifested as a printed figure and printed fabrics in the economic and environmental aspects of the production.

Therefore, the actuality and timeliness of research is quite obvious as it aims at creating technologies which usenatural compounds as textile-auxiliary substances not causing any danger for both biosphere and humankind. Bentonite, K-4 (on the basis of acrylates) and hydrolyze acryl emulsion (HAE)can be easily implemented for thickening printing inks, as they are produced in our Republic, inexistent and relatively inexpensive. In spite of these advantages, they are not widely used at present in domestic factories.

Thereby, it seems quite justified and expedient to develop new thickening compositions on the bases of natural and synthetic polymers, as the usage of high-quality, inexpensive and effective thickening compositions in printing is an important link in the chain of activities to ensure competitiveness and reduction of the cost of textile products.

To assess the effect of the sort and concentration of the polymer on the properties of the re-

sulting systems, the dependence of the viscosity of the composition (η) on the concentration of bentonite(C) was studied. It was found that the most low-concentrated systems with the necessary dynamic viscosity and good stability of the structure provide the composition with the component ratio: bentonite: K-4: HAE = 1: 0.05: 0.2, which is clearly visible from (Fig. 1).

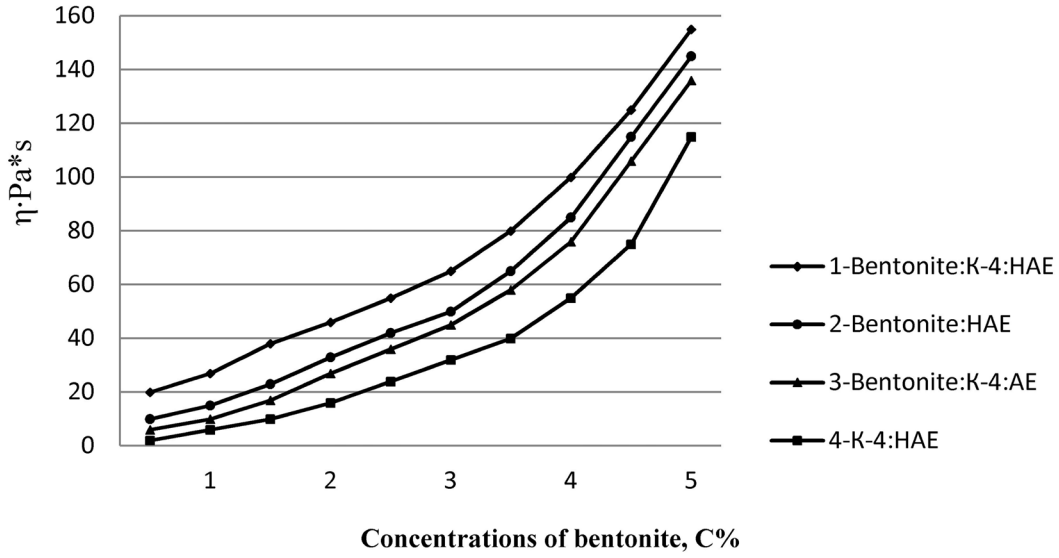

Figure1. Dependence of viscosity of compositions on concentration and sort of polymer

The main task with the use of active dyes is to ensure the highest possible degree of dye fixation. The implementation of the produced low concentrated clots, especially on the basis of bentonite, K-4 and HAE, create favorable conditions for this: first, by eliminating the side reaction of the dye with the polymer; secondly, due to a very permeable and thin film of printing ink, providing a more complete exit of the dye from it.

However, the noted positive factors may not be so significant if the optimal alkalinity of the ink is not ensured during its preparation, storage and in conditions of dye fixation. Due to the fact that the hydrogen index of the developed gelatinous and porous thickeners has a value of 10.0 ± 5, studies have been carried out to determine the effect of the concentration of the alkaline agent in the printing ink on the degree of dye fixation (DDF). The corresponding data for the dye is given in turquoise 4KP in (Fig. 2). from which it can be seen that when using the produced porous thickener, the concentration of sodium hydrogencarbonate should be about 15 g/kg. Similar dependences were obtained for other dyes as well.

When the ink is stored with a sufficiently high alkalinity (pH = 10), hydrolysis of the active dye can occur. In order to detect the effect of the storage time of the printing ink on the degree of hydrolysis of the active dye, one printing ink was used for printing immediately after its preparation and after 1, 2 and 24 hours.

It was found that the degree of fixation of active dyes during printing with the use of the developed bunch as a freshly prepared substance and after keeping it for a day did not decrease and but in the contrary it was by 10–25% higher than when using sodium alginate (Fig. 3), which can show the absence of hydrolysis. In addition, it should be noted that printing with a paint kept for an hour, provided a rise in the intensity of color. Presumably, this can be caused by the partial settling of bentonite included in the composition.

Next, we studied the dependence of the yield point of a thickener and ink, the degree of fixation of the dye by the fabric after printing, and the relative intensity of the color from the ratio of the constituent components of the thickening printing ink.

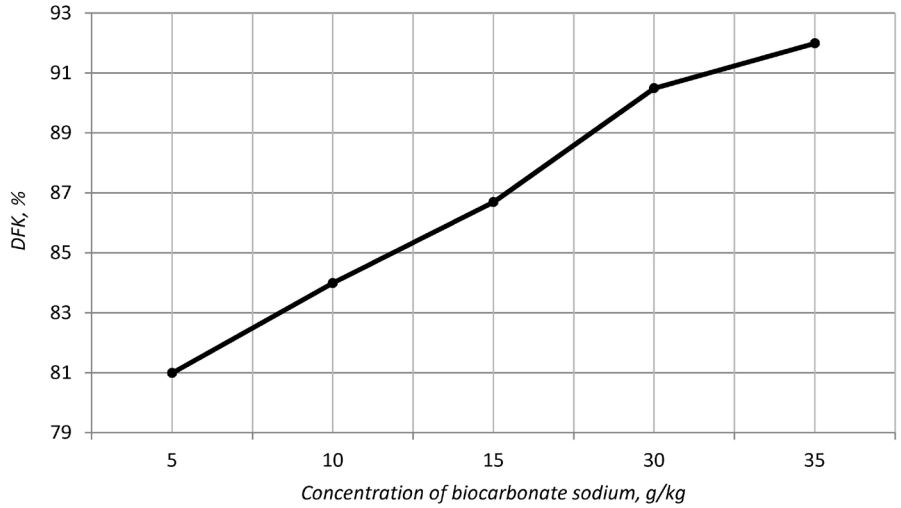

Figure 2. Dependence of the degree of fixation of active dyes active turquoise KP from concentration of alkali agent

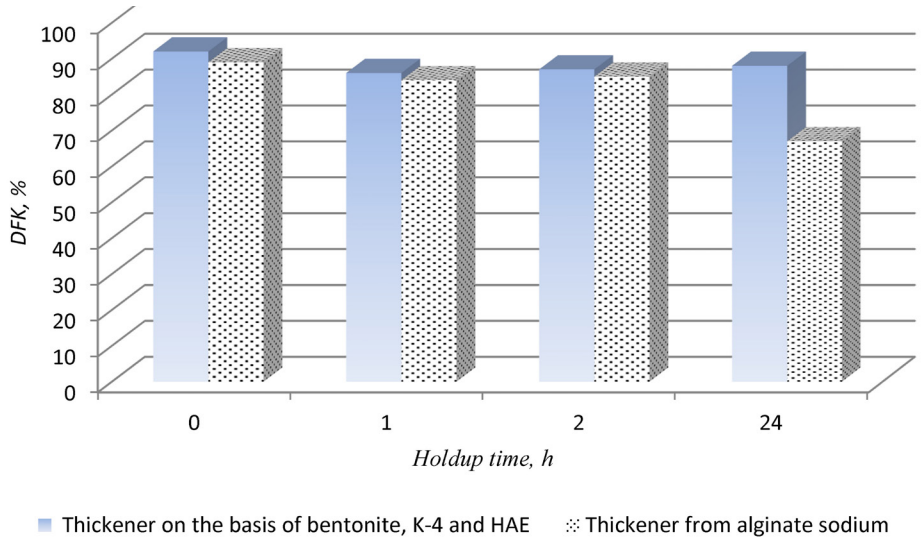

Figure 3. Dependence of the degree of usage of the active turquoise 4KP from the holdup time

Figure 4 shows a smooth course and the absence of minima on the yield strength (Pm) curves and the composition of the mixture, which indicates that the components of the thickening systems are well compatible, regardless of their ratio in the mixture (curve 2) and regardless of the additives of the ink components (curve 3). The presence of good compatibility is also confirmed by the high stability and uniformity of the mixtures obtained.

A smooth transition is also observed on the curves of the change in the colouristic indices of the printing of the composition substances shown in (Figures 5 and 6). From these graphs it can be observed that compositional thickenings, promoting a higher degree of fixation (Figure 5, curve 1), provide a lower color intensity.

It is of no less importance that the study of the structural-mechanical and rheological properties of the composition based on the synthesized oligomer in order to assess the possibility of its use in printing tissue.

The results obtained indicate a deeper penetration of printing inks thickened by the polymer composition into the interior of the tissue, compared to printing inks thickened with sodium alginate.

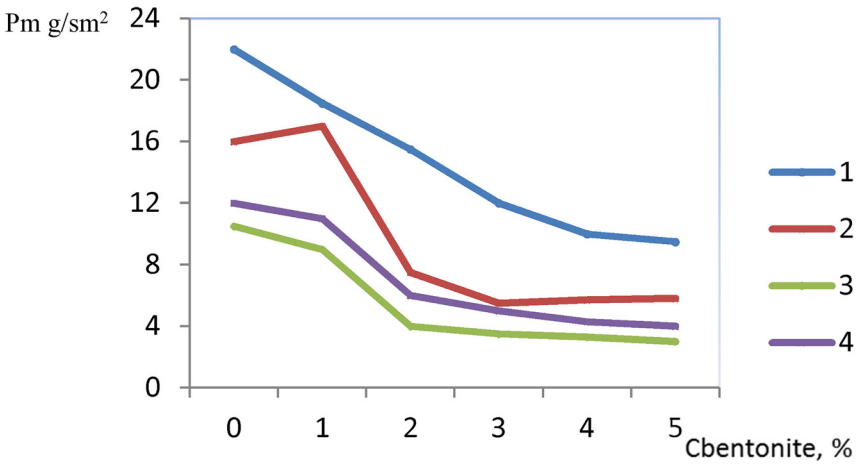

Figure 4. Dependence of the yield point of the thickener and the printing ink on the ratio of K-4 and HAE: 1 –thickeners on the basis of K-4; 2 – thickeners based on HAE; 3 – thickening on the basis of K-4 and HAE. 4 – printing ink

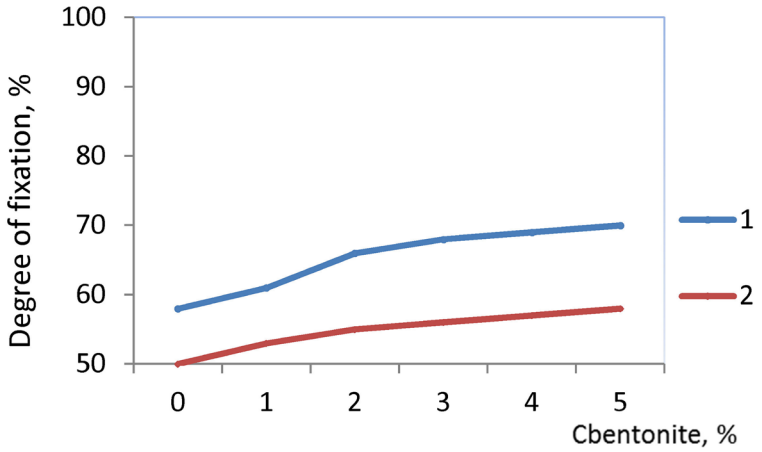

Figure 5. Dependence of the degree of fixation of the dye with tissue after printing: 1 – printing inks with a polymer composition; 2 – printing inks based on bentonite

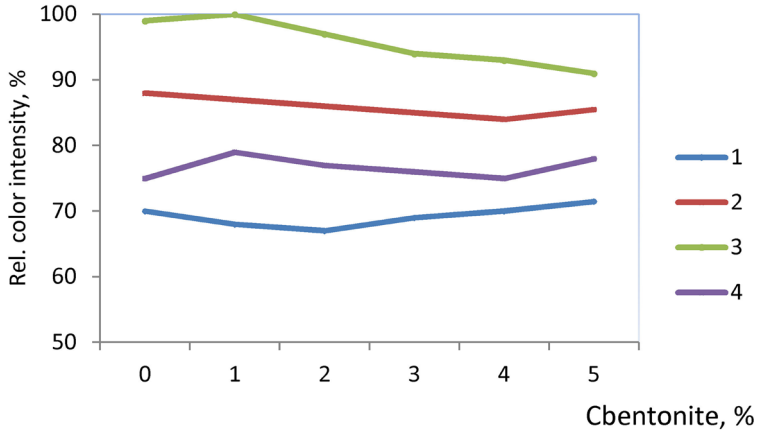

Figure 6. Dependence of the color change of the relative color intensity on the concentration of bentonite: 1 – Composition based on K-4; 2 – Composition based on HAE; 3 – Composition based on K-4 and HAE; 4 – Printing ink

It can be seen from Figures 5 and 6 that the relative content of bentonite, K-4 and HAE in the substance increases, the depth of penetration into the tissue and the degree of fixation of the dye increase. The addition of bentonite to the printed composite blobs promotes the production of sharper printing loops. Finally, the mixtures of bentonite-K-4-HAE and printing inks in question show an improvement in the rheological properties evaluated by the shape of the rheological curve.

Thus, it has been found that polymer compositions based on rice starch, bentonite-K-4-HAE, can be successfully applied as thickeners of paints for printing fabrics by compositions that helps to reduce the breakage, and also increases the degree of fixation of printing ink as compared to printing inks, thickened with sodium alginate.

References:

1. Nekrasova V. N., Shcheglova T. L., Belokurov O. A. // Technology of textile industry. 2009 – No. 2. – P. 49–52.
2. Nekrasova V. N., Shcheglova T. L., Belokurov O. A. // Technology of textile industry. 2010 – No. 2.– P. 50–53.
3. Melnikov B. N., Kirillova M. N., Moryganov A. P. Current state and prospects for the development of dyeing technologies of textile products.– M.: Light and Food Industry, 1983.– 232 p.
4. Breitman V. M., Senakhov A. *V.* Investigation of the influence of interaction between dyes and thickeners in printing inks fixed by a cloth during printing // Technology of textile industry. 1970.– No. 4.– P. 100–104.

Eshmuratov Bakhodir Beshimovich,
cand. tech. sciences, Tashkent Scientific Research Institute
of Chemical Technology of the Republic of Uzbekistan
E-mail: bbeshmuratov@mail.ru

Karimov Masud Ubaydulla ugli,
doc. tech. sciences, Tashkent Scientific Research Institute
of Chemical Technology of the Republic of Uzbekistan
E-mail: adler_219@mail.ru

Jalilov Abdulakhat Turapovich,
academician, doc. chem. Sciences, prof.,
Tashkent Scientific Research Institute
of Chemical Technology of the Republic of Uzbekistan
E-mail: a.t.djalilov@mail.ru

STUDY OF OPTIMIZATION OF SYNTHESIS METHYLDIETHANOLAMINE

Abstract: In the paper was studied the optimal ratio of ethylene oxide to methylamine for the preparation of methyldiethanolamine. The optimum molar ratio of methylamine with ethylene oxide having a degree of conversion of 60–70%, which allows to determine the upper limit of the degree of conversion of 70%.

Keywords: methylethanolamine, ethylene oxide, methylamine, methylmonoethanolamine, methyldiethanolamine.

In the production of methylethanolamines there is a large number of ethanolamines in the produced product. In the cleaning of natural gas, methyldiethanolamine is commonly used, and methylmonoethanolamine is used in small quantities or in no other way. Based on this, most manufacturers of methylethanolumineers have infused their technology for the production of methyldiethanolamine. Methyl monoethanolamine is added to the reaction mixture to increase the yield of methyldiethanolamine [1–2; 6–11].

In Fig. 1, the calculated behavior of methylethanolamine in the mixing reactor versus methanolamine and ethylene oxide is indicated. Methylamine was obtained on the basis of chloro-ammonium and formaline, and ethylene oxide was obtained on the basis of ethylene. The reactor is a type of autoclave and can withstand a pressure of 10–15 atm.

As seen from (Figure 1), in the absence of a methyl monoethanolamine (MMEA) recipe, the product obtained contains a large number of MMEAs. In (Figure 2), the estimated decoupling behavior of ethanolamines in the mixing reactor is relative to the methylamine and ethylene oxide ratio.

As seen from (Figure 2), with an increase in the amount of methylmonoethanolamine, the methyldiethanolamine production in the recycle increased and the output of methylmonoethanalamine decreased.

The dependence of the composition of ethanolamines, for the considered variant, on the amount of methyl monoethanolamine recycle in the initial mixture. When the value of the parameter, which corresponds to 3.2 kg of recycled methyl monoethanolamine per 1 kg of initial ethylene oxide, are obtained methyl ethanolamines composition of

MMEA: MDEA = 48 : 58 wt.%, indicating a very limited scope of this process.

Objectively, methyl monoethanolamine recycle, acceptable for today's production conditions, reflecting the market value of individual methylethanolamines and allowable energy costs, is at the level of 2 kg/kg. With such a recycle value of methyl monoethanolamine, the content of methyldiethanolamine is about 43% of the mass. The proportion of methyldiethanolamine can be increased, as mentioned above, by distributing the input of recycled methyl monoethanolamine.

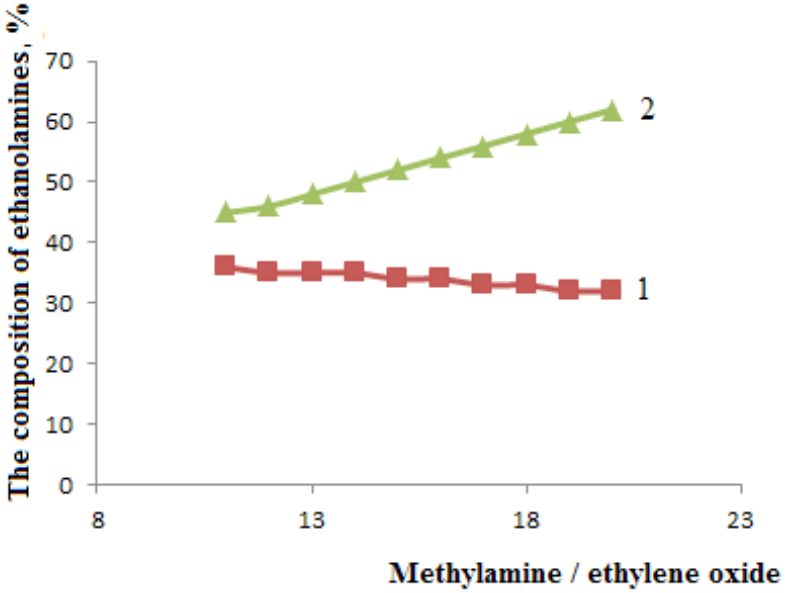

1 – methyldiethanolamin; 2 – methylmonoethanolamine

Figure 1. Recognizing the behavior of ethanolamines in the mixing reactor to reduce the methylamine and ethylene oxide in the distance of the MMEA at a temperature of 70 °C

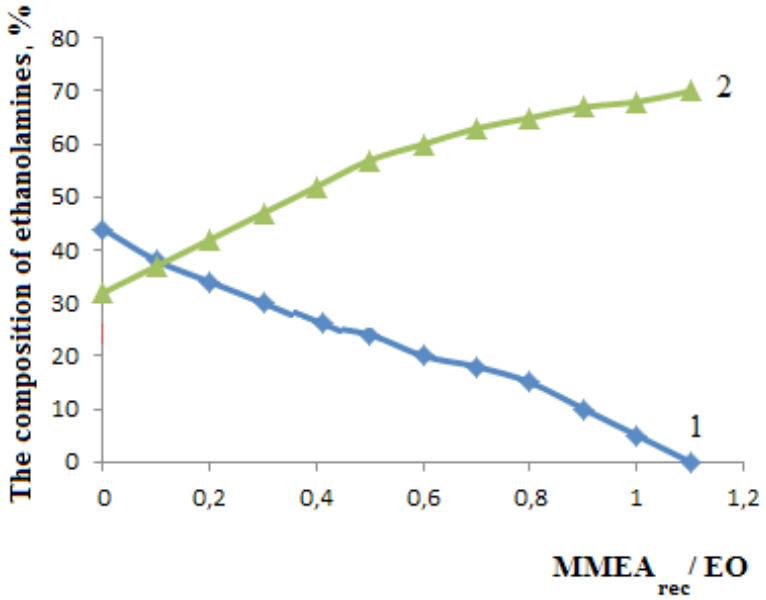

1 – Methylmonoethanolamine; 2 – Methyldiethanolamin

Figure 2. Calculation content of ethanolamines in the reactor for the mixing of methylamine and ethylene oxide at $MMEA_{rec}$

In (figure 3) shows the calculated dependence of the composition of methylethanolamines in the mixing reactor on the ratio of methyl monoethanolamine and ethylene oxide recycle with MMEA /OE = 21.

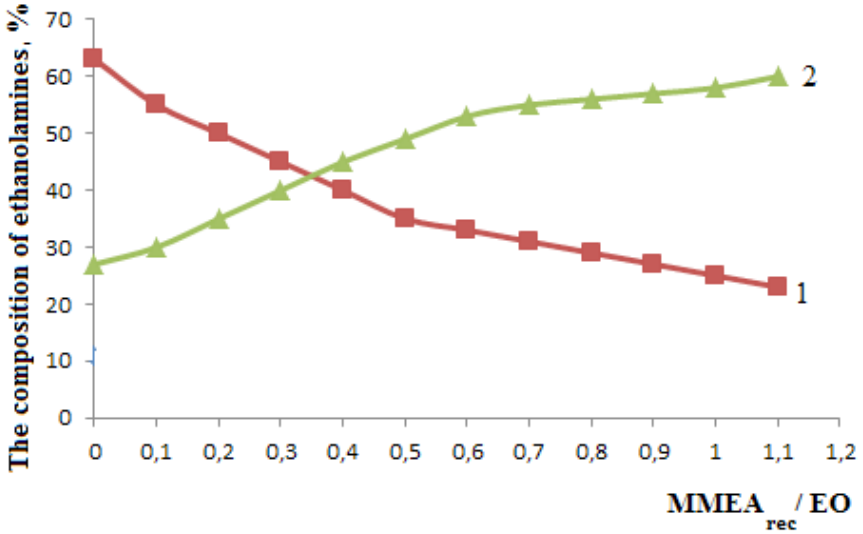

1 – methylmonoethanolamine; 2 – methyldiethanolamine

Figure 3. The calculated dependence of the composition of methylethanolamines in the mixing reactor on the ratio of methyl monoethanolamine and ethylene oxide recycle at $MMEA_{rec}/OE = 21$ and at a temperature of 70 °C

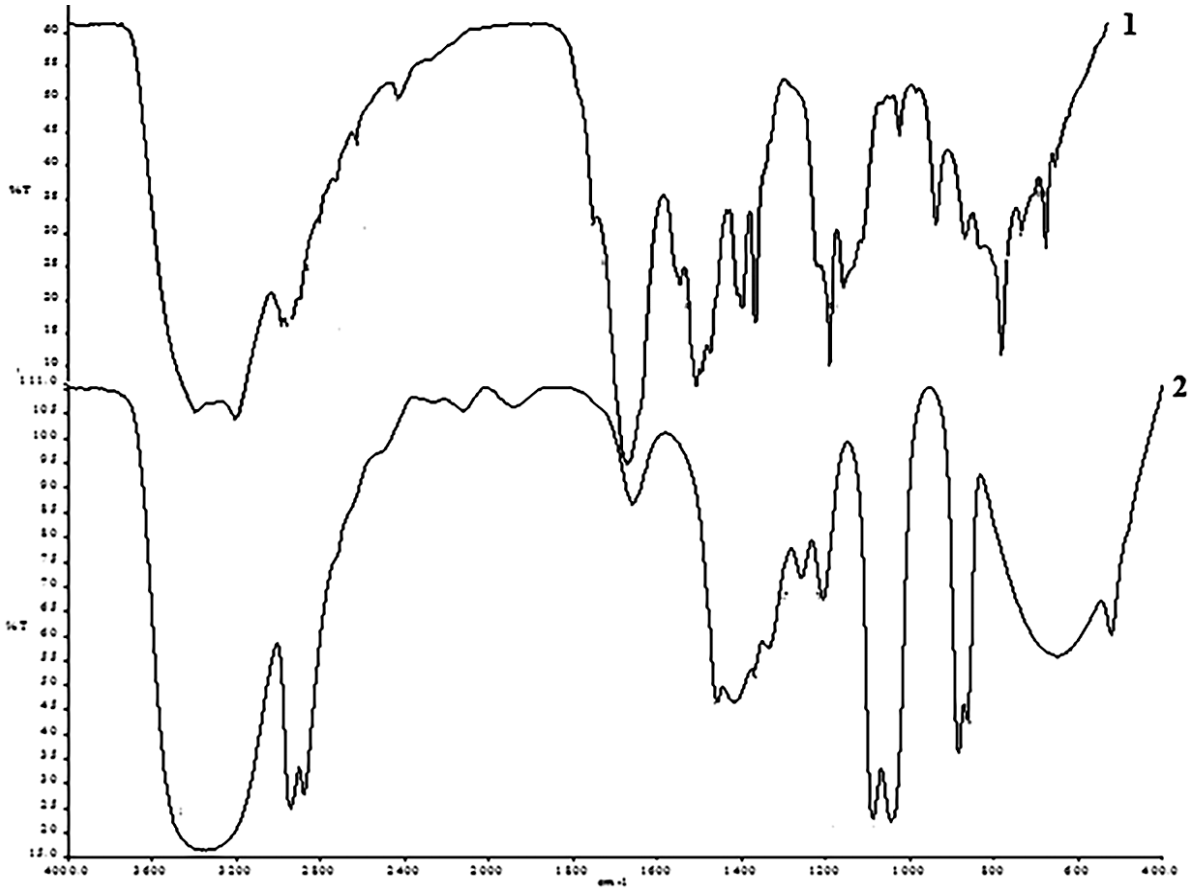

Figure 4. IR spectra of ethylene oxide (2) and methyldiethanol amine (1)

As can be seen from f(igure 3), an increase in the amount of methyl monoethanolamine in recycling leads to an increase in the amount of methyldiethanolamine.

To obtain a mixture with a high content of MDEA, MMEA is returned to the initial mixture and displaced.

The functional groups of the obtained methyldiethanolamine were studied by the method of IR spectroscopy and were compared with the IR spectra of ethylene oxide.

Figure 4 shows the IR spectra of ethylene oxide and methyldiethanolamine.

As can be seen in Figure 4 (2), the absorption bands in the regions 1050, 1250, 3350–3310, and 3500 cm^{-1} are characteristic of the $-CH_2$ – OH functional groups in the composition of ethylene oxide with water. Absorption bands in the region of 800–600 cm^{-1} are characteristic of –C – O– functional groups, which react with ammonia and form ethanolamines.

As can be seen in Figure 4 (1), the absorption bands in the region of 3350–3310, 3500 and 1580–1490 cm^{-1} are characteristic of the chemical bond – NH^-. Absorption bands in the region of 1050, 1250, 3640, 3350–3310, and 3500 cm^{-1} are characteristic for functional groups – CH_2 – OH in diethanolamine.

The intensity of the absorption bands in the region of 3350–3310 cm^{-1} is especially weak for diethanolamine. The absorption bands in the region of 1580–1490 cm^{-1} are usually difficult to determine, because they are masked by the oleiphyne band in the region of 1580 cm^{-1}.

In addition to these absorption bands, there are some absorption bands belonging to –C – O– bonds, which show the existence of nonreacting ethylene oxide.

Thus, when studying the IR spectra, it has been established that the ethanolamines obtained have characteristic absorption bands for the amine and methylol groups.

It was established that the optimum ratio of ethylene oxide and methylamine for the preparation of methylethanolamines is 1 : 21, and the optimum temperature is 70 °C. Experimental data show that the acceptable content of MDEA (methyldiethanolamine)60–70% at the exit is obtained at an initial molar ratio of methylamine-ethylene oxide 1: 19–25 and a conversion degree of 60–70%, which allows to determine the upper limit of the degree of conversion at 70%.

References:

1. Ethanolamines. Technical Bulletin "Oxiteno".– Brazil, 2002.– 4 p.
2. Ethanolamine. Monoethanolamine, diethanolamine, triethanolamine: Technical bulletin / "Dow Chemical Company". Midland, USA, 2003.– 20 p.
3. Patent № 2162461 RF, MKI S07S213G`04 Sposob polucheniya etanolaminov. Roleev G. I., Mixaylova T. A., Nikuhenko N. T., Lugovskoy S. A.(RF) – № 2000112562G`04, zayavl. 22.05.2000, Opubl. 27.01.2001, Byul. № 3.
4. Patent № 2167147 RF, MKI S07S215G`08 Sposob polucheniya etanolaminov G` Ro`leev G.I., Mixaylova T. A., Nikuhenko N. T., Lugovskoy S. A.(RF) – № 2000119218G`04, zayavl. 20.07.2000, opubl.20.05.2001 Byul. № 14.
5. Patent № 2225388 RF, MKI S07S213G`04. Sposob polucheniya etanolaminov T.A. Mixaylova, S. A. Lugovskoy, N. T. Nikuhenko, M. I. Nagrodskiy, I. A. Lavrentev (RF). № 2003105171G`04; Zayavl. 21.02.2003, Opubl. 10.03.2004, Byul. No. 7.
6. Sarkisov P. D. Problemo energo- i resursosberejeniya v ximicheskoy texnologii, nefteximii i biotexnologiiG`G` Ximicheskaya promo`shlennost, 2000.– No. 1.– P. 19–25.

7. Gruzinov V. P. Ekonomika predpriyatiya.– M.: Finanso` i statistika, 2000.– 326 p.
8. Djalilov A. T., Xamidov A. A., Eshmuratov B. B., Karimov M. U. Issledovanie polucheniya okisi etilena iz etilenaG`G`VIII Mejdunarodnaya nauchno-texnicheskaya konferentsiya "Gorno-metallurgicheskiy kompleks: dostijeniya, problemo` i sovremenno`e tendentsii razvitiya", Navoiyskiy gosudarstvenno`y gorno`y institut, g. Navai., 19–21 noyabr, 2015.– P. 18–19.
9. Djalilov A. T., Xamidov A. A., Eshmuratov B. B., Karimov M. U. Izuchenie sinteza etanolaminov iz etilenxlorgidrinaG`G` VIII Mejdunarodnaya nauchno-texnicheskaya konferentsiya "Gorno-metallurgicheskiy kompleks: dostijeniya, problemo` i sovremenno`e tendentsii razvitiya", Navoiyskiy gosudarstvennoy gorno`y institut, g. Navai., 19–21 noyabr, 2015.– P. 13–14.
10. Djalilov A. T., Xamidov A. A., Eshmuratov B. B., Karimov M. U. Issledovanie sinteza etanolaminovG` G`Respublikanskaya nauchno-texnicheskaya konferentsiya "Aktualno`e problemo` innovatsionno`x texnologiy ximicheskoy, nefte-gazovoy i pihevoy promishlennosti" – Tashkent, 2015.– P.18–20. noy-abr.– P. 33–34.

Contents

Section 1. Biology **3**

Rustamov Atham Ahmatovich, Kimsanboev Xojimurod Xamraqulovich, Jumaev Rasul Ahmatovich, Rajabov Shohrux
IN BIOCENOSIS THE DEGREE OF APPEARING ENTOMOPHAGOUS TYPES OF VERMINS WHICH SUCK TOMATOEY SOWINGS 3

Section 2. Biotechnology **6**

Shehu Matilda, Zekaj (Trojani) Zhaneta
CYTOLOGICAL DIVERSITY BETWEEN THREE POPULATIONS OF *SCILLA AUTUMNALIS* L. IN SOUTH ALBANIA 6

Section 3. Machinery construction **11**

Vasenin Valery Ivanovitch, Sharov Konstantin Vladimirovitch
STUDY OF THE GATING SYSTEM OPERATION WITH VERTICAL SLOT GATE 11

Section 4. Medical science **15**

Vashuk Mykola Anatoliiovych, Chesnakova Daria Dmytriivna, Somkina Yelizaveta Artemivna, Hloba Nataliia Serhiivna
PECULIARITIES OF SLEEP AS POSSIBLE RISK FACTOR OF OVERWEIGHT IN YOUNG PEOPLE 15

Section 5. Food processing industry **19**

Myrtaj Anisa, Malollari Ilirjan
PHYSIOCHEMICAL CHARACTERIZATION OF WASTEWATER FROM FRUIT JUICE AND BEVERAGE DRINK INDUSTRY IN ALBANIA 19

Section 6. Technical sciences **23**

Bukleshev Dmitry Olegovich, Sumarchenkova Irina Aleksandrovna, Buzuyev Igor Ivanovich
ANALYSIS OF METAL STRESS AND DEFORMATION DISTRIBUTION IN WELD-AFFECTED ZONES AT MAIN GAS PIPELINES 23

Vapaev Murodjon Dusummatovich, Akhmadzhonov Sardor Akhmadzhonovich, Teshabaeva Elmira Ubaidullaevna, Ibadullayev Akhmadzhon
INVESTIGATION OF MODIFIED ANGREN CAOLINE AS FILLING AND ACTIVATOR OF VULCANIZATION OF SOME ELASTOMERIC COMPOSITIONS 29

Vapaev M. D., Boborazhabov B. N., Teshabayeva E. U., Ibadullaev A. S.
ROAD COMPOSITIONS BASED ON MODIFIED BITUMENS 34

Kadirov Bakhodir Makhamadjanovich, Ergasheva Saodat Khasanova, Kodirov Khasan Ergashevich
RESEARCH OF THE EFFICIENCY OF COMPLEX INHIBITORS OF SALT DEPOSITION, CORROSION AND BIOFOULING 38

Mehtiyev Rafail Kerim oghlu, Jafarova Saida Allahverdi kizi
CONTİNİUSİNG SHEAR OF THROUGH CRACKS İN A COMPOSİTE REİNFORCED WİTH UNİDİRECTİONAL ORTHOTROPİC FİBERS 46

Orazimbetova Gulistan Jaksilikovna, Iskandarov Mastura Iskandarovna,
Mironyuk Nina Anatolievna, Kurbanova Aypara Djoldasovna
OPTIMIZATION OF RAW MATERIAL MIXTURES FOR BURNING
PORTLANDCEMENT CLINKERS at JV LLC "TITANCEMENT" 51

Orumbayev Rakhimzhan Kabievich, Kibarin Andrey Anatolievich,
Korobkov Maxim Sergeevich, Khodanova Tatyana Viktorovna
NEW ASEISMIC HORIZONTAL DESIGN KV-GM-55 HOT-WATER
BOILERS OPERATIONAL EXPERIENCE 56

Tuxtamushova Anisaxon Ubayevna, Yunusov Mirjalil Yusupovich,
Ikramova Zulfiya Adilovna, Alimxodjayeva Nazira Tillaxodjayevna,
Sulaymonova Gulchexra Gaybullayevna
INFLUENCE CRYSTALISTION ABILITIES OF GLASSES ON FORMATION
PYROXENES STRUCTURES 62

Section 7. Physics 66

Shukurlu Y. H.
KINETIC PARAMETERS OF THE FIRST AND SECOND STAGES
OF THE FISETIN MOLECULE DIFFUSION IN THE FIBROIN FIBER 66

Section 8. Chemistry 74

Islamova Yulduz Urolovna, Maksumova Oytura Sitdikovna,
Tadjieva SHaxnoza Abduvalievna
SYNTHESIS OF N-ACRYLOILOCARBAZOLE AND ITS
MODIFICATION TO POLYPROPYLENE 74

Klyuchnikova Natalya Valentinovna, Genov Ivan, Piskareva Anastasia Olegovna
INITIATION OF POLYMERIZATION BY THERMO-ACTIVATED
CALCIUM OXIDE 79

Usmonov Rasul Muratovich, Salikhanova Dilnoza,
Kuldasheva Shaxnoza Abdulazizovna, Eshmetov Izzat,
Abdurakhimov Saidakbar
CLEANING OF WASTE WATER FOR FATTY PRODUCTION
BY WASTE OF SUGAR PRODUCTION-DEFECATE 82

Ruzmetova Dildora Tulibaevna, Salikhanova Dilnoza Saidakbarovna,
Abdurakhimov Saidakbar Abdurakhmanovich, Eshmetov Izzat Dusimbatovich
DEVELOPMENT OF EFFECTIVE CLAY ADSORBENTS FOR CLEANING FATTY
ACIDS OBTAINED FROM COTTON 87

Sultonov Shavkat Abdullayevich, Amonov Muxtor Raxmatovich
THE STUDY OF THE RHEOLOGICAL PROPERTIES OF THE THICKENING
POLYMER COMPOSITIONS AND INK-BASE PRINTING 92

Eshmuratov Bakhodir Beshimovich, Karimov Masud Ubaydulla ugli,
Jalilov Abdulakhat Turapovich
STUDY OF OPTIMIZATION OF SYNTHESIS METHYLDIETHANOLAMINE 97